ANALYSIS OF *ANION EXCHANGER 1 (AE1)* GENE IN THAI PATIENTS WITH ENDEMIC DISTAL RENAL TUBULAR ACIDOSIS (EdRTA)

THITIMA TUNGSIRIKUL

A THESIS SUBMITTED IN PARTIAL FULFILLMENT
OF THE REQUIREMENTS FOR
THE DEGREE OF MASTER OF SCIENCE (MICROBIOLOGY)
FACULTY OF GRADUATE STUDIES
MAHIDOL UNIVERSITY
2000

ISBN 974-663-782-7

Thesis

entitled

ANALYSIS OF *ANION EXCHANGER 1* (*AE1*) GENE IN THAI PATIENTS WITH ENDEMIC DISTAL RENAL TUBULAR ACIDOSIS (EdRTA)

Thitima Tungsirikul
.....
Miss Thitima Tungsirikul
Candidate

Pa-thai Yenchitsomanus.
.....
Asst. Prof. Pa-thai Yenchitsomanus, Ph.D
Major-Advisor

P. Malasit
.....
Lect. Prida Malasit, M.D., F.R.C.P.
Co-advisor

Liangchai Limlomwongse
.....
Prof. Liangchai Limlomwongse, Ph.D.
Dean
Faculty of Graduate Studies

Uraiwan Kositanont
.....
Assoc. Prof. Uraiwan Kositanont, Ph.D.
Chairman
Master of Science Programme in Microbiology
Faculty of Medicine Siriraj Hospital

Thesis

Entitled

ANALYSIS OF *ANION EXCHANGER 1* (*AE1*) GENE IN THAI PATIENTS WITH ENDEMIC DISTAL RENAL TUBULAR ACIDOSIS (EdRTA)

was submitted to the Faculty of Graduate Studies, Mahidol University
for the degree of Master of Science (Microbiology)
on
March 21, 2000

Thitima Tungsirikul
.....
Miss Thitima Tungsirikul
Candidate

Pa-thai Yenchitsomanus.
.....
Asst. Prof. Pa-thai Yenchitsomanus, Ph.D
Chairman

P. Malasit
.....
Lect. Prida Malasit, M.D., F.R.C.P.
Member

Varaporn Akkarapatumwong
.....
Asst.Prof. Varaporn Akkarapatumwong, Ph.D.
Member

Somkiat Vasuvattakul
.....
Lect. Somkiat Vasuvattakul, M.D.
Member

Liangchai Limlomwongse
.....
Prof. Liangchai Limlomwongse, Ph.D.
Dean
Faculty of Graduate Studies
Mahidol University

Chanika Tuchinda
.....
Prof.Chanika Tuchinda, M.D., M.S., FAAP.
Dean
Faculty of Medicine Siriraj Hospital
Mahidol University

ACKNOWLEDGMENT

I would like to express my deepest gratitude and appreciation to my advisor, Asst. Prof. Dr. Pa-thai Yenchitsomanus for his continuous supervision, guidance, consultation, and encouragement, enabling me to accomplish this thesis. I am also extremely grateful to my co-advisor, Dr. Prida Malasit who is also the Head of Division of Medical Molecular Biology, for his valuable suggestions and comments in the writing of this thesis, and moreover for his supports and heedfulness all the time during my experimental study at the Division of Medical Molecular Biology.

My sincere thanks and appreciation are expressed to Dr. Somkiat Vasuvattakul for kindly providing the patients' samples and clinical data, educating me on the renal physiology, and being one of the examination committee members. I am also grateful to Asst. Prof. Dr. Varaporn Akkarapatumwong, the external examiner in the examination committee for her comments and corrections of this thesis.

I am greatly indebted to Nunghathai Sawasdee for her technical training, assisting, and friendship. Special thanks are also extended to Dr. Wanna Thongnoppakhun, Ajjima Treesucon, and Sumalee Oranwiroon for their kind and heartful helping for anything. I would like to thank all other members of the Divisions of Medical Molecular Biology and Molecular Genetics, Department of Research and Development, and of the Renal Unit, Department of Medicine, Faculty of Medicine Siriraj Hospital, for their kind assistance and friendship. I also thank to all friends in the Departments of Microbiology and Immunology for their sincerity and friendship. This thesis would not smoothly be completed without the financial supports from the National Science and Technology Development Agency (NSTDA) and from my aunt, Miss Wichittra Lailawitmongkol.

Finally, I wish to express my deepest appreciation and thankfulness to my parents and everybody in my family for their infinite love, understanding, support, encouragement, and attention. My success belongs to them.

Thitima Tungsirikul

3936703 SIMI/M : MICROBIOLOGY; M.Sc.(MICROBIOLOGY)
KEY WORDS : ENDEMIC DISTAL RENAL TUBULAR ACIDOSIS (EdRTA)/ *ANION EXCHANGER 1(AE1)* GENE/ *BAND 3* GENE/ SINGLE STRAND CONFORMATION POLYMORPHISM (SSCP)

THITIMA TUNGSIRIKUL: ANALYSIS OF *ANION EXCHANGER 1* GENE IN THAI PATIENTS WITH ENDEMIC DISTAL RENAL TUBULAR ACIDOSIS. THESIS ADVISORS: PA-THAI YENCHITSOMANUS, Ph.D., PRIDA MALASIT, M.D., F.R.C.P. (UK) 179 p. ISBN

Endemic distal renal tubular acidosis (EdRTA) is a unique form of distal renal tubular acidosis (dRTA), which is a common health problem in the northeastern region of Thailand. It is characterized by hyperchloremic metabolic acidosis due to the inability of the kidneys to excrete acid to urine, frequently accompanied by generalized muscle weakness, hypokalemia, nephrocalcinosis, and metabolic bone disease. The etiology of EdRTA could be related to either environmental or genetic factors or both. Evidence from past observations shows that many affected individuals were members of the same kindreds, suggesting that the genetic factor alone or in combination with the environmental factor(s) may involve in the pathogenesis of this disease. Although the acid excretion is controlled by several transporter proteins in the type A (acid-secreting) intercalated cells (IC) in the distal and collecting ducts of the kidneys, the defects of Cl^-/HCO_3^- exchanger (kAE1 or band 3), regulating Cl^-/HCO_3^- exchange across the basolateral membrane of type A IC, have recently been found to be associated with both autosomal dominant and autosomal recessive forms of dRTA. *AE1* mutation was therefore hypothesized to be the cause of EdRTA in the northeastern population of Thailand and the study in this thesis was carried out to prove this hypothesis.

Mutations of the *AE1* gene were screened in DNA samples from 10 EdRTA patients from 4 families by radioisotopic polymerase chain reaction and single strand conformation polymorphism (RI PCR-SSCP) technique, and from 7 affected and one unaffected members from a selected EdRTA family by non-RI PCR-SSCP. The analyses were also performed in 11 normal control DNA samples for comparison. From the results of screening of mutations in 18 regions of the *AE1* gene by both RI PCR-SSCP and non-RI PCR-SSCP analyses, mobility shifts were observed in 8 normal control subjects and 14 EdRTA patients in 5 regions including exons 4, 5, 9, 12, and 17. Sequencing analyses were performed in all 5 exons with the mobility shifts in 8 individuals who were selected as representatives of each group.

The results of sequencing analysis showed two nucleotide changes in the non-coding regions (IVS5+27C>T and IVS17+19G>A), two silent mutations (F266F and S438S), and four missense mutations (K56E, D38A, E72D, and G701D). The K56E (band 3 Memphis I) and D38A (band 3 Darmstadt) missense mutations, which were found in normal control subjects and patients, had previously been reported to be *AE1* polymorphisms. E72D is a new *AE1* missense mutation and proposed to be called 'band 3 Siriraj I'. This new mutation is most likely to be a non-disease mutation for the reason that it was present in normal control subjects as well as in only one of the patients resulting in a conservative amino-acid substitution. The G701D (band 3 Bangkok I) missense mutation was found in five patients but not in the normal control subjects. It is a reported disease mutation, which causes autosomal recessive dRTA in children, but its heterozygosity does not result in dRTA. DNA linkage analysis using microsatellite (D17S787) marker mapped close to the *AE1* gene was also carried out in a selected family with several members who were affected by EdRTA. The results of mutation analysis and DNA linkage study did not support the hypothesis that mutation of the *AE1* gene is involved the pathogenesis of EdRTA in the group of the northeastern Thai patients studied.

3936703 SIMI/M : สาขาวิชา: จุลชีววิทยา: วท.ม. (จุลชีววิทยา)

ฐิติมา ตั้งศิริกุล : การวิเคราะห์ยีนเออี-วัน ในผู้ป่วยไทยโรคไตผิดปกติในการขับกรดชนิดที่แพร่หลายในคนอีสาน (ANALYSIS OF *ANION EXCHANGER 1* GENE IN THAI PATIENTS WITH ENDEMIC DISTAL RENAL TUBULAR ACIDOSIS) คณะกรรมการควบคุมวิทยานิพนธ์: เพทาย เย็นจิตโสมนัส Ph.D., ปรีดา มาลาสิทธิ์ พ.บ., F.R.C.P.(UK). 179 หน้า

Endemic distal renal tubular acidosis (EdRTA) เป็นความผิดปกติในการขับกรดของท่อส่วนปลายของ nephron ซึ่งมีลักษณะจำเพาะ พบได้บ่อยและเป็นปัญหาสาธารณสุขของประชากรในภาคตะวันออกเฉียงเหนือของประเทศไทย โรคนี้มีภาวะที่ร่างกายมีการคั่งของกรดเนื่องจากไตไม่สามารถขับกรดออกทางปัสสาวะได้ และมักพบอาการกล้ามเนื้ออ่อนแรง โปแตสเซียมในเลือดต่ำ มีหินปูนหรือนิ่วในไต และความผิดปกติของกระดูก โรคนี้อาจมีสาเหตุจากปัจจัยทางสิ่งแวดล้อมและ/หรือปัจจัยทางพันธุกรรม จากหลักฐานของผลการศึกษาที่ผ่านมาพบว่าผู้ป่วยหลายคนมาจากครอบครัวเดียวกัน แสดงว่าพันธุกรรมหรือพันธุกรรมร่วมกับสิ่งแวดล้อมอาจจะมีส่วนเกี่ยวข้องในเชิงเป็นสาเหตุของโรคนี้ แม้ว่าการขับกรดจะถูกควบคุมโดยโปรตีนหลายชนิดในเซลล์ซึ่งทำหน้าที่ขับกรดในท่อส่วนปลายของ nephron ความผิดปกติของโปรตีน AE1 หรือ band 3 ซึ่งทำหน้าที่แลกเปลี่ยน Cl^- และ HCO_3^- ผ่าน basolateral membrane ของเซลล์ซึ่งทำหน้าที่ขับกรดได้มีการค้นพบเมื่อเร็วๆ นี้ว่า มีความสัมพันธ์กับโรค dRTA ทั้งชนิดที่ถ่ายทอดแบบ autosomal dominant และ autosomal recessive ดังนั้นจึงได้มีการตั้งสมมติฐานว่ามิวเตชั่นของยีน *AE1* น่าจะเป็นสาเหตุของโรค EdRTA ในประชากรภาคตะวันออกเฉียงเหนือของประเทศไทย และงานวิจัยในวิทยานิพนธ์นี้จึงทำการศึกษาเพื่อพิสูจน์สมมติฐานดังกล่าว

การตรวจกรองมิวเตชั่นของยีน *AE1* ในตัวอย่างดีเอ็นเอของผู้ป่วย 10 รายจาก 4 ครอบครัว กระทำโดยวิธี radioisotopic polymerase chain reaction and single strand conformation polymorphism (RI PCR-SSCP) และในผู้ป่วย 7 รายและญาติที่ไม่เป็นโรค 1 รายจากครอบครัว EdRTA โดยวิธี non-RI PCR-SSCP พร้อมทั้งทำการตรวจตัวอย่างดีเอ็นเอจากกลุ่มคนปกติจำนวน 11 รายเพื่อเปรียบเทียบ จากผลการตรวจกรองมิวเตชั่นทั้งโดยวิธี RI PCR-SSCPและ non-RI PCR-SSCP ในยีน *AE1* ทั้ง 18 บริเวณ (regions) พบว่ามี mobility shift ในคนปกติ 8 รายและผู้ป่วย 14 ราย ใน 5 บริเวณได้แก่ exon 4, 5, 9, 12 และ 17 ดีเอ็นเอที่พบว่ามี mobility shift ทั้ง 5 บริเวณซึ่งเลือกมาเป็นตัวแทนของแต่ละกลุ่มเพียง 8 รายได้นำมาทำการศึกษาโดยการวิเคราะห์ลำดับนิวคลีโอไทด์

ผลการวิเคราะห์ลำดับนิวคลีโอไทด์พบว่ามีการเปลี่ยนแปลงนิวคลีโอไทด์ในหลายตำแหน่งได้แก่ การเปลี่ยนแปลงนิวคลีโอไทด์ในบริเวณ non-coding 2 แห่ง (IVS5+27C>T และ IVS17+19G>A) มิวเตชั่นชนิดที่ไม่เปลี่ยนกรดอะมิโน 2 ชนิด (F266F และ S438S) และมิวเตชั่นชนิดที่เปลี่ยนกรดอะมิโน 4 ชนิด (K56E, D38A, E72D และ G701D) K56E และ D38A เป็น *AE1* polymorphism ที่เคยมีรายงานมาก่อนมีชื่อเรียกว่า band 3 Memphis I และ Darmstadt ตามลำดับ ส่วน E72D เป็นมิวเตชั่นใหม่ที่ยังไม่เคยมีรายงานมาก่อนจึงเสนอให้เรียกว่า "band 3 Siriraj I" มิวเตชั่นชนิดนี้ไม่น่าจะเป็นสาเหตุของโรค ด้วยเหตุผลที่พบมิวเตชั่นชนิดนี้ทั้งในคนปกติและผู้ป่วย และกรดอะมิโนที่เปลี่ยนอยู่ในกลุ่มเดียวกัน จึงไม่น่าจะมีผลต่อการทำงานของโปรตีน มิวเตชั่นชนิด G701D หรือ band 3 Bangkok I พบในผู้ป่วย 5 รายโดยไม่พบในคนปกติ มิวเตชั่นนี้เคยรายงานว่าเป็นสาเหตุของ autosomal recessive dRTA ในเด็ก แต่ในภาวะ heterozygote มิวเตชั่นชนิดนี้ไม่ทำให้เกิดโรค dRTA นอกจากนี้ยังได้ทำการศึกษา DNA linkage โดยใช้ microsatellite marker ชนิด D17S787 ซึ่งอยู่ใกล้กับยีน *AE1* ในครอบครัวของผู้ป่วย 1 ครอบครัวซึ่งมีสมาชิกหลายคนเป็น EdRTA ผลการวิเคราะห์มิวเตชั่นและการศึกษา DNA linkage ไม่สนับสนุนทฤษฎีที่ว่ามิวเตชั่นของยีน *AE1* เกี่ยวข้องในเชิงเป็นสาเหตุของโรค EdRTA ในกลุ่มผู้ป่วยจากภาคตะวันออกเฉียงเหนือของประเทศไทยซึ่งได้นำมาทำการศึกษาในวิทยานิพนธ์นี้

CONTENTS

LIST OF TABLES

Table **Page**

LIST OF FIGURES

Figure **Page**

LIST OF ABBREVIATIONS

bp	=	base pair
BUN	=	blood urea nitrogen
C-terminus	=	carboxyl terminus
°C	=	degree Celsius
dATP	=	deoxyadenosine-5′-triphosphate
dCTP	=	deoxycytidine-5′-triphosphate
dGTP	=	deoxyguanosine-5′-triphosphate
dTTP	=	deoxythymidine-5′-triphosphate
dNTP	=	dATP, dCTP, dGTP, dTTP
DNA	=	deoxyribonucleic acid
EDTA	=	ethylenediamine tetraacetic acid
H^+	=	hydrogen ion
HCO_3^-	=	bicarbonate ion
i.e.	=	*id est* (that is)
IVS	=	intervening sequence
K^+	=	potassium ion
kb	=	kilobase pair
kDa	=	kilodalton (s)
M	=	molar
mEq	=	milliequivalent
mg	=	milligram(s)

μg	=	microgram(s)
$MgCl_2$	=	magnesium chloride
ml	=	milliliter(s)
μl	=	microliter(s)
mM	=	millimolar
μM	=	micromolar
mRNA	=	messenger ribonucleic acid
Na^+	=	sodium ion
ng	=	nanogram
NH_4Cl	=	ammonium chloride
nt	=	nucleotide(s)
N-terminus	=	amino terminus
OD_{260}	=	optical density at 260 nm
OH^-	=	hydroxide ion
PAGE	=	polyacrylamide gel electrophoresis
PBS	=	phosphate buffer saline
PCR	=	polymerase chain reaction
pmol	=	picomole
RBC	=	red blood cell
RNA	=	ribonucleic acid
RNase	=	ribonuclease
rpm	=	revolutions per minute
SDS	=	sodium dodecyl sulfate
TAE	=	tris acetate EDTA

Taq	=	*Thermus aquaticus*
TEMED	=	N,N,N′,N′-tetramethyl-ethylenediamine
TM	=	transmembrane
Tm	=	melting temperature
U	=	units(s)
UV	=	ultraviolet
WBC	=	white blood cell
%	=	per cent
′	=	minute
″	=	second

CHAPTER I

INTRODUCTION

Distal renal tubular acidosis (dRTA) is a health problem found in the northeastern region of Thailand (1-3). It is found associated with other conditions such as hypokalemic periodic paralysis and renal stone (1-6). This disease is characterized by hyperchloremic metabolic acidosis with inability of the kidney to acidify urine, frequently accompanied by hypokalemia, nephrocalcinosis, metabolic bone disease, and growth retardation (7-10). The etiology of the so-called 'endemic renal tubular acidosis (EdRTA)' in the northeastern Thai population is still unknown. Either environmental or genetic factors or both may contribute to the pathogenesis of the disease (1-3, 5, 11, 12). It has been suggested that high level of vanadium (V) in the environment and then in the dwellers (6, 12), or low level of potassium (K) in their diets causing potassium deficiency (1-3, 5, 6, 11, 13) may be possible causes of the disease. However, both hypotheses remain to be proven. On the other hand, from the observation that many affected individuals were members of the same kindred, the role genetic, alone or in combination with environmental factor(s) has also been proposed (1).

Kidney has an important function in maintenance of acid-base balance by bicarbonate reabsorption and acid excretion. The acid excretion in the kidney is

substantially mediated by type A (acid-secreting) intercalated cells (IC) of the renal collecting ducts. Defects in transporters of the type A IC required for transluminal acid secretion may cause dRTA (7-9, 11, 14). The acid excretion is mediated mainly by H^+-ATPase pumps located in the apical membrane of type A IC of the distal nephron, in association with bicarbonate reabsorption across the basolateral membrane of these cells, which is moderated by kidney Cl^-/HCO_3^- exchanger (kAE1) (14-16). Other components include cytoplasmic carbonic anhydrase II (CA II) whose activity provides both H^+ for luminal secretion by the H^+-ATPase and HCO_3^- for basolateral extrusion by kAE1 (14, 16), and H^+/K^+-ATPase locating in the apical membrane and functioning in H^+ secretion in exchange with K^+ ion (14, 16).

Both autosomal dominant (17-19) and autosomal recessive (20) patterns of inheritance have been observed in kindreds with primary dRTA, with a broad spectrum of clinical severity. Some patients with autosomal dominant dRTA remain asymptomatic until adolescence or adulthood. Patients with autosomal recessive dRTA are usually severely affected in infancy, with bone abnormalities, growth retardation, and early nephrocalcinosis causing eventual renal insufficiency. Many patients with autosomal recessive dRTA also have sensorineural deafness (21). Mutations of a gene encoding B1 subunit of the H^+-ATPase, which is composed of several subunits, have been reported in autosomal recessive dRTA with sensorineural deafness (22). Several autosomal recessive mutations of *CA II* gene have been described that result in proximal renal tubular acidosis and metastatic calcinosis (8, 14, 16). dRTA in association with defective H^+/K^+-ATPase has not been detected.

AE1 gene encodes both erythroid (eAE1) and kidney (kAE1) isoforms of Cl^-/HCO_3^- exchanger 1 protein. The eAE1 isoform or band 3 is a major integral membrane of red cells. *AE1* mutations are associated with approximately 20% hereditary spherocytosis (HS) (23) and Southeast Asian ovalocytosis (SAO), a common red cell abnormality observed in Southeast Asian and Melanesian population (23, 24). The kAE1 isoform, which is encoded by the same gene, using alternative promoter and skipping the first 3 exons (25), is involved in $Cl^-/HCO3^-$ exchange across the basolateral membrane of type A IC. Therefore, *AE1* mutation is believed to result in dRTA (23). Usually, dRTA is not present in these conditions. However, at least two families with elliptocytosis (this term is sometime used as a synonym of ovalocytosis) associated with dRTA were reported (26, 27). Recently, several *AE1* mutations have been found to be associated with autosomal dominant dRTA in many patients and kindreds (28-31). However, autosomal recessive dRTA associated with homozygous *AE1* mutation (32) and with compound heterozygous mutations (33) have also been recently described. *AE1* mutations are thus associated with both autosomal dominant and autosomal recessive dRTA. These observations strongly indicate that mutations of the *AE1* might be a possible pathogenetic factor causing EdRTA found in the northeast of Thailand. This thesis is an attempt to answer this hypothesis.

CHAPTER II

OBJECTIVES

The objectives of the study in this thesis are:

1. To establish polymerase chain reaction and single strand conformation polymorphism (PCR-SSCP) technique for screening of *AE1* mutations,
2. To use PCR-SSCP techniques to screen for potential mutations of the *AE1* gene in EdRTA patients and normal individuals,
3. To characterize *AE1* mutations as identified PCR-SSCP,
4. To study the association between *AE1* mutations and EdRTA.

CHAPTER III

LITERATURE REVIEW

Acid-base balance, which refers to regulation of hydrogen (H^+) ion concentration in the body fluids (34), is important of the body's homeostatic mechanisms for normal body functions. Acids and bases continually enter the blood from the metabolism of food consumed in our diet (15, 34). Both volatile and nonvolatile acids are produced continuously during normal metabolism. Approximately 13,000 to 15,000 mmol of CO_2 (or volatile acid in form of H_2CO_3) are formed daily in normal adult. The nonvolatile (or fixed) acid is generated 1.0 to 1.5 mEq/kg body weight per day from the metabolism of high protein diet. These dietary acids are generated as sulfuric acid, organic acid phosphoric acid, and hydrochloric acid (35). Despite the metabolic production of acids in the body, a normal pH in blood and interstitial fluid is preserved in a healthy person. Buffers in the body fluid stabilize the pH. The first line of defense of pH consists of chemical buffers in extracellular and intracellular fluids. HCO_3^-/H_2CO_3 is the major extracellular buffer system. The second is the lungs, which buffer blood pH by disposing of carbon dioxide as rapidly as it is formed. When there is excessive production of acids (or bases) in the body, lung ventilation changes in order to reduce the deviation from normal blood pH. The third is the kidneys, which buffer blood pH by excreting hydrogen ions in the urine

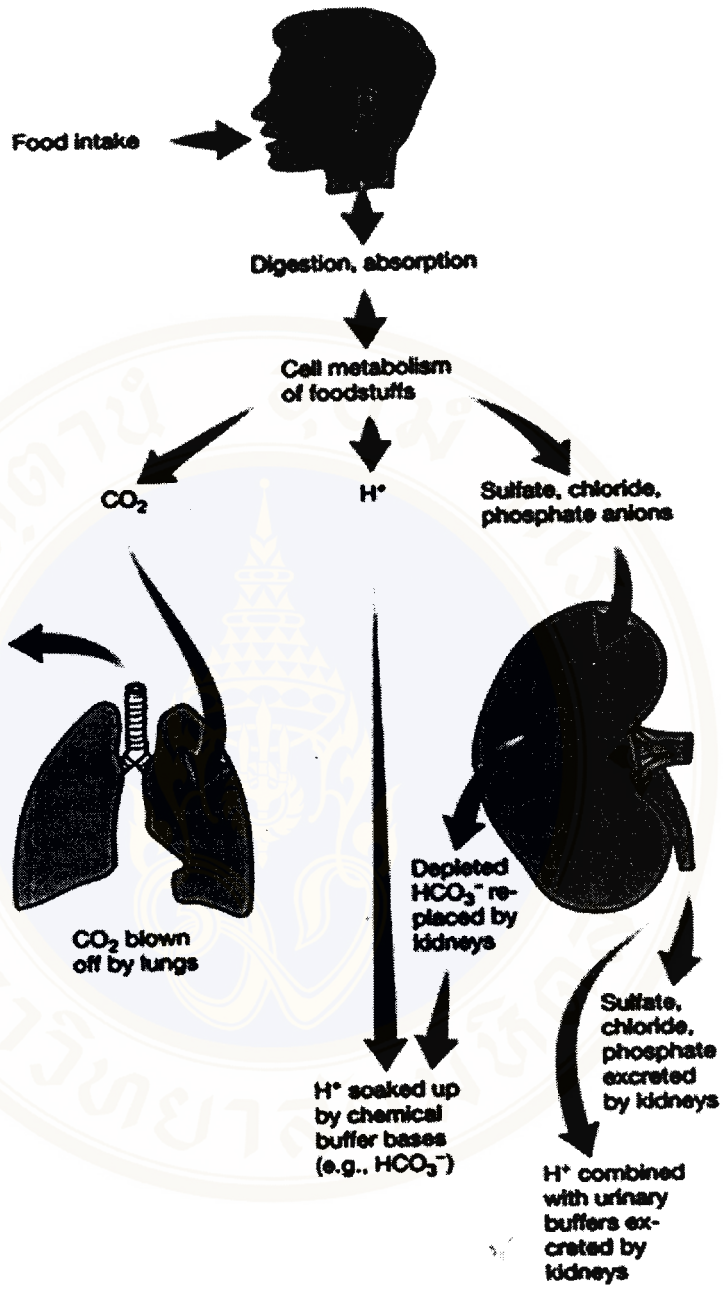

Figure 1. The pathway of human acid-base homeostasis (36).

This diagram shows the pathways for maintenance of acid-base balance. Despite the acid threat posed by cell metabolism of foodstuffs three major systems plays role to stabilize blood pH in the normal narrow range, 7.35-7.45. The first line of defense of pH consists of chemical buffers in extracellular and intracellular fluids and buffer in bone. The second is the lungs, which buffer blood pH by disposing of CO_2. The third is the kidneys, which buffer blood pH by excreting hydrogen ions in the urine.

(36). Figure 1 sketches the pathways for maintaining a stable blood pH despite the acid threat posed by cell metabolism of foodstuffs.

1. Role of the kidney in acid –base homeostasis

Besides the excretion of the waste products especially urea, the control of acid-base balance is the main function of the kidney. The functional unit of the kidney is the nephron. In a human kidney, there are about a million nephrons. As shown in Figure 2, the structure of the nephron consists of two major parts, glomerulus and renal tubules. The acid-base control mainly occurs in the tubule part. The renal tubules can be divided into at least 4 anatomically distinct segments. There are proximal tubule, loop of Henle, distal tubule, and collecting tubule.

For acid-base balance, the kidneys play the pivotal role by preserving plasma bicarbonate at normal concentration and excreting 50 to 100 mmol non carbonic acid each day (9, 35). This regulation occurs via three crucial processes. The first process is the reclamation of filtered bicarbonate (HCO_3^-). This occurs mainly in proximal convoluted tubule, for preventing HCO_3^- efflux into the urine. Figure 3(A) depicts the model of HCO_3^- reclamation. Hydrogen ion (H^+), which secreted into the tubular urine via Na^+/H^+ exchanger combine with bicarbonate ion that, has been filtered by the glomeruli. This leads to formation of carbonic acid in the urine. The dehydration of this acid to CO_2 rapidly diffuses into the tubule cell. Within the cell, H^+ ion and HCO_3^- are generated from CO_2 and water. The H^+ ion is actively transported into the lumen, while HCO_3^- exits the basolateral membrane. The net result is the removal of HCO_3^- from the urinary fluid and the additional of HCO_3^- to the blood.

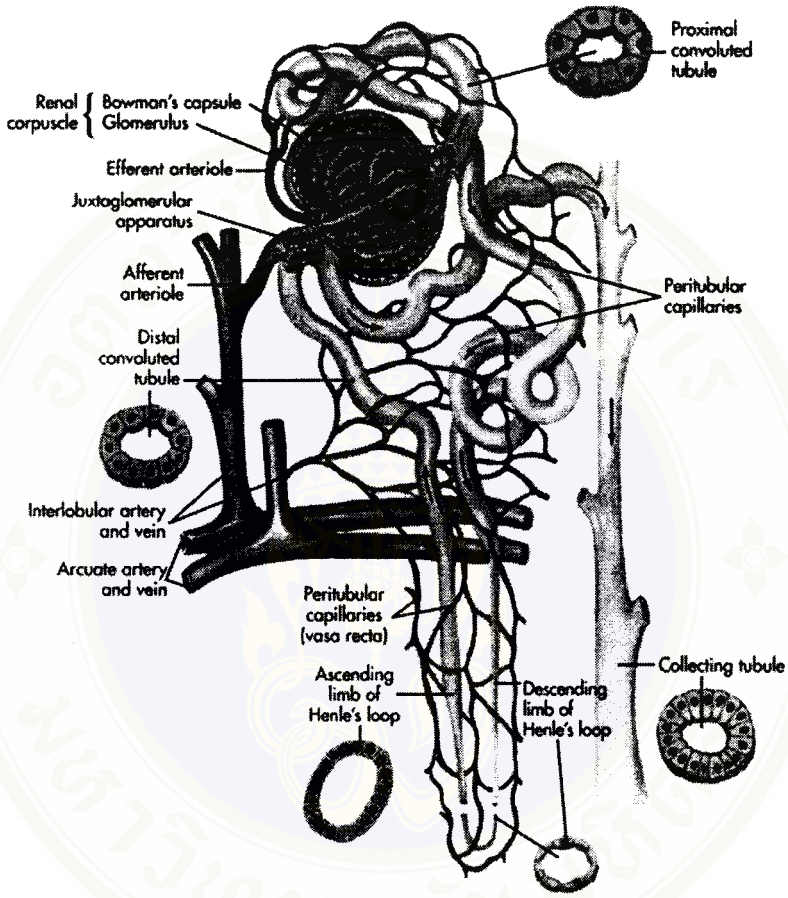

Figure 2 The anatomy of nephron (34).

The structure of nephron, functional unit of the kidney, consists of renal corpuscle and its tubule. The renal tubule can be divided into 4 parts that are proximal tubule, loop of Henle, distal tubule, and collecting tubule.

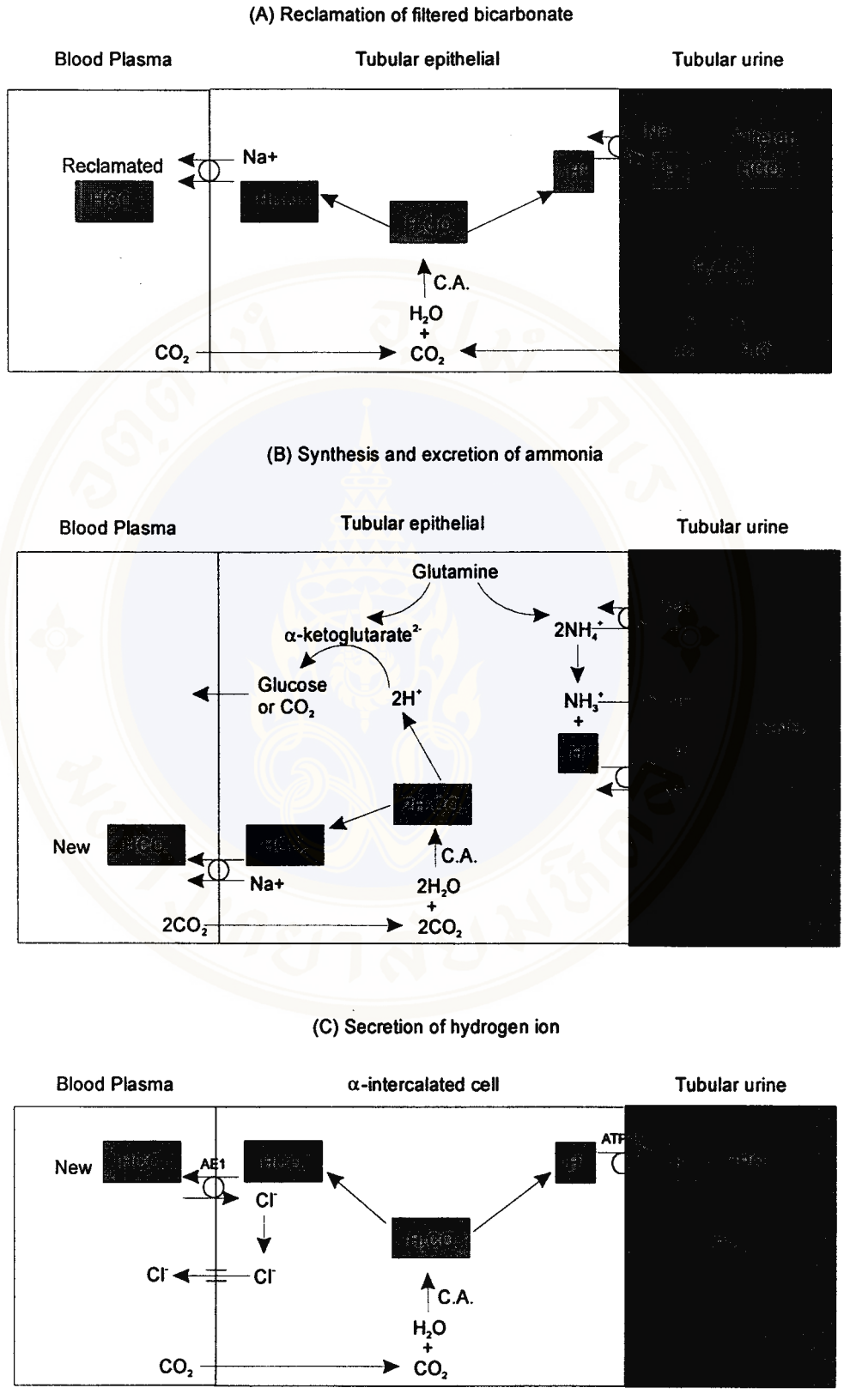

Figure 3. Schematic representation of the three processes involved in renal acid-base balance.

The second process is the synthesis and excretion of ammonia. Figure 3(B) summarizes the role of ammonia in urinary acidification. The major part of excreted ammonia is synthesized in the renal proximal tubule cells by the metabolism of glutamine. At the physiological pH, two ammonium (NH_4^+) ions and divalent anion α-ketoglutarate are the major products of glutamine metabolism. Each ammonium ion yields one molecule of free base ammonia (NH_3) and one H^+ ions. Ammonia is secreted into the urine by two metabolisms. First, in the proximal tubule, the Na^+/H^+ exchanger actively secretes ammonia. In addition, NH_3 also diffuses through cell membranes into the urine and combines with a secreted hydrogen ion to form an ammonium ion. In the cell, hydration of CO_2 produces H^+ and HCO_3^- ions. These H^+ ions are consumed when α-ketoglutarate is metabolized to form glucose or CO_2. The HCO_3^- ions are reabsorbed together with sodium ions. For each H^+ ion excreted in the urine as ammonia (ammonium ion), an equivalent quantity of "new bicarbonate" serves to restore the bicarbonate lost in the blood.

The last process is the secretion of H^+ ion. Hydrogen ion secretion mainly occurs in the distal and collecting tubules that consist of at least two cell types, principal cells and intercalated cells which are further divided into type A (α) and type B (β). The α-intercalated cells secrete H^+ ions through a luminal proton or H^+-ATPase pump; bicarbonate then exits the cell through a basolateral Cl^-/HCO_3^- exchanger (anion exchanger 1 or AE1). The β-intercalated cells secrete bicarbonate. They resemble the α-intercalated cells except the Cl^-/HCO_3^- exchanger and proton pumps are reversed in polarity.

The α-intercalated cells play the most important role in H^+ ions secretion. The mechanism of acid secretion in this cell type is shown in Figure 3(C). The intracellular CO_2, which enters from the blood, is changed to carbonic acid by carbonic anhydrase. This carbonic acid dissociates into hydrogen and bicarbonate ions by none-enzymatic process. The H^+ ion is secreted into the tubular lumen, where it is buffered phosphate or ammonia in the urine, by the luminal H^+-ATPase. The bicarbonate ion is transported to the blood in exchange for chloride by AE1, and the chloride ion that has moved into the cell leaves through chloride selective channel.

If the kidney tubules fail to reabsorb filtered bicarbonate or have an impaired ability to secrete H^+ ion, this leads to a type of metabolic acidosis called renal tubular acidosis (36).

2. Renal tubular acidosis (RTA)

Renal tubular acidosis is a group of disorders that have renal acidification defect in the presence of well-preserved glomerular function (glomerular filtration rate >20 ml/min). The consistent findings of RTA are a normal anion gap, hyperchloremic metabolic acidosis with hypokalemia, normokalemia, or hyperkalemia depending on the type of RTA (8, 35, 37, 38).

Traditional classification of RTA is based on which nephron segment is thought to have an abnormal function (38). This classification is shown in Table 1 (7).

Table 1 Traditional classification of RTA.

Type	
I	Distal or classic RTA (hypokalemic type)
II	Proximal RTA
III	Distal RTA with bicarbonate wasting
IV	Type IV RTA (hyperkalemic type)
Other	Incomplete RTA

The original type III RTA was considered to be either or severe forms of type I RTA or mixed disorders of types I and II. Now, this type is no longer used in classification. Therefore, the most common 3 types are a distal form (dRTA or type I), a proximal form (pRTA or type II) and a hyperkalemic form associated with hypoaldosteronism or aldosterone resistance (type IV). Some authors suggested that the term type IV RTA should be used to refer to only one of mechanisms, namely hypoaldosteronism or aldosterone resistance. However, some have used the term type IV RTA for all hyperkalemic forms of RTA, including voltage defects and combined defects as occurs after kidney obstruction. Table 2 (8, 39) summarizes the biochemical, clinical, and diagnostic features of each class of RTA.

Table 2 Guide to the differential diagnosis of renal tubular acidosis.

Finding	Type of RTA		
	Type II (Proximal RTA)	**Type I (Classic RTA)**	**Type IV (Hyperkalemic dRTA)**
Plasma Cl^-	High	High	High
Plasma K^+	Low	Low	High
Aminoaciduria and/ or Phosphaturia	Present	Absent	Absent
Osteomalacia	Present	Present	Absent
Nephrolithiasis and/ or Nephrocalcinosis	Absent	Present	Absent
Citrate excretion	Normal	Low	Normal
Fractional HCO_3^- excretion	>15%	<5%	<5%
Urine pH with acidosis	<5.5	>5.5	<5.5

Besides the above classifications, Kamel *et al* (38) proposed an alternative classification based on pathophysiology and the components of net acid excretion (NAE) that is abnormal. They also suggested expanding the definition of the NAE that should include a term that describes the renal handling of metabolizable organic anions because their loss in the urine represents the loss of HCO_3^-. Hence, their revised classification of renal acidosis includes three categories: low excretion of NH_4^+, excessive excretion of HCO_3^-, and excessive excretion of metabolizable organic anions (potential HCO_3^-) as shown in Equation 1 and Table 3 (38). It was claimed that this alternative classification not only provide new insights into the

pathophysiology of the disorders, but also permit more precise molecular identification of suspected underlying lesions.

Equation 1

Net acid excretion (NAE) = $(NH_4^+ + H_2PO_4^-)-(HCO_3^- + \text{Potential } HCO_3^-)$

Table 3 Classification of RTA based on formation of net acid excretion.

Type of disorder
1. Low rate of NH_4^+ excretion
i) Low NH_3 availability
Low production of NH_3
Usually low GFR, hyperkalemia, alkaline proximal ICF pH, and high delivery of fat-derived fuels to the kidney (e.g., TPN)
Low NH_3 delivery to the medullary interstitium
Usually medullary interstitial diseases
ii) High distal nephron luminal pH
Low distal nephron H^+ secretion
H^+ ATPase or K^+/H^+ ATPase pump failure, voltage defect, H^+ backleak
Excessive delivery of HCO_3^- to the distal nephron (low proximal H^+ secretion)
2. Excessive excretion of HCO_3^-
Defect in proximal or distal H^+ secretion
3. Excessive excretion of potential HCO_3^- (metabolizable organic anions)
For example: excessive ketonuria,

2.1 Proximal renal tubular acidosis (Type II RTA)

Since the proximal tubule is the major site of bicarbonate reabsorption, a defect at this site resulting in massive bicarbonaturia (35, 39). Proximal RTA (pRTA) can be divided into two categories, one in which acidification is only defective function and one in which there is a more generalized proximal tubule dysfunction. Proximal RTA resulted from an isolated defect of acidification in the proximal tubule is rare. Such a disorder would involve a selective defect in the Na^+/H^+ antiporter, the H^+-ATPase, or the $Na^+/ HCO_3^-/ CO_3^{2-}$ symporter. The majority of cases of proximal RTA fit into the category of generalized proximal tubule dysfunction. Patients with this generalized abnormality, the Fanconi syndrome, usually have glycosuria, aminoaciduria, citraturia, and phosphaturia. Numerous investigators have noted an association between vitamin D deficiency and a generalized Fanconi syndrome (8, 40). Another model for isolated proximal tubular acidosis is inherited carbonic anhydrase (CA) deficiency. As already discussed, CA II is present in the cytoplasm of renal cells and, thus, its deficiency occurring associates with an acidification defect. However, for most the pathophysiology is as yet unclear (10, 40).

Furthermore, it has been shown that patients with pRTA also have an impaired ammonia production within the proximal tubule cells (9, 10). The precise mechanism underlying the observed reduction in proximal acidification in pRTA is not known (39). The diagnosis of pRTA is based on the demonstration of a chronic hyperchloremic metabolic acidosis (HCMA) frequently associated with an acid urine pH ($\leq$ 5.5). The fractional excretion of bicarbonate is higher than 15 percent at

normal plasma bicarbonate concentration. Hypokalemic is common. Bone disease, which commonly accompanies this disorder, is expressed as rickets in children and osteopenia in adult (8, 39). The goal of therapy in pRTA is to maintain a near-normal serum bicarbonate concentration while avoiding potassium deficiency. Concomitant administration of thiazide diuretics to reduce intravascular volume and secondarily to reduce the filtered load of bicarbonate is often beneficial (8).

2.2 Distal renal tubular acidosis (Type I RTA)

The distal renal tubular acidosis (dRTA), formerly known as classic or type I RTA, is more common than others type of RTA. It is a clinical syndrome of hypokalemic hyperchloremic metabolic acidosis due to impairment in distal nephron acidification that is manifested by an inability to lower urine pH in the presence of metabolic acidosis. This syndrome was originally described in infants and children and later in adults in whom osteomalacia was a prominent finding. This disorder is also associated in some patients with nephrocalcinosis, nephrolithiasis, and osteomalacia (in the adult form) or rickets (in the infant and children form) (39). The striking feature of dRTA is a urine pH above 5.5 during acidosis, which distinguishes this disorder from other forms of RTA (40). Because chronic metabolic acidosis also decreases renal production of citrates, the resulting hypocitraturia in combination with hypercalciuria creates an environment favorable for urinary stone formation and nephrocalcinosis. Nephrocalcinosis appears to be a reliable marker of dRTA because it does not occur in other type of RTA (40). Patients with dRTA frequently present with a history of lethargy, fatigue, bone pain, polyuria, polydipsia, and sometimes

with nephrocalcinosis and nephrolithiasis. In infants and children, failure to thrive and growth retardation are common presenting complains. Adult patients may occasionally present with profound muscle weakness, acute respiratory failure, and cardiac arrhythimias in association with life-threatening hypokalemia. Defective urinary concentrating ability is commonly observed (39). The syndrome of dRTA maybe either hereditary or acquired and maybe primary or associated with a systemic illness (35). Both autosomal dominant and autosomal recessive patterns have been observed in kindreds with primary dRTA. Some patients with autosomal dominant dRTA remain asymptomatic until adolescence or adulthood, whereas others, and those with recessive disease, may be severely affected in infancy. Many patients with recessive dRTA also have sensorineural deafness, which is confined to a subset of patients with dRTA (21, 22). dRTA may also occur sporadically in association with a number of systemic autoimmune disorders, metabolic diseases, cirrhosis and in renal transplant recipients. In addition, amphotericin B and toluene poisoning have been reported to induce a dRTA-like syndrome. It can also be associated with genetic disorder such as elliptocytosis and carbonic anhydrase deficiency. The causes and conditions associated with dRTA are shown in Table 4 (39).

Untreated dRTA produces growth retardation that is responsive to alkali therapy. Correction of the acidosis by alkali administration leads to correction of hypokalemia, sodium depletion, and hypercalciuria, and also results in an increase in citrate excretion. Progressions of nephrocalcinosis and nephrolithiasis are usually arrested. Restoration of normal growth and prevention of nephrocalcinosis are the major goals of therapy (8).

Table 4 Causes and conditions associated with dRTA.

Hereditary
Family
Genetic
Elliptocytosis
Ehless-Danlos syndrome
Carbonic anhydrase B deficiency
Marfan's syndrome
Wilson's disease
Nephrocalcinosis
Hypervitaminosis D
Chronic hyperparathyroidism
Idiopathic hypercalciuria
Hypergamma globulinemic purpura
Sjögren's syndrome
Amyloidosis
Multiple myeloma
Renal transplant rejection
Cryoglobulinemia
Cirrhosis
Medullary sponge kidney
Toluene intoxication
Amphotericin B therapy
Hyperthyroidism

2.3 Hyperkalemic dRTA (Type IV)

Hyperkalemic dRTA is a unique form of RTA characterized by hyperkalemia and hyperchloremic metabolic acidosis. It results from impaired renal potassium and net acid excretion. This syndrome occurs most often in adult patients but has also been described in children. More often than not it is associated with some degree of chronic renal insufficiency. Renal hyperkalemia in this disorders is out of proportion to that expected for the degree of renal insufficiency, which indicates an impairment in renal tubular potassium secretion. Hyperkalemic dRTA comprises a heterogeneous group of disorders of diverse pathophysiologic origins. Basically, patients with this syndrome can be divided into two broad categories. Those with mineralocorticoid deficiency and those with normal mineralocorticoid reserve. In those cases associated with mineralocorticoid deficiency, primarily manifested as hypoaldosteronism, both hyporeninemia and subnormal renin secretion rates have been reported. However, normo- or hypoaldosteronism has also been observed. In contrast to patients with type I RTA, patients with type IV RTA secondary to hypoaldosteronism maintain the ability to maximally lower urine pH in the presence of systemic acidosis. Patients with type IV RTA present with hyperkalemia and metabolic acidosis of varying severely, depending in part upon dietary potassium intake. Most patients with type IV RTA have diabetic nephropathy as an underlying disease. The underlying disorder may also influence the degree of hyperkalemia (39). Patients with hyporeninemic hypoaldosteronism and chronic renal insufficiency may require cation exchange resins, alkali therapy, and a loop diuretic to enhance renal potassium and salt excretion (8).

2.4 Others type

2.4.1 Incomplete RTA

The syndrome of incomplete RTA refers to a condition wherein an ability to maximally acidify the urine during ammonium chloride loading occurs in the absence of systemic metabolic acidosis. A number of disease-states have been associated with acidification defects determined by ammonium chloride loading and by the infusion of nonreabsorbable Na^+ salts. Many patients with incomplete RTA present with nephrocalcinosis or nephrolithiasis and are incidentally discovered to have an abnormally high urine pH. Furthermore, several patients with this defect have been family members of patients with a complete form of distal type I RTA. Some of these patients manifest mild degree of systemic metabolic acidosis, although most of them have normal plasma bicarbonate concentrations. In contrast to patients with complete RTA, patients who have incomplete RTA show significant reduction in urine pH when sodium sulfate is infused (39).

2.4.2 dRTA with nerve deafness

This is a variant of dRTA associated with deafness, which many occur at birth or late in childhood (41). It has speculated that children with nerve deafness may suffer from a more severe type of dRTA. It is well- known and has been showed that deafness was present in familial case with autosomal recessive dRTA. There are also numerous sporadic reports worldwide (16). This syndrome has been found to associate with inactive mutant form of red cell carbonic anhydrase II (41). However, a recent study has shown that mutations in the gene encoding B1 subunit of H^+-

ATPase (*ATP6B1*) cause dRTA with sensorineural deafness in many kindreds (22). They also demonstrated expression of ATP6B1 in cochlea and endolymphatic sac, where endolymph pH is control.

3. Endemic dRTA in northeastern Thailand

As previously described, most of the literatures on dRTA reported either sporadic or familial cases or small groups of patients with particular clinical and biochemical manifestation. A large series of endemic cases confined to a particular geographical area has been reported in 1990 by Nilwarangkur *et al* (1). They are the first group who studied of a large number of patients with primary classical dRTA, in a homogeneous (Lao-Thai) population, endemic within a particular geographical region. This group of patients (103 patients) was admitted in two provincial hospitals in northeastern Thailand because of hypokalemic paralysis and muscle weakness. They found that the age distribution of the patients peaked at the second to fourth decades, with a female preponderance (F: M= 3.3: 1). High incidences of nephrocalcinosis (27.2%) and osteomalacia (23.3%) have also been described. Moreover, high incidence of familial association was found in some patients. The dRTA clustered within the northeastern region of Thailand is called endemic distal renal tubular acidosis (EdRTA). Its etiology is still unknown. In the same year, this group further reported the composition of the urine in the indigenous population in the northeastern area and compare their values with data obtained from a group of age matched adults, living in Bangkok (4). They found that daily urinary sodium, potassium, chloride and phosphate of the villagers were significantly lower than those

of Bangkokians. The villagers had significantly lower amounts of Na^+ and relatively higher urinary calcium. These data combined with their previously study showing the low values of urinary citrate in the villagers in the same areas, strongly indicate that the indigenous population is at high risk in developing urolithiasis. The causes for these electrolyte abnormalities are still unknown. This group suggested that low contents of major electrolytes in their diets might play an important role. Low phosphate output indicates low protein diets. Other factors such as excessive loss through hot weather and /or strenuous activities in exposed fields, renal tubular defect, and other environmental factors may all contribute to the above abnormalities.

A few years later, Tungsanga *et al* studied renal acidification in 29 renal stone patients who were living in rural Northeast of Thailand (5). Hypokalemia, hypokaliuria and hypocitraturia were found in 10%, 83% and 93% of patients, respectively. An abnormal response to acid loading was found in only 1 patient. Thus, hypokaliuria and hypocitraturia in these renal stone subjects were infrequently due to dRTA. This suggests that perhaps potassium depletion might be contributing factor in the metabolic abnormalities. However, the dRTA patients also have been reported with gastric hypoacidity (42). It was suggested that they might have an abnormality in H^+/K^+-ATPase activity. There have been published reports on the high vanadium, an inhibitor of H^+/K^+-ATPase, contents of the soil and water in the Northeast of Thailand (12, 43). In addition, the local population has a higher than normal concentration of vanadium in urine and tissue (6, 12, 43). In this area, the dRTA affects not only humans but also water buffaloes, indicating it to be an environmental inhibitor of the H^+/K^+-ATPase pump (43). This observation is very

appealing, but further work may be required to support this hypothesis. Recently, it has shown that vanadate had no effect on either ammonium excretion or total net acid excretion, nor did it lead to distal RTA (44).

In 1996, Nimmannit *et al* reported the result of survey study on EdRTA in 5 villages (total population of 3,606) within the Northeast of Thailand. The following findings were made. First, the urinary citrate excretion of the inhabitants in the area was low, 30% of the population having urinary citrate less than 0.3 mmol/l (range in people from Bangkok 0.8-1.9 mmol/l). Second, a high prevalence (2.8%) of renal acidification defect, failure to lower the urine pH below 5.5 after short acid-loading test, most without systemic metabolic acidosis. Twenty-five of the 85 EdRTA subjects had serum potassium of 3.5 mEq/l or lower. Third, the prevalence of both EdRTA and renal stone correlate inversely with the socioeconomic status, i.e. higher in poorer villages. The latter observation strongly indicated that environmental factors play major role in their pathogenesis (3). In the same year, this group examined environmental factors that are known to be associated with RTA in the EdRTA patients and their first-degree relatives. The focus of this study was on potassium and renal medullary function because of obvious hypokalemia and its known associated with a concentrating defect and distal RTA. They have demonstrated a spectrum of EdRTA in the villagers of an area known to have a high prevalence of EdRTA and potassium deficiency (2). Combined with the results from duplicated meal survey in 5 villages within this area presented that the potassium content in the diets of the indigenous population was lower than the recommended dietary allowance. These findings coupled with the high possibility of excess loss of

potassium through sweating because of the persistently hot climate, indicate that chronic potassium deficiency exists in this population (11). They, therefore, postulated that potassium deficiency might be the important pathogenetic factor of EdRTA in the northeastern Thailand.

The pathogenesis of EdRTA is still unclear. Although there are evidences that support environmental factor as a cause of EdRTA, the presences of disease in members of the same families and hereditary form of dRTA indicate that genetics factor may play role as the cause of this disease.

4. Molecular basis of dRTA

Studies of distal renal tubular acidification disorders have traditionally relied on physiologic tests and maneuvers, which provided indirect evidence and were mostly descriptive (14, 16). In the past several years, significant advances have been made in understanding on the molecular and cellular mechanisms of H^+/HCO_3^- absorption and secretion in distal nephron. Several concepts on the cellular and molecular basis of distal acidification defects have been reviewed by Arruda and Cowell (14), Bastani and Gluck (16), and Sabatini (45). However, the pathogenesis of the dRTA syndromes has not yet been completely elucidated. The suggested concepts include defects in any one of several transporters of the α-intercalated cell required for transepithelial acid and bicarbonate reabsorption. These components are multiple gene products that comprise the H^+-ATPase, the H^+/K^+-ATPase, the cytoplasmic carbonic anhydrase II (CA II), and the Cl^-/HCO_3^- exchanger or anion exchanger 1 (AE 1).

4.1 H^+-ATPase

An electrogenic hydrogen adenosine triphosphatase (H^+-ATPase) is one of the two major proton pumps in distal nephron. It is located on the apical surface of the α-intercalated, acid-secreting cell. It was first discovered as the primary transporter responsible for urinary acidification. The H^+-ATPase is currently believed to be the ATPase chiefly responsible for regulated proton secretion in the distal nephron (16). If the H^+-ATPase does not pump protons effectively, distal acid excretion will fail to meet metabolic demand, and metabolic acid will ensure (45). There are at least 2 evidences showed that the H^+-ATPase might be involved urinary acidification of dRTA patients. Firstly, staining of renal biopsy material by using antibody to the H^+-ATPase in three dRTA patients with primary Sjögren's syndrome. In two of them, staining to a subunit of the H^+-ATPase showed complete absence of the enzyme throughout the collecting duct, although electron microscopy showed intercalated cells to be present (16, 45). Secondly, the other two patients with lupus nephritis and dRTA, the H^+-ATPase was present in the collecting duct but it was essentially nonfunctional. Thus, abnormal function or distribution of H^+-ATPase in the distal nephron appears to result in a defect to normal urinary acidification (45). In addition, the recent report demonstrated that mutation in *ATP6B1* gene, encoding the B1 subunit of the H^+-ATPase, cause autosomal recessive dRTA with sensorineural deafness in many kindreds (22).

4.2 H^+/K^+-ATPase

An electroneutral proton-potassium-exchanging ATPase (H^+/K^+-ATPase) was first identified and isolated from gastric parietal cells (46). Its distribution has been determined immunocytochemically using antibodies to the gastric isoform. It is also located in the apical membrane of α-intercalated cell, with a polarized distribution similar to the H^+-ATPase (16). It has also been suggested that hypokalemia and dRTA could arise from a defect in the renal H^+/K^+-ATPase (47). If H^+/K^+-ATPase pump fails, then both the acid retention and the potassium wasting are explained at once. The data that directly describes the biochemistry of the pump lesion in case of dRTA is not available. Because there is no appropriate antibody to H^+/K^+-ATPase, no data is obtained on this enzyme. However, there are clinical observations suggest that the renal H^+/K^+-ATPase pump is defective in dRTA (47). It has been proposed that the possible cause of endemic dRTA with hypokalemia in northeastern Thailand may be a generalized H^+/K^+-ATPase defect from vanadate toxicity. There are evidences suggest that well water and soil in this area were found to rich in vanadate, an inhibitor of H^+/K^+-ATPase, and high concentrations of vanadate have also been found in tissues and urine from affected individuals (12, 43). In experimental models, rats chronically treated with vanadate developed hypokalemic dRTA (48). Intraperitoneal administration results in high renal vanadate concentrations, and the activity of the H^+/K^+-ATPase is marked depressed (47). Since Na^+/ K^+-ATPase is also inhibited by vanadate, it is not clear what causes dRTA. Furthermore, no measurements of the activities of these pumps have been made in the subjects from Thailand (45).

4.3 Carbonic anhydrase II (CA II)

Carbonic anhydrase in the cytosol of the intercalated cell is responsible for catalyzing the condensation of intracellular OH^-, generating luminal H^+ secretion, with CO_2 to form bicarbonate, which exits the cell through the basolateral membrane. H^+ secretion is dependent on adequate carbonic anhydrase activity because this enzyme is required for proximal bicarbonate reabsorption as well as distal acidification. Reduction or absence of cytosolic carbonic anhydrase II (CA II), leading to increased bicarbonate secretion, could also impair distal urinary acidification. Type II carbonic anhydrase deficiency is an autosomal recessive disorder producing a distinctive syndrome of RTA, osteopetrosis, cerebral calcification and mental retardation (16). Patients with CA II deficiency may have any of an array of distal, proximal, or mixed proximal and distal causes of RTA, but they show no consistent pattern of acidification defects (14).

4.4 Cl^-/HCO_3^- exchanger or anion exchanger 1(AE 1)

The generated bicarbonate, inside α-intercalated cells as a result of apical proton secretion, exits from the cell in exchange for Cl^- through an anion exchanger in the basolateral membrane. This Cl^-/HCO_3^- exchanger, previously known as band 3 protein in erythrocyte, is called anion exchanger 1 (AE1). It is a member of electroneutral anion exchanger family, which consists of at least three distinct proteins: AE1, AE2 and AE3. AE1 is expressed in two types of cells, red blood cells and α-intercalated cells in distal and collecting tubule of kidney. Changes in the kinetic, cellular content, and distribution of kidney AE1 all contribute to the renal

response to acid-base disorders (16). Recently, there are many reports provide evidences that abnormalities in AE1 are the cause of the familial form of dRTA (28-33). In two reports, AE1 mutations were found to be associated with both red cell abnormalities and dRTA (28, 33). Both autosomal dominant and autosomal recessive dRTAs have been reported to be associated with AE1 mutations.

5. Molecular and cellular biology of human anion exchanger 1 (AE1)

5.1 Organization of *AE1* gene

The human *AE1* gene locates on chromosome 17, between 17q21 and qter (49, 50). Linkage analysis using a *Pst*I polymorphism has shown that *AE1* is closely linked to the nerve growth factor receptor (NGFR) gene, which narrows the localization to 17q21-q22 (51, 52). The entire human *AE1* gene has been cloned and sequenced by two groups (25, 53). The human *AE1* encompasses approximately 20 kb and contains 20 exon and 19 intron. Extensive similarity between the human and mouse *AE1* genes were observed (25). No TATA or CCAAT boxes are present in the upstream region of the *AE1* gene. However, the consensus sequences for the binding sites of variety of transcription factors are contained in this region. These transcription factors consensus binding sites (Figure 4) are Ap1 (activator protein 1), Ap2 (activator protein 2), CACCC boxes, GATA (erythroid factor 1, eryF1], E-boxes (53). Downstream of a cluster of these binding sequences, the human *AE1* contains TATA and CCAAT boxes in intron 3. There are two initiation codons downstream of the TATA box that are inframe with the human *AE1* coding sequence. One is located in intron 3 and the other is located in exon 5. The ATG in both sites, intron 3 and

exon 5, are good consensus translation initiation sequences. A diagram of the human *AE1* gene is shown in Figure 5. The exon designated as K1 is nonerythoid and contributes to the first exon of the truncated AE1 transcript found in α- intercalated cells of kidney. Approximately 30 bp upstream of this exon is a consensus TATA box. With the exception of exon 20, which is 2153 bp in length, exon sizes are relatively small and range from 62 to 254 bp in length (Table 5). All exon-intron boundaries conform to the consensus found in other human genes. In the 3′ acceptor sequence (consensus: $Y_n$agG), ag is invariably present, preceded by a pyrimidine-rich tract, while, gt is invariably present in all 5′ donor site (consensus: Aggtragt). In addition, the downstream end of exon 20 (defined as the RNA cleavage site or the poly(A) addition site was identified by cloning the very 3′ end of the cDNA. The total length of the 3′ non-coding region is 2075 bp. A consensus polyadenylation signal (AATAAA) is located 20 nucleotide upstream of the RNA cleavage site.

Nine *Alu* repeat elements are found within the body of the human *AE1* gene. Eight of these are within intron sequences and one is in the 3′ non-coding region of exon 20. Like other primate *Alu* sequences, the human *AE1* gene repeats are ~300 bp in length and consist of related left and right subunits that are separated by an adenine- rich linker sequence (AAAAATACAAAAA), and each repeat is followed by a poly(A) or A-rich sequence (53).

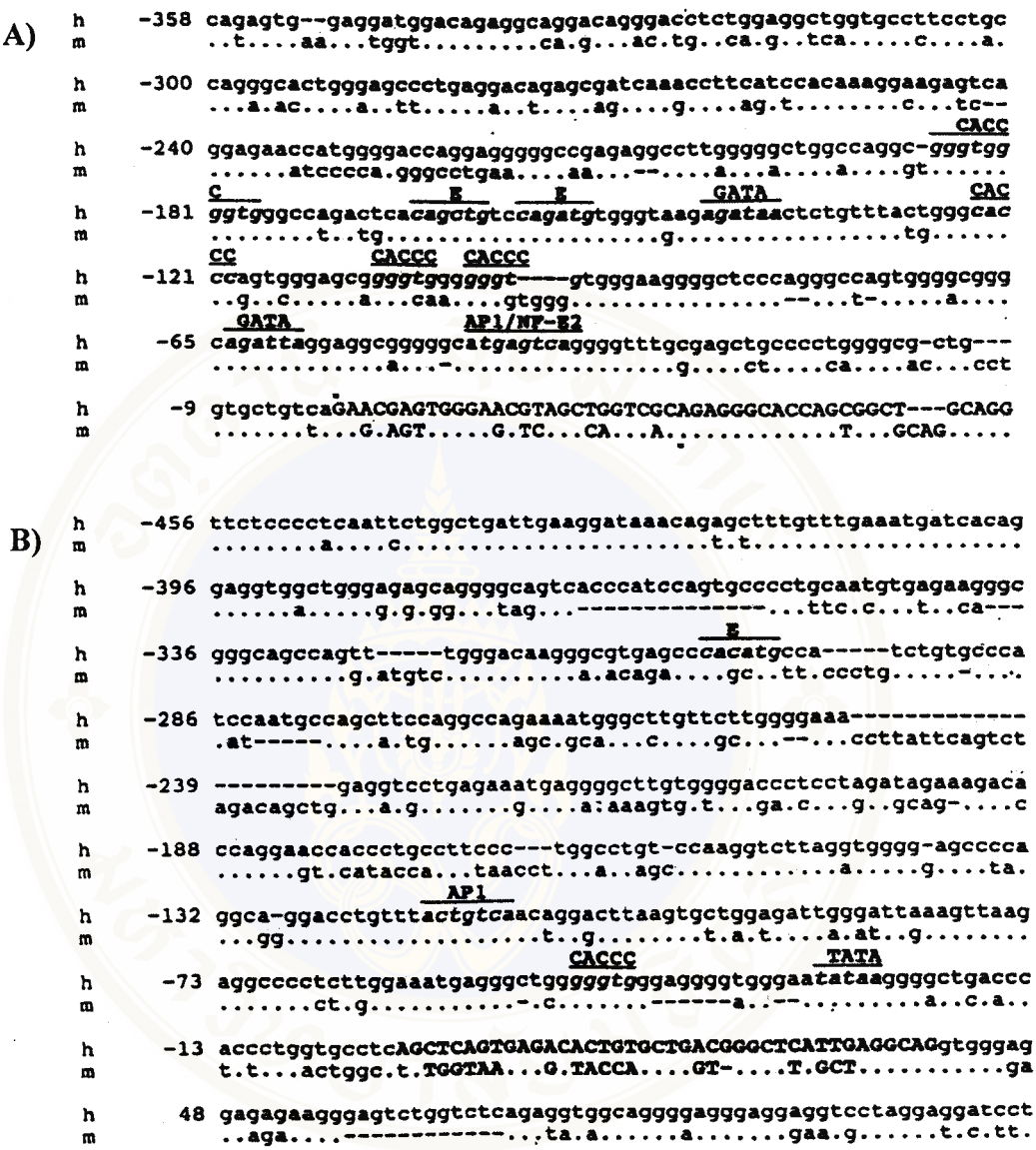

Figure 4 Alignment of promoter regions of human and mouse *AE1* sequences (53).

Potential E-box, CACCC, GATA, and AP1/NF-E2 sequences that are conserved between the human and mouse genes are labeled. Identical sequences are indicated by a dot and insertions by a dash. A) An alignment of ~358 bp of upstream sequence of *AE1*. The upstream sequence is shown in lowercase letters, while exon 1 sequence is shown in uppercase. B) Aligned sequences of the internal potential promoter region of *AE1* that contribute to the 5′ end of the kidney truncated AE1 transcript (exon K1). Exon K1 sequence is shown in uppercase letter. A potential TATA box is present ~30 bp upstream of this sequence.

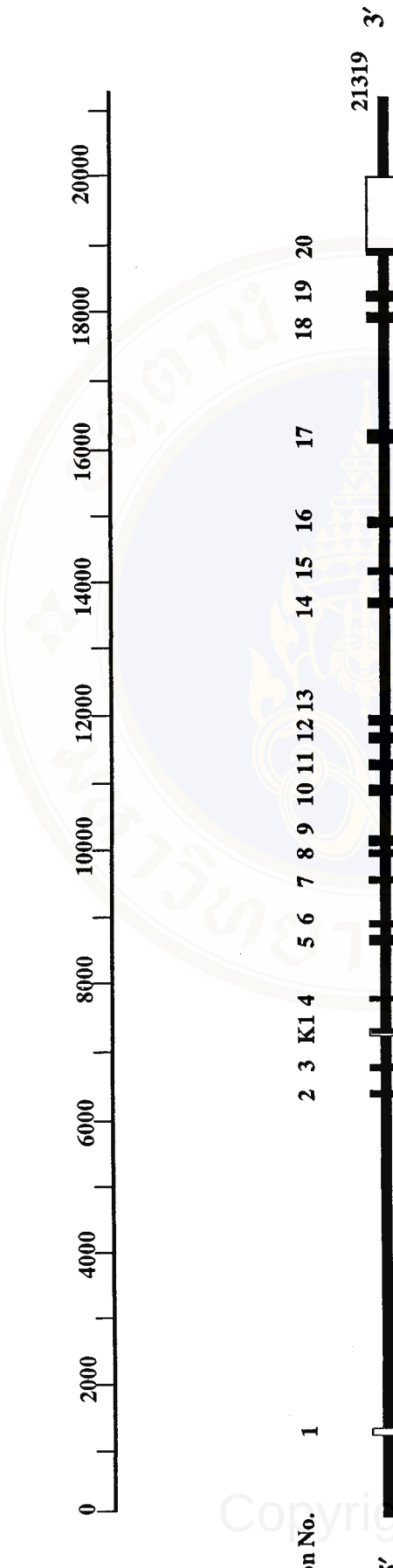

Figure 5 Diagram of the human *AE1* gene.

The positions of exon 1 through 20 are indicated; coding exons are represented by solid boxes and the non-coding exons or regions by open boxes. The locations of erythroid (ATG$_E$) and kidney (ATG$_K$) translation start sites and of exon K1 that forms the 5′ end of kidney *AE1* mRNA transcript are also indicated.

Table 5 Exon-intron size of human *AE1* gene (53).

Exon No.	Exon Size (bp)	Intron No.	Intron Size (bp)
1	~86[a]	1	5123
2	83	2	125
3	91	3	1000
4	62	4	767
5	181	5	96
6	136	6	471
7	124	7	229
8	85	8	152
9	182	9	538
10	211	10	227
11	195	11	180
12	149	12	114
13	174	13	1501
14	90	14	380
15	90	15	544
16	167	16	1127
17	254	17	1519
18	170	18	86
19	174	19	620
20	2153		

[a] The approximate size of exon 1 of the human *AE1* estimated by alignment with the mouse and rat *AE1* sequences.

5.2 AE1 mRNA transcript

A composite human *AE1* cDNA sequence assembled from the published cDNA sequence (50, 54) and the complete 3′ non-coding region of exon 20 (53) is predicted to be 4,959 bp in length (53). Schofield et al also reported that the human *AE1* cDNA sequence contains 4,906 nucleotides (nts), excluding the poly(A) tail, 4,756 nts from ATG codon to the polyadenylation site and 150 nts of 5′ non-coding

region (25). Both are compatible with the approximate 4.7 kb *AE1*-mRNA observed in northern blots of human reticulocyte mRNAs (25, 53). In addition to erythrocyte, the human *AE1* is expressed in the α-intercalated (acid–secreting) cells of the distal tubule of kidney. Two potential promoter regions within the human *AE1* gene are located, transcriptions initiating from different promoters give rise to different transcripts found in erythroid cells and in the kidney. The kidney transcript lacks exon 1 through exon 3 of erythroid transcript (25). Kollert-Jons *et al* (55) demonstrated that the sequence containing the codons for Met-1 and Met-33 in erythroid mRNA is missing in the kidney transcript, whereas the sequence coding for Met-66 is present. Moreover, DNA sequence data derived from cloning the 5′ end of the human kidney *AE1* mRNA clearly showed that the 5′ untranslated region comprises a part of intron 3, the complete exon 4, and part of the exon 5 (55) (Figure 7). By this splicing pattern, the ATG codon encoding Met-66 becomes the site of translation initiation, which it is part of the consensus sequence GTGATGGAC for translation initiation (55).

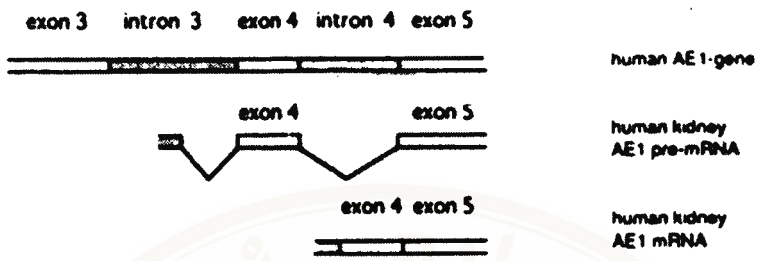

Figure 6 The splicing pattern of human kidney *AE1* mRNA (55).

The 5′ untranslated region of the human kidney *AE1* mRNA comprises a part of intron 3, the complete exon 4, and the first part of the exon 5.

5.3 Structure and function of AE1 protein

The human anion exchanger 1 (AE1) protein is a multifunctional integral membrane glycoprotein. It is expressed in erythrocytes and in the acid-secreting cells of the distal tubule of the kidney (23). In both cell types it mediates the electroneutral exchange of chloride (Cl^-) and bicarbonate (HCO_3^-) across the plasma membrane (56-58). Because of this function it is called anion exchanger 1, which is a member of anion exchanger (AE) protein family (59). The human erythroid AE1 is the most abundant protein in the human red blood cell membrane. It has a copy number of 1.2 million per cell and makes up approximately 25% by weight of the protein in the membrane (23, 60). It is a 911 amino acid glycoprotein with a single site of N-glycosylation at Asn 642 (60). In sodium dodecyl sulphate-polyacrylamide gel electrophoresis (SDS-PAGE), this protein appears as the third band so called 'band 3'

from its relative position on the SDS-PAGE (15) (Figure 7). It migrates as a diffuse band due to heterogeneity in size of the carbohydrate chain present on the molecule (51). Band 3 has a molecular weight about 95 kDa. It consists of 2 structural domains, each having distinct functions. The two domains can be physically separated by trypsin cleavage at Lys 360 (60). The amino-terminal 40 kDa domain is hydrophilic and extends into the cytoplasm. This domain acts as the membrane-binding site for several cytoplasmic proteins including hemoglobin, glycolytic enzymes such as aldolase, phosphofructokinase, and glyceraldehyde-3-phosphate dehydrogenase, and for cytoskeletal components band 4.1 and ankyrin (23, 53, 56, 60). The carboxyl-terminal 55 kDa domain is hydrophobic and is predicted to transverse the lipid bilayer and functions as an anion transporter, mediating the electroneutral exchange of chloride and bicarbonate ions. This domain is glycosylated with a single N-glycan chain at Asn 642. This N-glycan chain is heterogeneous in size on different band 3 molecules, because of variation in the number of repeating N-acetyllactosamine units present in each lactosaminoglycan chain (51). However N-glycosylation of band 3 is not essential for the transport function (60). The kidney AE1 isoform is otherwise identical to erythroid AE1 but lacks the N-terminal 65 amino acids of erythroid isoform. Therefore, it lacks the capacity to bind to the cytoskeletal proteins but still maintains the anion transport activity.

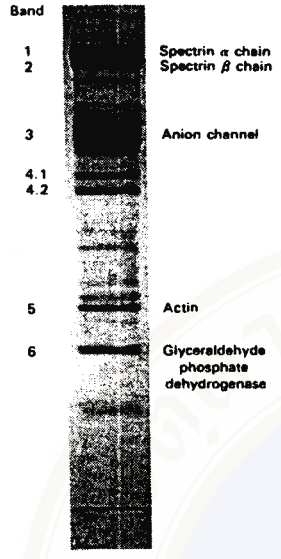

Figure 7 The pattern of AE1 protein migration in sodium dodecyl sulfate-polyacrylamide gel electrophoresis (SDS-PAGE).

AE1 migrates as a diffuse band and appears as the third band, so it is called 'band 3'. It has a molecular weight of about 95 kDa.

The topology of AE1 membrane domain is still controversial regarding the number of the membrane spanning segments (23). Previously, hydropathy analysis of the amino acid sequence combined with experimental evidence derived from covalent labeling studies with impermeant reagents, proteolysis and antibody epitope mapping have led to models for the folding of the protein which contain 14 transmembrane (TM) spans (Figure 8). This model is proposed by Reithmeier *et al* in 1993 (61). It is the current model until few years ago two new models, which have different numbers of transmembrane spans, 12 and 13 TM, were proposed (62, 63). These models differ in their detailed predictions in the C-terminal portion of the protein, especially around predicted transmembrane segments 9 and 10. Absolute determination of the topology of AE1 awaits a crystal structure of the protein (63).

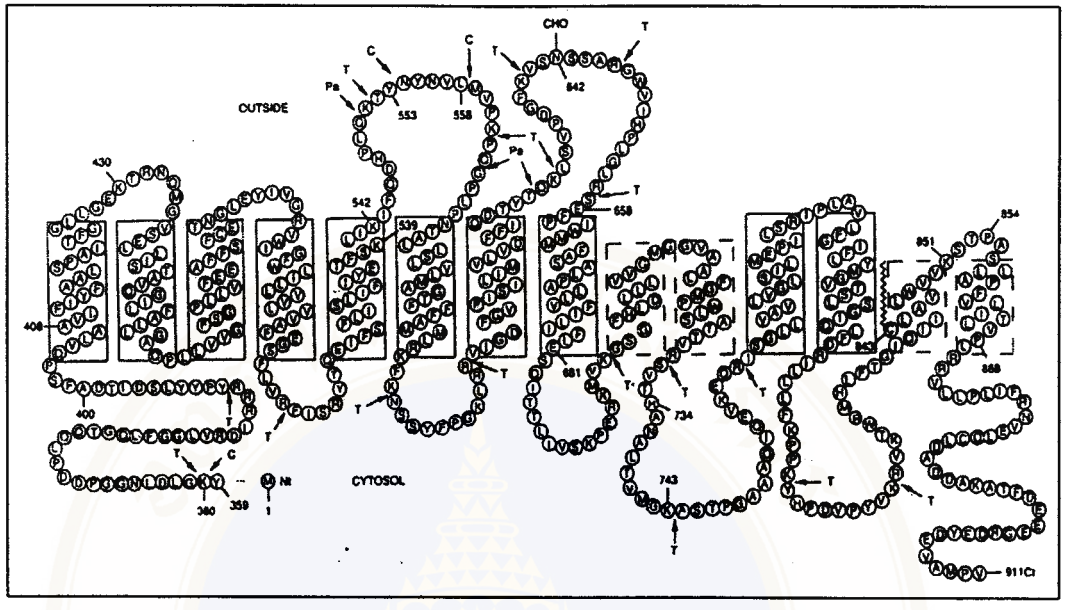

Figure 8 A model of topology of human AE1 transmembrane (TM) domain (amino acids 359-911).

The transmembrane domain of human AE1 in this model contains 14 TM spans. The amino-terminal cytosolic domain is not shown. Asn 642 is the single site of glycosylation indicated by CHO and cysteine 843 is fatty acylated. Nt, N-terminus, Ct, C-terminus, T and C denote trypsin- and chymotrypsin-sensitive sites, respectively. The membrane domain is generated by trypsin cleavage at Lys 360.

The structure of AE1, like most other polytopic membrane proteins with a high helical content, is thought to be based on a tightly packed helical bundle with the loop that connect the helical spans extending outside the membrane (64). AE1 exists in the erythrocyte membrane as a mixture of dimers, tetramers, and higher oligomers. Dimers are the predominant species with the rest composed mostly of tetramer (60). Three-dimensional structure of AE1 has been proposed (57). It is a dimer with

dimensions of ~60x110 A° and a thickness of 80 A° (Figure 9), the U-shaped structure with an opening on the top and sides like a canyon. The basal domain is 40 A° thick and probably spans the lipid bilayer. The protrusions forms the sides of converges into a depression at the center of the dimer on the top of the basal domain. This depression may represent the opening to a transport channel located at the dimer interface. Based on the available biochemical data, it is believed that the protrusions on the upper side of the basal domain are the cytosolic side of the membrane and the smooth surface on the lower side is extracytosolic (57).

Band 3 has two major functions on the red cell. The anion exchange activity of protein increases the ability of blood to carry carbondioxide from the tissues to the lungs. By allowing bicarbonate formed within the red cell by carbonic anhydrase to enter the plasma in exchange for chloride, both the cell and plasma phases can be used to carry bicarbonate (23). It is also important in the mechanical properties of the red cell and maintains the stability and integrity of the cell by anchoring the cytoskeletal proteins to the lipid bilayer. The bifunction nature of AE1 in the red cell is reflected in its domain structure that has been previously described. Besides these two important functions, AE1 is also thought to have a role in the turnover of red cells by acting as a senescence antigen for aged and damaged red cells (23). The kidney AE1, the truncated isoform which lacks the amino-terminal 65 residues of erythroid AE1, provides major exit route for bicarbonate in the exchange for chloride across the basolateral membrane of the α-intercalated cell during urinary acidification.

Figure 9 Three-dimensional structure of dimeric AE1 protein (57).

The U-shaped structure has an opening on the top. The bulky basal domain is probably embedded in the lipid bilayer, indicated by the two semi-transparent planes which are separated by 35 A°. The longest dimension of the basal domain is 110 A°. The protrusions that above the basal domain are on the cytosolic side of the membrane, forming two sides of a canyon that leads to a depression which is probably the entrance to a pore.

5.4 Mutations and polymorphisms of *AE1* gene

Many mutations and polymorphisms of *AE1* gene have been reported in the literatures. As AE1 is present on both the red cell membrane and the basolateral membrane of the kidney α-intercalated cell, *AE1* mutations may result in abnormalities of the red cell morphology due to structural or functional changes of band 3 or of the anion exchange function of the kidney α-intercalated cell.

5.4.1 *AE1* mutations associated with red blood cell abnormalities

A common *AE1* mutation is the mutation causing Southeast Asian ovalocytosis (SAO) (23, 24, 51, 65), which is a unique form of hereditary elliptocytosis widely distributed in Southeast Asia such as the South of Thailand, Malaysia, Indonesia, Papua New Guinea, and Philippines. Microscopy of blood films shows 20-50% rounded elliptocytes or 'ovalocytes', some of which have one or two transverse bars that divide the central clear space (Figure 10a). These distinctive red cells are not seen in other conditions (24). SAO is found in areas where malaria has been endemic since it is believed to afford protection against cerebral malaria in children (23). SAO red cells are also much more rigid than normal; their resistance to malarial is attributed to the change of membrane mechanical properties (51). The molecular defect of SAO has been shown to be the band 3 containing deletion of the amino acid residues 400-408 due to deletion of 27 bp in exon 11 of the *AE1* gene (66). This nine amino acids are at the boundary between the N-terminal cytoplasmic domain and the membrane domain of band 3 and the deletion of these residues disrupts the structure of the membrane domain of SAO band 3 (65). The abnormal

protein is misfolded in the membrane and does not transport anions or bind anion transport inhibitors such as 4,4'-diisothiocyanatostibene- 2, 2' disulfonic acid (DIDS) or eosin maleimide. The mutant protein also has an abnormal N-glycan chain (23). All the known individuals with SAO are heterozygous for band 3 SAO associated with the Memphis I (Lys 56→ Glu) polymorphism (23, 65). The details of this polymorphism will be described below. Although SAO occurs with high frequencies in parts of Southeast Asia, no individuals homozygous for this mutation have been observed, suggesting that the homozygosity for this mutation is lethal (23).

Hereditary spherocytosis (HS) is the most common congenital hemolytic anemia, characterized by spherocytic red cells with increased osmotic and mechanical fragility. The spherocytic shape of these cells results from loss of membrane surface area relative to intracellular volume (65). HS can be found to be associated with abnormalities in any of the red cell skeletal components, which are involved with stabilizing the lipid bilayer, including spectrin, ankyrin, band 3, and protein 4.2 (24, 65). About 20% of the cases of HS result from band 3 defects, and are often characterized by the presence of mushroom-shaped or 'pincered' erythrocytes in blood smears (Figure 10b), which are not seen in other forms of HS (24, 65). A murine model of band 3 deficiency showed that band 3 is essential for stability of membrane lipid bilayer but not for assembly of the membrane skeleton (67). A large number of band 3 mutations that give rise to HS are known. These mutations are located in both membranous and cytoplasmic domains of band 3 and are of two types. The first group result in the absence of mutant mRNA because of its instability and are mainly associated with the occurrence of premature stop codons

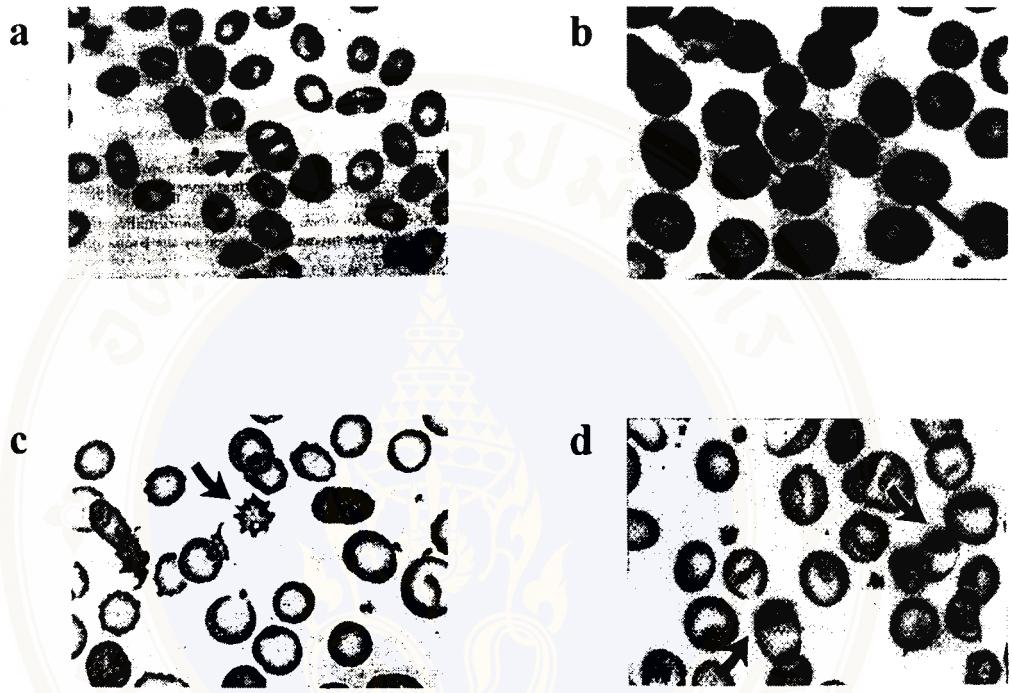

Figure 10 Abnormal red blood cell morphologies associated with *AE1* mutations.

(a) Southest Asian ovalocytosis (SAO) which red cells are oval and often contain a transverse bar, (b) hereditary spherocytosis which some red cells show mushroom-shaped or pincered morphology, (c) acanthocytosis, and (d) xerocytosis. Typical morphology for each type of the abnormality is indicated by arrow.

because of nonsense or framshift mutations. In the other group, the mRNA is present but the mutant protein is absent or decreased in the red cell membrane. These mainly comprise missense point mutations (often at highly conserved residues) and probably result in abnormal targeting to the plasma membrane or abnormal membrane insertion, causing decreased stability of the protein (23). The reported band 3 mutations associated with HS are listed in Table 6. Recently, band 3 mutations have been reviewed by Tse and Lux in 1999 (24). Many changes in the band 3 gene that result in null mutations have been identified in patients with HS. Band 3 Hodouin, Lyon, Noirterre, Osnabrück I, and Trutnov have nonsense mutations that cause mRNA instability and band 3 deficiency (68-71). Band 3 Bicètre II, Bohain, Brü ggen, Foggia, and Smichov have single nucleotide insertions in the coding region that produce frameshift mutations, whereas band 3 Evry, Hobart, NapoliI, Princeton, and Worcester have single nucleotide deletions (72, 73). Band 3 Campinas and Pribam result from splicing defects, and band 3 Prague occurs because of a 10-nucleotide duplication in the gene (74, 75). Missense mutations or short in-frame deletions have also been found in HS patients. Many mutations are located in the transmembrane domain and probably cause poor incorperation of band 3 into the membrane. In band 3 Bicètre I, Dresden, Hradec Kralove, Jablonec, Prague II, and Prague III, substitutions of highly conserved arginine residues positioned at the internal boundaries of transmembrane segments probably interfere with cotranslational insertion of band 3 into the membrane of the endoplasmic reticulum (68, 72, 76). In band 3 Benesov, Birmingham, Chur, Most, Napoli II, Okinawa, and Philadelphia, other highly conserve amino acids crucial for stabilization of band 3 within the lipid

bilayer are substituted (73, 77, 78). A 22-residue insertion in the transmembrane domain in band 3 Malino prevents incorperation of the peptide into the membrane (79), and a single amino acid deletion in the transmembrane domain is found in band 3 Osnabrück II (68). Mutations causing changes in the cytoplasmic domain of band 3 can interfere with its binding to other membrane skeleton proteins, resulting in a functional defect. In band 3 Nachod, a deletion of five amino acids from the ankyrin binding site disrupts this binding (69). An amino acid substitution in the cytoplasmic domain in band 3 Fukuoka causes defective protein 4.2 binding. A compound heterozygote carrying both band 3 Fukuoka and band 3 Okinawa has complete absence of protein 4.2 (78). Patients with band 3 Montefiore and Tuscaloosa have spherocytic hemolytic anemia with protein 4.2 deficiency (80, 81). Both of these alleles have missense mutations in the cytoplasmic domain, but symptoms are manifest in heterozygotes with band 3 Tuscaloosa and only in the homozygote with band 3 Montefiore. The reason for this difference is unclear. Band 3 Coimbra has a substitution in the putative second ectoplasmic loop of band 3 protein, causing mild HS (82). Several mutant band 3 alleles modulate the severity of the disease. Band 3 Mondega and Montefiore, which both have missense mutations in the cytoplasmic domain, aggravate the HS symtomps of band 3 Coimbra when either is co-inherited. A normally silent promoter mutation in band 3 Genas increases the clinical severity of HS in a patient with band 3 Lyon (82).

The other red cell abnormality associated with *AE1* mutation is acanthocytosis (Figure 10c). The band 3 in these cells migrated slower than the normal protein on SDS-PAGE and anion transport activity was increased due to an

increase in V_{max} compared to normal cells. This variant band 3 with increased transport activity and has since been described as band 3 high transport (HT). Band 3 HT has a single base substitution at position 2,603 (C→T) resulting in the Pro868→ Leu mutation (65). A study of the kinetics of binding of band 3 HT to different stillbene disulphonates suggested that although there was no difference in the binding of DIDS, covalent binding of H_2DIDS to band 3 HT was on order of magnitude slower than to the normal protein. This work suggests that structural effects of the mutation are limited to the C-terminal region of the protein (23).

The xerocyte-like dumbbell red cells (Figure 10d), were observed in two Thai sibling dRTA patients who had homozygous band 3 Bangkok I mutation, accompanied by homozygous hemoglobin E (32). Band 3 Bangkok I occurs from a GGC to GAC transition at codon 701 in exon 17 of the *AE1* gene, resulting in Glu to Asp (G701D) substitution. The genetic and functional data have suggested that the homozygous G701D mutation also cause recessively transmitted dRTA, with apparently normal erythroid anion transport. The details of this mutation with respect to dRTA will be discussed in the next section.

5.4.2 *AE1* mutations associated with dRTA

At present, at least 7 *AE1* mutations associated with dRTA have been reported (Table 7), with both autosomal dominant (28, 30, 31, 79) and autosomal recessive (32) modes of inheritance. The six mutations are due to nucleotide substitutions and one due to nucleotide insertion. Three of the six nucleotide substitutions are mutations occurred at codon 589, which is the code for arginine

(R589) of transmembrane domain 6 (TM6) of the AE1 polypeptide. These mutations including (R589H, R589S and R589C), were found in multiple unrelated families (30, 31). Another missense mutation (S613F) resulted from C to T transition in exon 15 of the *AE1* gene. This amino acid substitution is in TM7 of AE1. Band 3 Pribram has a G to A substitution at the splice donor site (nt +1) of intron 12 of *AE1*. It was found in two incomplete dRTA patients with hereditary spherocytosis (28). This mutation encodes a C-terminally truncated band 3 containing only the cytoplasmic domain and the first three putative transmembrane segments. The other *AE1* mutation associated with dRTA is an intragenic 13-bp duplication in exon 20 of *AE1*. This duplication does not alter the encoded protein through codon 900, but as the result of an introduction of premature termination codon at position 901, the mutant protein is truncated by 11 amino acids (30). The molecular mechanism related to these mutations which lead to pathogenesis of the autosomal dominant dRTA is still unknown. Some particular mutations of *AE1* were observed in autosomal recessive dRTA. A homozygous missense, G701D, mutation of *AE1* was reported in autosomal recessive dRTA in two Thai siblings (32). The same mutation, G701D, in compound heterozygosity with 27-bp deletion in exon 11 that results in Southeast Asian ovalocytosis (SAO), could also cause autosomal recessive dRTA and SAO (33).

Band 3 Bangkok I (G701D) is the only one so far reported to cause autosomal recessive dRTA. It is also found to be associated with two benign mutations, M31T and K56E (band 3 Memphis I), on the same allele. Band 3 Bangkok I has an impaired trafficking to the surface when it was expressed in *Xenopus* oocyte. Coexpression of Band 3 Bangkok I with the erythroid band 3 chaperone, glycophorin

A, rescued both band 3- mediated Cl^- transport and its surface expression in oocytes (32). The functional data in oocytes suggest that the G701D mutation leads to decreased or absent kAE1 accumulation at the basolateral plasma membrane of type A IC in the renal collecting duct (32).

Table 6 *AE1* mutations in hereditary spherocytosis.

Variant	Codon	Mutation	Effect	Reference
Genas	-	G→A at +89nt from the capsite in 5' UTR	Reduced AE1 mRNA	(71)
Montefiore	40	GAG (Glu) →AAG (Lys)	Reduced protein 4.2	(81)
Foggia	54-55	ACCCAC→ACCAC (delete C)	Reduced AE1 mRNA from premature termination (after addition of 10 amino acids)	(73)
-	81	CGCTGGG→CGCGGG (delete T)	Reduced AE1 protein from premature termination (after addition of 30 amino acids)	(72)
Hodonin (Praque IV)	81	TGG (Trp) →TGA (stop)	Mutant mRNA not detected from premature termination	(69)
Napoli I	100	TCT→TTCT (insert T)	Mutant mRNA not detected from premature termination (after addition of 9 amino acids)	(73)
Nachod (Hradec Kralove II)	117-121	Acceptor splice site in intron 5 mutated from CAG→AAG	Reduced AE1 protein from deletion of highly conserved amino acids GTVLL (117-121) from the ankyrin binding site	(69)
Fukuoka	130	GGA (Gly) →AGA (Arg)	Reduced AE1 protein	(83)
Mondego	147	CCT (Pro) →TCT (Ser)	Reduced AE1 protein when combines with Montefiore	(71)
Osnabrück I	150	CGA (Arg) →TGA (stop)	Reduced AE1 protein	(71)
Worcester	170-172	TGGGGGGT→ TGGGGGGGT (insert G)	Mutant mRNA not detected from premature termination (after addition of 4 amino acids)	(69)
Campinas	202	Donor splice site in intron 8 mutated from G→T	Exon 8 skipping and premature termination (after addition of 13amino acids)	(75)
Princeton	273-275	GCCCCCCAC→ GCCCCCCCAC (insert C)	Mutant mRNA not detected from premature termination (after addition of 23 amino acids)	(69)
Boston	285	GCT (Ala) →GAT (Asp)	Reduced AE1 protein (effect highly conserved amino acids)	(69)
Tuscaloosa	327	CCC (Pro) →CGC (Arg)	Reduced protein 4.2	(80)
Noirterre	330	CAG (Gln) →TAG (stop)	Reduce AE1 mRNA	(70)
Brüggen	419	TCACCCG→TCACCG (delete C)	Reduce AE1 protein	(68)
Milano	447	Insert 69 bp duplication	Reduce AE1 protein	(79)
Bicetre II	454-455	TGGGGGC→ TGGGGC (delete G)	Reduced AE1 protein from premature termination (after addition of 17 amino acids	(72)
Benesov (PlaqueV)	455	GGG(Gly) →GAG(Glu)	Reduced AE1 protein (effect highly conserved amino acids)	(69)
Pribram (PraqueVI)	477	G→A at+1nt of intron 12	Reduced AE1 mRNA from premature termination (after addition of 8 amino acids)	(69)

Table 6 *AE1* mutations in hereditary spherocytosis (continue).

Variant	Codon	Mutation	Effect	Reference
Coimbra	488	GTG (Val)→ATG (Met)	Reduced AE1 protein	(82)
Bicetre I	490	CGC (Arg)→TGC (Cys)	Reduced AE1 protein	(72)
Every	496	TTCTGG→TTCGG (delete T)	Reduced AE1 protein from premature termination (after addition of 17 amino acids	(72)
Dresden	518	CGC (Arg)→TGC (Cys)	Reduced AE1 protein (effect highly conserved amino acids)	(68)
Smichov (PraqueVII)	616	ATCATG→ATATG (detete C)	Mutant mRNA not detected from premature termination (after addition of 48 amino acids)	(69)
Trutnov	628	TAC (Tyr)→TAA (stop)	Mutant mRNA not detected from premature termination	(69)
Hobart	646-647	CGGGGC→ CGGGC (delete G)	Mutant mRNA not detected from premature termination (after addition of 17 amino acids)	(69)
Osnabrück II	663	TGGATGATG→ TGGATG (delete ATG)	Reduced AE1 protein	(68)
Most (Praque VIII)	707	CTG (Leu)→CCG (Pro)	Reduced AE1 protein (effect highly conserved amino acids)	(69)
Okinawa	714	GGG (Gly)→AGG (Arg)	Reduced AE1and protein 4.2	(78)
Praque II	760	CGG (Arg)→CGA (Gln)	AE1 protein not detected (effect highly conserved amino acids)	(76)
Hradec Kralove	760	CGG (Arg)→TGG (Trp)	Reduced AE1 protein (effect highly conserved amino acids)	(76)
Praque	767	Insert 10 bp duplication	Reduced AE1 protein from premature termination	(84)
Chur	771	GGC (Gly)→GAC (Asp)	Reduced AE1 protein	(77)
Napoli II	783	ATC (Ile)→AAC (Asn)	Reduced AE1 protein	(73)
Jablonec	808	CGC (Arg)→TGC (Cys)	Reduced AE1 protein (effect highly conserved amino acids)	(76)
Birmingham	834	CAC (His)→CCC (Pro)	Reduced AE1 protein (effect highly conserved amino acids)	(69)
Philadelphia	837	ACG (Thr)→ATG (Met)	Reduced AE1 protein (effect highly conserved amino acids)	(69)
Praque III	870	CGG (Arg)→TGG (Trp)	Reduced AE1 protein	(76)
Veruvio	894	ACC→AC (delete C)	Reduced AE1 protein	(85)

Table 7 *AE1* mutations associated with dRTA.

Variant	Codon	Mutation	Phenotype	Reference
Pribram	477	G→A at nt +1 of intron 12	Incomplete dRTA	(28)
R589H	589	CGC (Arg)→ CAC (His)	AD dRTA	(29)
R589S	589	CGC (Arg)→AGC (Ser)	AD dRTA	(30)
R589C	589	CGC (Arg)→TGC (Cys)	AD dRTA	(29)
S613F	613	TCC (Ser) →TTC (Phe)	AD dRTA	(29)
Bangkok I	701	GGC (Gly) →GAC (Asp)	AR dRTA	(32)
-	901	13 bp duplication in exon 20	AD dRTA	(30)

5.4.3 *AE1* polymorphisms

Several *AE1* polymorphisms, which appear to be clinically benign, have been reported, including band 3 Memphis (variant I and II) and other AE1 variants associated with blood group antigens. These have been reviewed in several reports (23, 51, 65, 86). Band 3 Memphis I is a relatively common *AE1* polymorphism, found in 6% to 7% of random human blood samples. It is particularly common in American Indians (up to 25%), African Americans (15%), and Japanese (29%) (65). It migrates with a higher apparent molecular weight than normal band 3 on SDS-PAGE. It is readily distinguished from normal band 3 in membrane from chymotrypsin treated red cells because the N-terminal fragment of the abnormal band 3 has M_r 63,000 compared with the M_r of 60,000 found for the normal fragment. Yanoukakoa *et al* (87) shown that band 3 Memphis I has a glutamic acid at position 56 replacing the lysine of normal band 3. It results from a single base substitution (AAG→GAG) in codon 56 (88). The surprisingly large change in SDS-PAGE

electrophoretic mobility from this point mutation probably results from differences in SDS binding and hydrodynamic properties of the variant (51). The Memphis I polymorphism appears to have little effect on the normal functioning of band 3, although the red cells with band 3 Memphis I have slightly reduced phosphoenolpyruvate transport activity, and a possible increased affinity for hemoglobin and glycolytic enzymes (51, 65).

Band 3 Memphis II is a mutation that occurs against a background of band 3 Memphis I. This shows the same abnormal mobility on SDS-PAGE as Memphis I, but differs in its covalent binding of the anion transport inhibitor H_2DIDS (51, 65). Band 3 Memphis II has Pro 854→Leu as well as Lys 56→Glu but the mutation does not effect the anion transport activity of the protein. Memphis II is associated with the occurrence of a new red cell antigen, the Diego a antigen (Di^a), which is common in the indigenous people of North America. The mutation is close to the site of crosslinking by H_2DIDS at Lys 581, and the Memphis II variant was originally detected because it was more readily covalently labeled by H_2DIDS than the normal band 3 (23).

In addition to the Di^a antigen associated with the Memphis II variant described above, a number of other serologically defined blood group antigens have been linked with band 3 mutations. Many of these antigens result from point mutations in amino acids present in the third extracellular loop of band 3. For examples, the Waldner (Wd^a) antigen results from Val557→Met, while the Warrior (WARR) and Redelberger (Rb^a) antigens result from Thr 552→Ile and Pro 548→Leu, respectively. (23). The reported *AE1* polymorphisms are listed in Table 8.

Table 8 Reported *AE1* polymorphisms.

Variant	Codon	Mutation	Phenotype	Reference
Darmstadt	38	GAC (Asp)→GCC (Ala)	-	(73)
Memphis (I)	56	AAG (Lys) →GAG (Glu)	-	(88)
L73M	73	CTG (Leu) →ATG (Met)	-	(73)
$ELO^{+}Ag$	432	(Arg) →(Trp)	ELO^{+} blood group Ag	(89)
Rb (a+)Ag	548	CCA (Pro) →CTA (Leu)	Rb (a+)blood group Ag	(74)
Tr (a+)Ag	551	AAG (Lys) →AAC (Asn)	Tr (a+)blood group Ag	(74)
WARR Ag	552	ACT (Thr) →ATT (Ile)	WARR (a+)blood group Ag	(74)
Wd (a+)Ag	557	GTG (Val) →ATG (Met)	Wd (a+)blood group Ag	(74)
Wu+ Ag	565	GGC (Gly) →GCC (Ala)	Wu+ blood group Ag	(90)
Wr (a+)Ag	658	GAG (Glu) →AAG (Lys)	Wr (a+)blood group Ag	(91)
Memphis II (Di^{a})	854	CCT (Pro) →CTT (Leu)	Di^{a} blood group Ag	(65)

6. Methods for screening mutations and polymorphisms

Identification of disease gene by the candidate gene approach requires a definite proof that a certain mutation is involved in pathogenesis of the disease. Analysis of mutation is therefore an important step of this approach. Before the analysis is carried out, mutation and polymorphism of a gene of interest have to be screened. This section deals with the methods, which have been developed and

currently used for screening mutation and polymorphism. The ideal method should be simple, rapid, sensitive, cost effective, harmless, reproducible, and practical for screening a large number of sample (92).

6.1 Single strand conformation polymorphism (SSCP)

SSCP, a PCR-based screening method, is one of the most widely used techniques because of its simplicity and versatility (93, 94). It is based on the principle that single stranded DNA (ssDNA) molecules take one specific sequence-based secondary structure or conformation which is determined by intramolecular interactions (Figure 11) under nondenaturing conditions. DNA molecules differing by as little as a single base substitution may form different conformations and migrate differently in a nondenaturing polyacrylamide gel (93). In the original method described by Orita *et al* (95, 96), DNA sequence of interest was amplified and simultaneously radiolabeled by PCR. The PCR product was denatured prior to being separated on a sequencing size polyacrylamide gel, and the bands of ssDNA molecules were visualized by autoradiography. Subsequent improvements of the method have reduced the gel size and eliminated the radiolabeled by using ethidium bromide or silver staining (97). Recently fluorescence-based SSCP has been established in the automated DNA sequencer system (98).

Conformational changes and migration of ssDNA fragments are critically influenced by the size and sequence of DNA fragment, electrophoresis temperature, gel additives, percentage of acrylamide, acrylamide cross linking, and ionic strength of the buffer. These parameters have been empirically found to effect sensitivity of

SSCP analysis. Therefore, PCR-SSCP is most suitable for the identification of higher power increases temperature and destroys the conformational changes of ssDNA (97). Unless a laboratory is air-conditioned the ambient temperature will vary both diurnally and seasonally, thus affecting the reproducibility of SSCP results. Results of SSCP analysis are more easily replicated when electrophoresis is carried out in a cold room at 4°C, where temperatures fluctuate vary little (99).

Many SSCP protocols recommend the inclusion of additives such as glycerol (93, 96, 100, 101) and polyethylene glycol (102) to the gel matrix. The addition of glycerol in particular has been reported to increase the sensitivity of SSCP analysis. Markoff *et al* (102) reported that the addition of polyethylene glycol helps to improve the differential separation of ssDNA in a much shorter time than conventional SSCP and broadens the applicability of SSCP analysis from 150 to as much as 500 bp of DNA fragment.

Acrylamide is the commonly used matrix for SSCP. The percentage of acrylamide and the ratio of acrylamide to bis-acrylamide cross-linker determine the sieving properties of the gel (103). The percentage of acrylamide may vary from 5% to 20%. Savov *et al* (104) reported that high percentage of acrylamide gels improve revolution in SSCP analysis allowing the detection of a PCR fragment > 400 bp in one instance. Furthermore, Hongyo *et al* (105) presented that 20% polyacrylamide showed the sharpest SSCP bands most consistently, but 4-20% gradient gels were found to be convenient because band mobilities were almost 50% faster and gel-running times were consequently shorter. However, Spinardi *et al* (100) reported that

increasing the polyacrylamide concentration above 6% did not result in any improvement.

The ratio of acrylamide cross linking used in SSCP protocol is very variable, some groups use a 19:1 ratio (106) others a 29:1 (104), 39:1 ratio (105) or 49:1 (107). Gels with a low level of acrylamide: bis-acrylamide cross-linking (49:1) are popular because it is thought to improve the efficiency of SSCP analysis (99, 103). The type and concentration of buffer in the chamber of the gel unit is another important parameter, affecting the clarity of the SSCP bands (97). In most cases 1x Tris-borate-EDTA (TBE) yielded the sharpest SSCP bands. Decreasing the ionic strength of the electrophoresis buffer to 0.5xTBE many reduce the occurrence of smeary signal bands, but also lowers the buffer capacity (97). It has been empirically known that using TBE with glycerol as a buffer system in the electrophoresis, mutations could be detected at a high sensitivity (94). The glycerol effect in SSCP analysis is explained by the decrease of pH of the buffer caused by interaction of glycerol with borate. The reason for increase mobility shifts in low pH is unclear. Perhaps, by lowing pH, the charges of phosphates in the nucleic acid backbone are suppressed, and more nucleotide residues become involved in maintaining the tertiary structure (108).

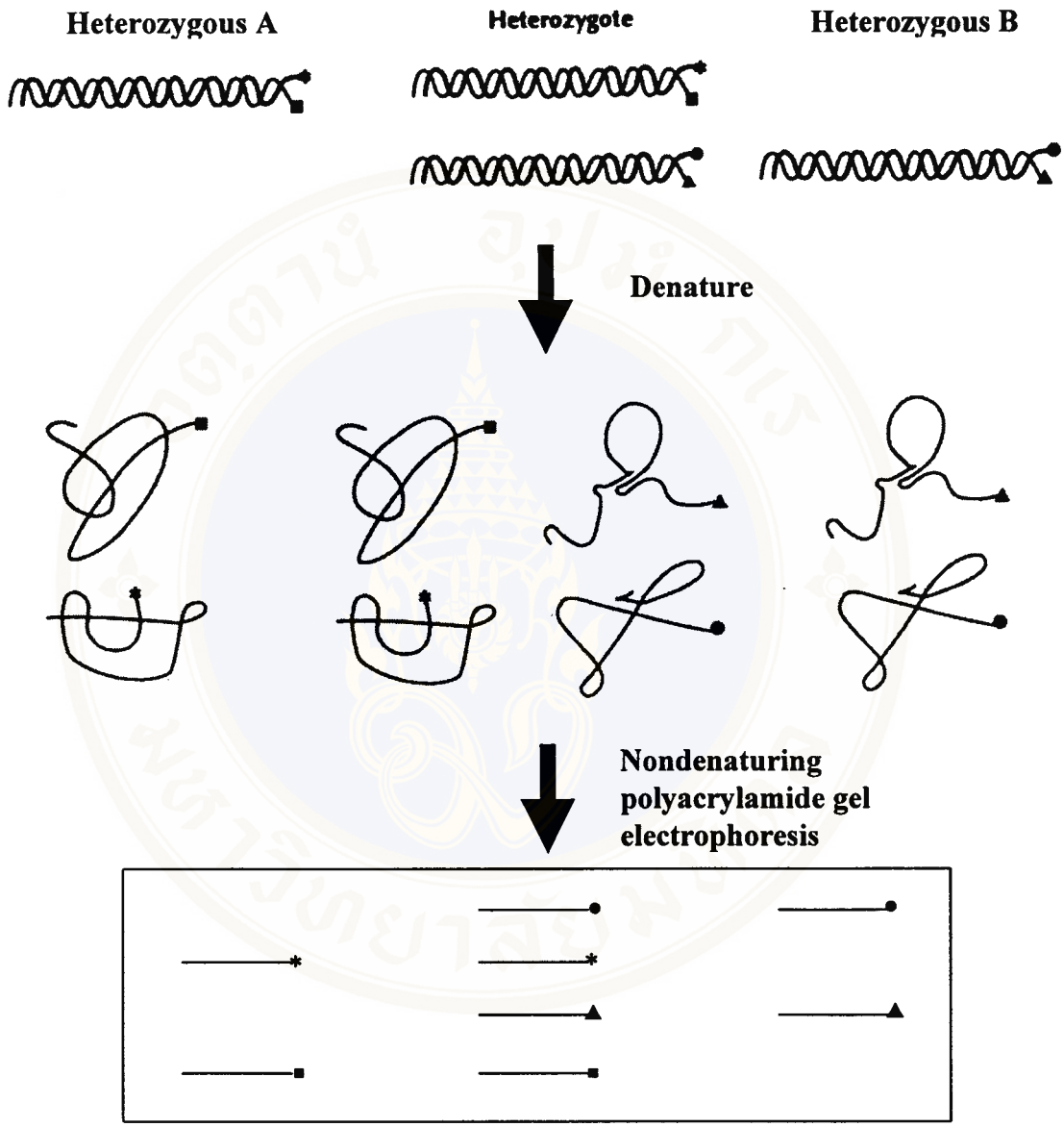

Figure 11 Principle of single strand conformation polymorphism (SSCP).

DNA fragment is amplified by PCR and denatured into ssDNA molecules. The secondary structure or conformation of each ssDNA molecule occurs due to intramolecular interaction in nondenaturing condition during electrophoresis on polyacrylamide gel. Different conformations result in different migrations of ssDNA molecules. The 'A' and 'B' forms of DNA molecules may have only one different nucleotide.

6. 2 Heteroduplex analysis (HA)

Heteroduplex analysis is one of the most widely and practical method used for screening mutations. It is a PCR-based technique, which involves the denaturation of allelic (PCR-amplified) DNA fragments of wild-type and mutant and subsequently reannealing of single stranded DNA molecules to give a hybrid of both wild type and mutant strands. The products are mixtures of the homoduplex of wild-type, homoduplex of mutant, and novel heteroduplexes (109). A bulge or bend is generated at the site of base mismatch in the hybrid molecules of wild type and mutant strands. This structural feature produces different mobilities on nondenaturing polyacrylamide gel (92, 109). Heteroduplexes usually migrate more slowly than their corresponding homoduplexes due to a more "open" double stranded configuration surrounding the mismatched bases (106). Its sensitivity of detection is about 80% of mutations (109). A recent development has been the introduction of denaturing high performance liquid chromatography (DHPLC) to analyse the heteroduplexes (92, 110). This adds more precision and speed to the method and avoids the pouring of the gels. Automation would allow the high throughput without radioactivity but expensive equipment is required.

6.3 Denaturing gradient gel electrophoresis (DGGE)

This method is based on the electrophoretic mobility and the different melting points of DNA duplexes. Melting temperature (Tm) of each DNA fragment is largely depend on its nucleotide sequence. The DNA fragments are analysed on denaturing gradient polyacrylamide gel containing a linearly increased temperature or

concentration of denaturing agents such as formamide and urea (111). The DNA duplexes migrate until they reach positions of the gel where the concentrations of the denaturing agent equal to their melting temperatures (Tm_s); consequently they partially denatured (branch) and do not migrate much further. Only a single nucleotide difference between normal and mutant DNA duplexes is sufficient to cause branching at different positions along the gel allowing their separation. Base changes in the undenatured slower-melting domain are not detected. Once the molecules are completely denatured, their positions in the gradient again become solely a function of size. The technique therefore requires that molecules maintain an undenatured (clamped) end (109). The addition of the GC-clamp, GC-rich sequence, at the 5' end of one primers has been found to increase the percentage of mutation detection of DGGE (112). DNA fragment with the length up to 1 kb can be screened for mutation by DGGE but it is most efficient with fragments of 100-500 bp. Its sensitivity for detection is close to 100% and does not require radioactive labeling of DNA fragment. Once set up, it is excellent for repeated analyses of same DNA regions from different samples (109). The more recent modifications have included using capillary and two-dimensional electrophoresis (113).

6.4 Dideoxy fingerprinting (ddF)

Dideoxy fingerprinting (ddF) is a hybrid between Sanger dideoxy sequencing and SSCP that can detect the presence of single base and other sequence changes in PCR-amplified DNA segment (114). In ddF, a Sanger sequencing reaction is performed with one dideoxy terminator, which yields ssDNA fragments of different

sizes for running on a nondenaturing polyacrylamide gel electrophoresis. Mutations can be detected on the basic of missing fragments, additional fragments or differences in migration pattern of the ssDNA (97). Dideoxy fingerprinting provides information about the location of the sequence change, and efficiency of detection is independent on the length of the amplified product (114). The ddF can detect all mutations in a 300 bp length of DNA (114-116).

6.5 Ribonuclease (RNase) cleavage assay

The RNase cleavage assay or ribonuclease protection assay is the oldest of the cleavage methods for mutation detection (92). This method is based on the property of RNase to cleave RNA at a mismatch site in heteroduplexes which are the hybridization of a radioactively labeled wild-type RNA probe to mutant DNA or RNA (117). The RNase cleavage RNA fragments are separated by size on denaturing polyacrylamide gel. Tests are scored as positive for mutation based on the presence of subfragments seen in the test lanes and absent from a no mismatch control (118). The original method, using RNase A, has a detection efficiency of only 30-60% (109). Since RNase A is an inefficient cutter of single base pair mismatches, especially on RNA probe at a purine i.e., G:G, G:A, G:T, A:A, A:C and A:G (117, 119). To improve the efficiency of this method, other enzymes (RNase I or RNase T2) can be used inplace of RNase A (120). A recent technique of non-isotope RNase cleavage assay, NIRCA™ commercial kit (Ambion), has encouraged the use of this method in a new mode (118). The RNase cleavage assay has a disadvantage that the contact with RNase has to be carefully prevented during RNA isolation. Therefore, the addition of

RNase inhibitors are recommended (97). This method has ability to scan mutation in a large DNA fragment and can also determine the position of mutation on the fragment.

6.6 Chemical cleavage of mismatch (CCM)

CCM is a method for detection of point mutation, which depends upon the chemical modification and cleavage of mismatched bases in heteroduplex DNA. It relies upon the principles of Maxam-Gilbert sequencing in which radioactively end–labeled DNA fragments are exposed to reagents that modify specific bases so that subsequent cleavage of the DNA sugar-phosphate backbone occurs at the modified sites (121). The heteroduplexes are reacted with either hydroxylamine that recognizes mismatched C bases or osmium tetroxide that recognizes mismatched T bases. The respective chemicals modify any mismatched or unmatched C or T bases so that the modified strand can be cleaved with piperidine at the site of the mismatch. The products are analysed by electrophoresis on a denaturing polyacrylamide gel and the size of the fast running cleavage bands indicates the site of mismatch (122). This technique has a number of advantages that it scans large DNA fragments, in virtually 100% efficiency, and specifically locates the mutation for subsequent sequencing. However, the practical disadvantages are that it is labor-intensive and uses noxious chemicals and radioactivity (121).

6.7 Enzyme mismatch cleavage (EMC)

The enzyme mismatch cleavage (EMC) method is one of a few techniques capable of quickly detecting and locating a single nucleotide mutation within kilobase stretches of DNA. The EMC is analogous to the chemical cleavage of mismatch (CCM) in that it cleaves heteroduplex DNA at base pair mismatch; however, it does not require toxic chemicals or multiple steps. Denaturing and re-annealing wild-type and mutant DNA in the same tube results in heteroduplexes. The EMC exploits the activity of a bacteriophage T4 enzyme endonuclease VII that cleaves heteroduplex DNA at single base pair mismatch or site of insertion/deletion. The cleavage products which are radioactively labeled can then be detected by electrophoresis on a denaturing polyacrylamide gel (123). However, the cleavage of heteroduplex DNA by T4 endonuclease VII does not occur precisely at the site of base mismatch but within 6 nucleotides downstream from the point of DNA perturbation (124).

6.8 Conformation sensitive gel electrophoresis (CSGE)

This assay is base on the assumption that mildly denaturing solvents in an appropriate buffer can amplify the tendency of single base mismatches to produce conformational changes such as bends in the double helix, and thereby increase the differential migration of DNA heteroduplexes and homoduplexes (125, 126). DNAs are detected by polyacrylamide gel electrophoresis and ethidium bromide staining. The advantages of CSGE are that it is simple, requires little standardization, requires no special equipment or preparation of PCR samples, uses a standard polyacrylamide

electrophoretic gel, and does not use radioactivity (126). Its disadvantage is that the sequence alterations within 50 bp of the ends of DNA fragment may not be detected.

6.9 Protein truncation test (PTT)

The PTT is a specific test for nonsense, framshift, or splice site mutations that produce truncated protein products. It is based on *in vitro*-coupled transcription and translation of PCR amplified coding sequences (127). PCR is carried out using a special forward primer comprising a high activity promoter sequence, such as T7 promoter, followed by translation initiation signal (AUG), and an inframe gene specific sequence (128). The resulting PCR product is used as template for *in vitro* transcription and translation. Incorporation of a labeled amino acid is necessary for detection of the synthesized protein production on sodium dodecyl sulfate-polyacrylamide gel (SDS-PAGE). Both radioactive and nonradioactive labels are available. If a truncating mutation is present then the translation product will be shorter than that from the normal sequence, and thus resolved by SDS-PAGE (128). An advantage of PTT is that a large coding segment (2-3 kb) can be screened in a single assay. Neutral polymorphism, silent, and missense mutations will be not detected by PTT. Its sensitivity is 95-100% (128). It is not widely used because of some limitations such as inability to detect missense mutation, high cost, radioisotope requirement, and complicated procedure (127, 128).

6.10 DNA sequencing

DNA sequencing is the "gold standard" method to identify changes in DNA sequence (97). Since PCR product can now directly be used for sequencing and the automated sequencing method is rapid and less expensive, in some circumstances DNA sequencing may be conducted without preliminary screening for mutations. Two different techniques for effective DNA sequencing have been described. The Maxam-Gilbert chemical method is based on the specific chemical usage to break the end-labeled DNA strands at only one type of nucleotide at random positions (129). The Sanger chain-termination method, which is now the most commonly used, is based on incorporation of a dideoxynucleoside triphosphate (ddNTP), the a nucleotide analog that lacks the hydroxyl group at the 3' position of sugar necessary for further dNTP attachment (130). The automated sequencing has been developed to improve the sequencing rate. Its principle still relies on Sanger's dideoxy method (130) with replacement of isotopic labeling by fluorescent dyes.

6.11 DNA chip

Basic principle of DNA chip technology is microscopic arrays of oligonucleotides attached on small chips by a special process for hybridization with fluorescent-labeled mutant or wild-type DNA (92). Distinct sequences are attached to the chip with the differences as small as a single base for the detection of nucleotide changes (131). Scanning of fluorescent chips requires a special confocal microscope (92). Differing patterns of hybridization between wild type and test samples signal the nucleotide change. This method was initially conceived for rapid DNA

sequencing. There is a major development towards using this method to assay known and unknown mutations in known stretches of DNA have been made.

Certain characteristics of all methods that have been described are compared in Table 9.

Table 9 Summary and comparison of methods for screening mutations.

Method	Precise location	Efficiency of detection	Size of fragment	Advantage	Disadvantage
SSCP	No	~90% (but lower efficiency reported)	≤200 bp	- rapid and simple - not expensive	- conditions require careful selection - low detection when fragment >200 bp - mutation not precisely located
HA	No	~80%	200-500 bp	- rapid and simple -not expensive	- limited sensitivity - mutation not precisely located
DGGE	No	100%	<500 bp	- rapid and simple (after initial setting up) - 100% detection - heterozygote detection - not expensive	- effort required to establish the technique - mutation not precisely located
ddF	nearly	100%	300 bp	- 100% detection - approximately provide location of mutation	- effort required to establish the technique
RNase	Yes	60-90%	1-2 kb	- scans large fragments - precisely locates mutation - no hazardous chemicals	- low efficiency of detection - requires cloning - multiple step

Table 9 Summary and comparison of methods for screening mutations (continue).

Method	Precise location	Efficiency of detection	Size of fragment	Advantage	Disadvantage
CCM	Yes	100%	1-2 kb	- scans large fragments - precisely locates mutation - heterozygote detection	- multistep and labor intensive - uses hazardous chemical
EMC	within 6 bp	~100%	1-2 kb	- scans large fragments - precisely locates mutation - no hazardous chemicals	- multistep and labor intensive
CSGE	No	~100%	450 bp	- simple - no used hazardous agent - not expensive	- mutations within the 50 bp of the end of fragment maybe missed
PTT	nearly	95-100%	2-3 kb	- detected debilitating mutation only - polymorphism and silent mutation not be detected	- unable to detect missense mutation - expensive - complicated procedure
DNA Sequencing	Yes	100%	<500 bp	- 100% detection - not required further step - automated sequencing (rapid and simple)	- expensive - technical demanding - labor intensive if few mutations are expected
DNA chip	Yes	100%	1-16.6 kb	- high accuracy and throughput	- general applicability unproven

CHAPTER IV

MATERIALS AND METHODS

1. Materials

1.1 dRTA patients and normal subjects

dRTA patients who were studied in this thesis were diagnosed, treated, and followed up at Sappasitthiprasong Hospital, Ubolrajathani Province. This group of patients has been thoroughly investigated and followed up for a period of more than 10 years by a team of clinicians and nephrologists leading by Professor Sumalee Nimmannit of Siriraj Hospital and Professor Wipada Chaowakul of Sappasitthiprasong Hospital. dRTA was diagnosed from the history of illness, clinical symptoms, laboratory investigations, and renal physiological studies. Short acid loading test (ALT) was performed in all the patients by oral administration of 0.1 gm/kg NH_4Cl as described (132). Blood and urine samples were collected during the test for measuring venous blood pH, serum creatinine, BUN, HCO_3^-, Na^+, K^+, Cl^-, creatinine clearance, pH, and NH_4^+. dRTA was defined by a low rate of NH_4^+ excretion and inability to lower the urine pH below 5.5, in the presence of systemic acidosis, HCO_3^- <20 mEq/liter. Fifteen dRTA patients (9 females and 6 males) from 4 families were included in the study in this thesis. The patients' codes are given in Table 10 and their pedigrees are shown in Figure 12.

Table 10 dRTA patients and normal control subjects studied in this thesis.

Subject	Code	Sex	Age (years)
dRTA patients	P 1	Female	57
	P 2	Female	52
	P 3	Female	27
	P 4	Male	48
	P 5	Male	57
	P 6	Female	23
	P 7	Female	75
	P 8	Male	56
	P 9	Female	68
	P 10	Female	60
	P 11	Male	74
	P 12	Female	65
	P 13	Male	66
	P 14	Male	64
	P 15	Female	39
Normal control	N 1	Male	42
	N 2	Female	33
	N 3	Male	29
	N 4	Male	26
	N 5	Female	27
	N 6	Female	25
	N 7	Female	25
	N 8	Female	23
	N 9	Female	23
	N 10	Female	34
	N 11	Female	43
	N 12	Female	56

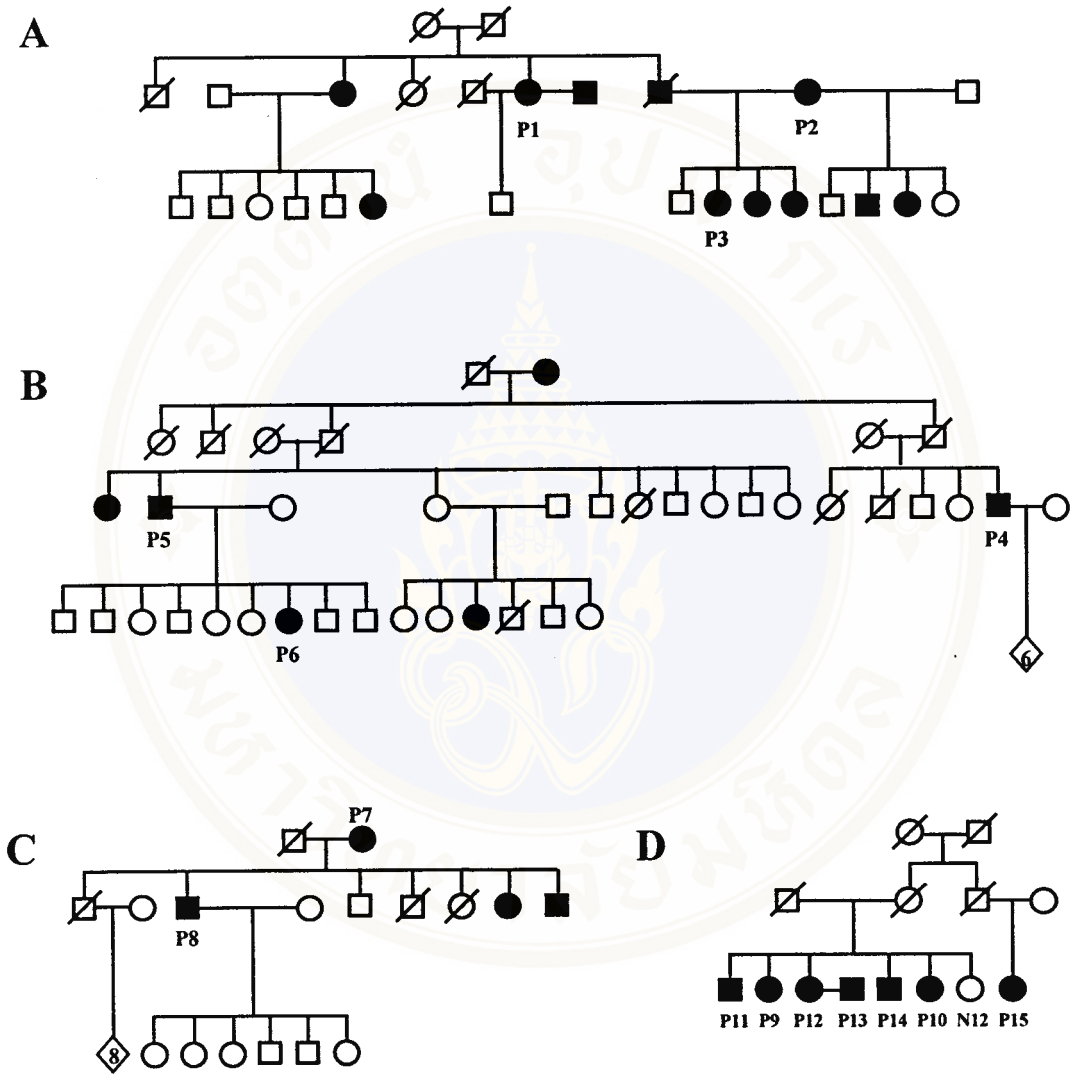

Figure 12 Truncated pedigrees of 4 unrelated families with EdRTA selected for the study in this thesis.

Fifteen patients (coded under symbols) from these 4 families were included in the study. ○ Unaffected female, □ unaffected male, ● affected female, ■ affected male, ⊘ dead female, ⊠ dead male.

Normal control subjects were 11 healthy laboratory personnels (7 females and 4 males) who were working in the Medical Molecular Biology Unit (MMBU) and had no history of dRTA (Table 10).

1.2 Blood samples

Approximately 10 ml of peripheral venous blood were taken from the patients and normal controls for DNA studies The blood sample was collected into a sterile plastic tube containing 0.1 ml of 20% (w/v) EDTA solution as anticoagulant. The patients' blood samples were transported on ice from Ubolrajathani to Bangkok within 48 hours after the collections and processed in laboratory within a few days.

1.3 PCR primers

PCR primers for amplifications of the *AE1* gene were available at MMBU laboratory. These primers were designed from the *AE1* genomic sequence (HUMAE1ERY; GenBank Accession number: L35930) by Dr. Pa-thai Yenchitsomanus and Ms. Nunghathai Sawasdee (33) using a computer program-MacVector version 4.5.1 (Kodak, Inc.). The criteria for designing included:

(1) length of primer between 20-30 nucleotide,

(2) average GC content of about 50% with random distribution,

(3) melting temperature (Tm) between 50-85 degree Celsius,

(4) no primer dimer formation between same and pair of primers, and

(5) no possibility of long hairpin loop and secondary structure formation.

Table 11 Oligonucleotide primers for amplifications of *AE1*.

Region	Primer name	Sequence (5′→3′)	Position	Tm (°C)	Product size (bp)
Promoter	AE1Int3.1L	CAGTTTGGGACAAGGGCGTG	IVS3, nt 242 to 261	64	491
	AE1Int3.1R	TGATGAAGTGAAGGGACCTCTCC	IVS3, nt -269 to -291	70	
Exon 4	AE1Ex4L	GTCTCTGAGGCTCACAGTGGATG	IVS3, nt -81 to -59	72	226
	AE1Ex4R	ATCCCCTTGCTCCTCTCTTCC	IVS4, nt 63 to 83	66	
Exon 5	AE1Ex5L	TGAGCACCCACTATGCCCTG	IVS4, nt -61 to -42	64	299
	AE1Ex5R	CAGCACCCCACAACAATCCTC	IVS5, nt 37 to 57	66	
Exon 6	AE1Ex6L	AGATGAGGATTGTTGTGGGGTG	IVS5, nt 33 to 54	66	262
	AE1Ex6R	CAAGTGGGCTGGGGAAGTG	IVS6, nt 44 to 62	62	
Exon 7	AE1Ex7L	CACCACTGATAGCTCAGCCTGAAC	IVS6, nt -60 to -37	54	243
	AE1Ex7R	TGAGAAAGCTCTCTCCTTGCCC	IVS7, nt 38 to 59	58	
Exon 8	AE1Ex8L	GAGAATGGGAAGGGGAGGATG	IVS7, nt -60 to -80	66	244
	AE1Ex8R	GGTCCAGGCTGAGGGAAAGAC	IVS8, nt 59 to 79	68	
Exon 9	AE1Ex9L	TCTTCAGCACACCCACCCTG	IVS8, nt -59 to -40	64	299
	AE1Ex9R	TCAGCCACCATGCAGGTCC	IVS9, nt 40 to 58	62	
Exon 10	AE1Ex10L	TCCTTTCCCTCCGCAGGTC	IVS9, nt -51 to -33	62	332
	AE1Ex10R	ACAGAGGCTACGCTGAGGTGTC	IVS10, nt 49 to 70	70	
Exon 11	AE1Ex11L	CCTCACCTCCTCCAGCTACTCC	IVS10, nt -52 to -31	72	318
	AE1Ex11R	CAGAAGTTGGGGCTGAGACAGAG	IVS11, nt 49 to 71	72	
Exon 12	AE1Ex12L	GCTCTATGGGCTCCTGGAAATG	IVS11, nt -61 to -40	68	293
	AE1Ex12R	AAAGGGTCTTGGGGCAAGG	IVS12, nt 65 to 83	60	
Exon 13	AE1Ex13L	CTGTCATGTCCCCCGCAC	IVS12, nt 27 to 44	60	339
	AE1Ex13R	TGTCTCAGTCTTATACACAACCTCC	IVS13, nt 32 to 56	72	
Exon 14	AE1Ex14L	TGGTGGTATTTTCCAGCCCAAG	IVS13, nt -65 to -44	66	320
	AE1Ex14R	GCACTGAGGAATTTGGAGCGG	IVS14, nt 61 to 81	66	
Exon 15	AE1Ex15L1	AAGGCAGGAGGTGGGGAGTGACTG	IVS14, nt -58 to -35	78	201
	AE1Ex15R1	GGAAATGAGGACCTGGGGGGTATC	IVS15, nt 30 to 53	76	
Exon 16	AE1Ex16L	TCCTGCTCCCACCCTTCCCC	IVS15, nt -64 to -45	68	276
	AE1Ex16R	TCTGCCTCCCACCCTCCCAG	IVS16, nt 26 to 45	68	
Exon 17	AE1Ex17L	TGGAGGAGGCAGGGGAGAAC	IVS16, nt -51 to -32	66	347
	AE1Ex17R	GGGGCAGGAGGATGGTGAAG	IVS17, nt 23 to 42	66	
Exon 18	AE1Ex18L	ATATGGTGCCTGTGTTTTATTCCC	IVS17, nt -99 to -76	68	332
	AE1Ex18R	TGCCTATCACACCCCAGCAC	IVS18, nt 44 to 63	64	
Exon 19	AE1Ex19L	GGTACAGGACCCTTTTCTGG	nt-1 of 3'Ex18 to nt 19 of IVS18	62	334
	AE1Ex19R	GCCTGCCCTAGTTCTGAGAC	IVS19, nt 54 to 73	64	
Exon 20	AE1Ex20L1	TCTCACCCTGTCTCTCTCCTG	IVS19, nt –35 to -15	66	198
	AE1Ex20R1	GAGGTGCCCATGAACTTCTG	nt 66 to 85 of 3'Ex20	62	

Altogether 18 pairs of primers for *AE1* were designed to amplify in the kidney promoter (in intron 3) and exon 4-20 regions. Each pair of primers in the latter set would amplify a region covering the exon, exon-intron junctions, and parts of its flanking introns (Figure 13). They were designed to anneal to the flanking intronic sequences, approximately 25 nucleotides from the exon-intron junction. Names and locations of these primers, and the expected sizes of PCR products are also shown in Figure 13. The detailed features of these primers including nucleotide sequences, positions, number of nucleotides, melting temperatures (Tm), and sizes of the products are presented in Table 11. These primers were ordered from GENSET, Tokyo, Japan and BioService Unit (BSU), the National Center for Genetic Engineering and Biotechnology (NSTDA), Bangkok, Thailand.

1.4 PCR primers for amplification of microsatellite DNA marker

A pair of PCR primers for amplification of a microsatellite DNA marker linked to *AE1* were also designed for linkage analysis (Table 12). They were also ordered from BSU.

Table 12 Oligonucleotide primers for amplification of microsatellite DNA marker linked to *AE1*.

Microsatellite markers	Primer name	Sequence (5′→3′)	No. of nt	Tm (°C)	Product size (bp)	Location
D17S787	D17S787L	TGGGCTCAACTATATGAACC	20	58	142	17q22.31
D17S787	D17S787R	TTGATACCTTTTTGAAGGGG	20	56	142	17q22.31

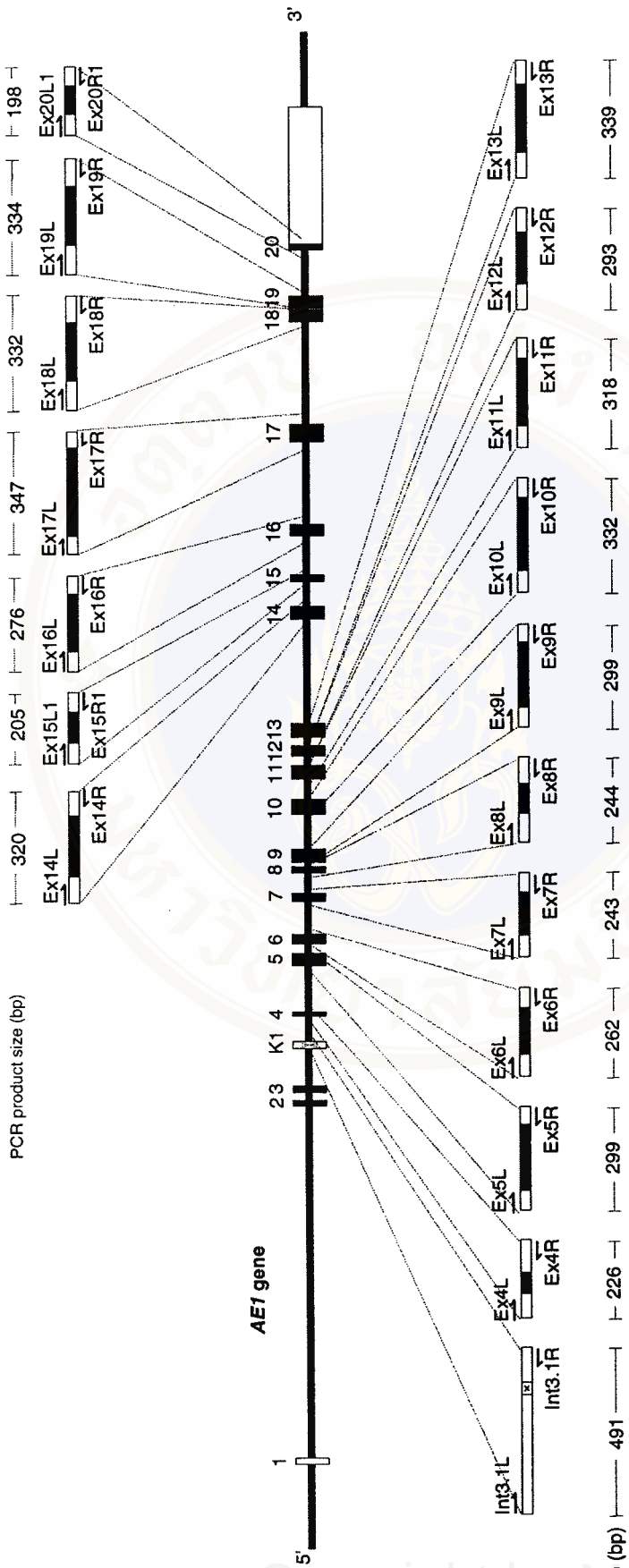

Figure 14 Schematic diagram showing PCR primers for amplification of *AE1*.

The gene is represented by a long horizontal line and its vertical bars. Eighteen pairs were designed to amplify the kidney prometer (intron 3 and exon 4-20 regions. All primers were specific to sequences in in introns. The regions amplified by all pairs of primers are magnified to show more details. The names of primers and sizes of PCR products are also indicated. The 5'->3' direction of primer is shown by half arrow.

1.5 Other materials

Chemicals, instruments, enzymes, reagents, and other materials are listed in Appendix.

2. Methods

2.1 Experimental strategy

Patients' DNAs extracted from white blood cells isolated from venous blood samples were screened for *AE1* mutations by polymerase chain reaction and single strand conformation polymorphism (PCR-SSCP). Eighteen regions of *AE1* (Figure 13) were amplified by PCR and screened by SSCP. Both radioisotopic (IR) and non-radioisotopic (non-IR) methods of PCR-SSCP were performed. The RI PCR-SSCP was used for screening DNA samples from 10 dRTA patients from 4 families. In addition, DNA samples of 8 dRTA patients (from one family) and of 11 normal control subjects were also screened for *AE1* mutations by a later developed non-RI PCR-SSCP. In non-RI PCR-SSCP, the single stranded DNA (ssDNA) molecules were detected by staining with silver nitrate ($AgNO_3$), and electrophoresis was carried out in 4 different conditions. Normal DNA samples were concurrently studied. Mobility shift of ssDNA in SSCP gel indicated the presence of nucleotide change which might result from *AE1* mutation or polymorphism. The DNA fragment showing mobility shift in SSCP would therefore be reamplified, purified, and subjected to sequencing analysis. Furthermore, linkage analysis using a polymorphic microsatellite DNA marker linked to *AE1* was also conducted to examine the possible involvement of *AE1* in one of the dRTA families studied. The experimental strategy is summarized in Figure 14.

2.2 White blood cell isolation

White blood cells (WBCs) were isolated from EDTA-blood sample. The blood sample (about 10 ml) was centrifuged at 2,000 rpm, 4°C, for 10 minutes. Plasma was discarded and whole cells were washed twice with phosphate buffered saline (PBS), pH 7.4 (see Appendix); in each washing, the cells were harvested by centrifugation in the same condition as mentioned above. Red blood cells were lysed by adding 3 volumes of RBC lysis buffer (see Appendix), leaving at room temperature for 10 minutes, and spinning. After that, RBC lysate was discarded and WBCs were collected. The lysis step was repeated once again. WBCs were then washed with PBS and collected by centrifugation at the same conditions as described. They were stored in a 15-ml screw-cap tube at -70°C until used for genomic DNA preparation.

2.3 Genomic DNA preparation

Frozen WBCs were thawed in the 15-ml storage tube and added with 4 ml of TE 20-5 buffer (see Appendix). The cell pellet was resuspended by vigorously shaking until all clumps disappeared. Two hundred microliters of 2 mg/ml proteinase K (Promega) in TE 20-5 buffer and 200 µl of 10% SDS solution were added into the suspension. The slimy mixture was mixed gently several times and incubated at 37°C overnight.

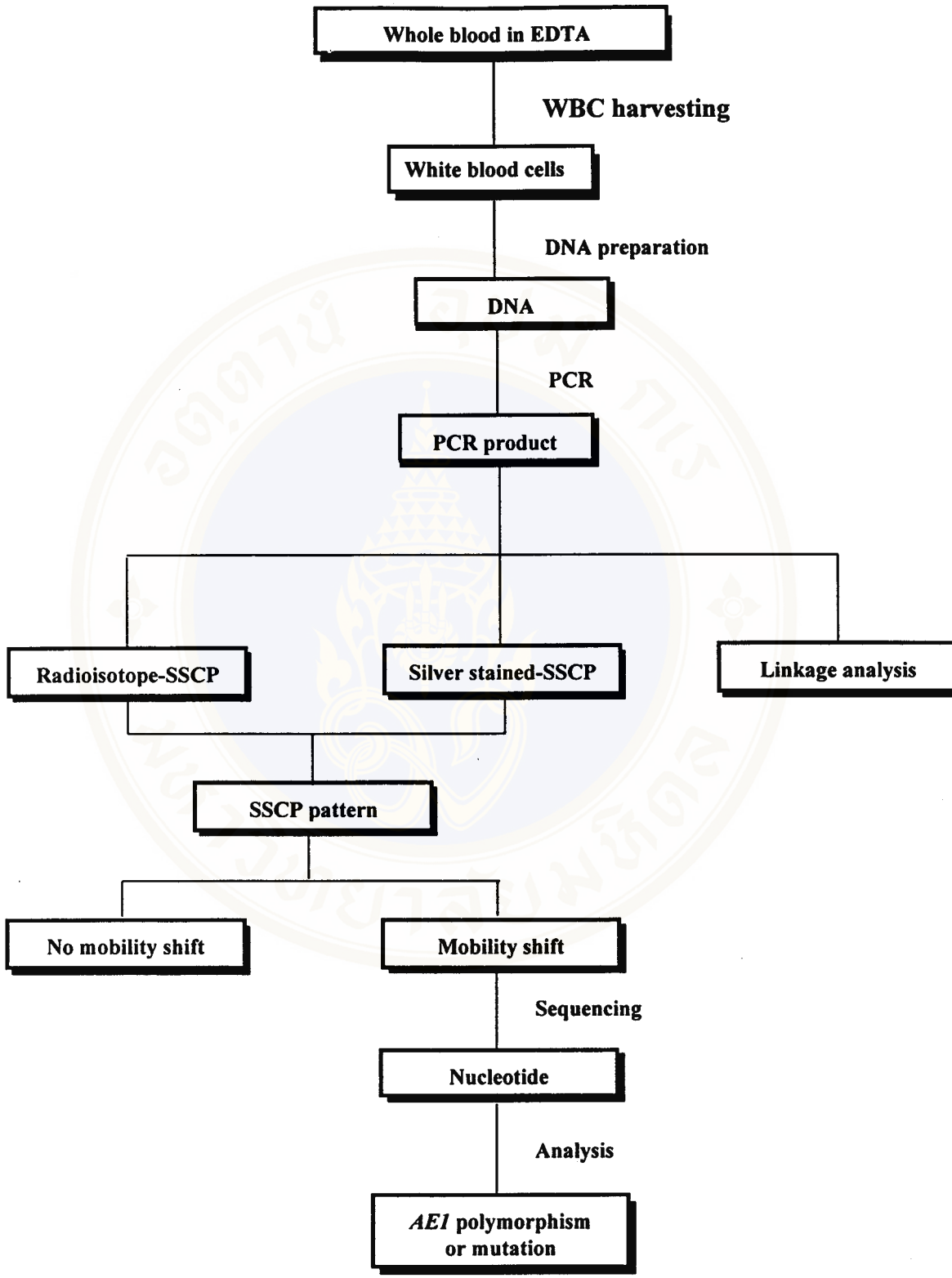

Figure 14 Flow-chart showing experimental strategy in the study of *AE1* mutations in dRTA patients.

Two milliliters each of saturated phenol solution and chloroform-isoamyl alcohol (24:1) mixture (see Appendix) were added into the sample tube. The tube was capped and mixed gently but thoroughly for 3-5 minutes until the mixture had a homogeneous milk-like appearance. After centrifuge at 2,500 rpm, 4°C, for 10 minutes, the lower organic phase under the aqueous phase was manually aspirated with a Pasture pipette. The step of phenol/chloroform-isoamyl-alcohol extraction was repeated once again. Then, 4 ml of chloroform-isoamyl alcohol (24:1) was added to the aqueous phase. The mixture was mixed gently but thoroughly, and centrifuged at 2,500 rpm, 4°C, for 10 minutes. The lower organic phase was again removed. This chloroform-isoamyl-alcohol extraction was repeated one more time.

DNA was then precipitated out of the aqueous phase by adding 1/10 volume of 4 M NaCl and 2 volumes of chilled absolute ethanol with gently mixing. DNA pellet was collected by centrifugation at 2,500 rpm, 4°C, for 10 minutes. It was air-dried at room temperature and dissolved in approximately 500 µl of sterile distilled water. Ten microliters of DNA solution were diluted with 990 µl distilled water (1:100 dilution). Then, optical densities (ODs) at wavelength 260 and 280 of the diluted DNA solution were measured. The ratio of OD260/OD280, which should be close to 1.8, indicated purity of DNA. DNA concentration could be estimated from its OD260 by the following formula: OD260 x 50 x dilution = DNA concentration in µg/ml.

2.4 Radioisotopic polymerase chain reaction and single strand conformation polymorphism (RI PCR-SSCP)

DNA fragments of 18 regions of *AE1* amplified from genomic DNA were labeled with ^{32}P by direct incorporation of α-^{32}P dCTP during amplifications. The labeled PCR products were denatured into ssDNA and run on non-denaturing polyacrylamide gel. SSCP pattern on the dried gel was detected by autoradiography.

2.4.1 RI PCR

PCR mixture for amplification and radioactive labeling of a DNA fragment was made up by mixing 125 ng of DNA sample, 1x PCR buffer, 1.5 mM $MgCl_2$, 0.5 units of *Taq* DNA polymerase (Promega or Perkin-Elmer), 0.2 mM dNTPs, 12.5 pmol each of L- and R-primers, 0.75 μCi α-^{32}P dCTP (Amersham). Sterile distilled water was added to the reaction to adjust total volume to 25 μl. The reaction was mixed well, briefly spun to collect splashing, and overlaid with 2 drops of mineral oil to prevent vaporization. PCR was performed in a DNA Thermal Cycler 480 (Perkin-Elmer). An initial denaturation at 94°C for 5 minutes was followed by 35 or 38 cycles of PCR consisting of denaturation at 94°C for 1 minute, annealing at 58-70°C for 1 minute and extension at 72°C for 1 minute, with a final extension at 72°C for 5 minutes. The details of PCR cycles for amplifications of all regions of *AE1* are presented in Table 13.

Table 13 Thermal cycling profiles for amplifications of regions in *AE1*.

Amplified region	Primers	Thermal cycling profile			Total cycle
		Denaturing[a]	Annealing	Extension[b]	
Promoter	AE1Int3.1L/AE1Int3.1R	94°C, 1′	67°C, 1′	72°C, 1′	37
Exon 4	AE1Ex4L/AE1Ex4R	94°C, 1′	63°C, 1′	72°C, 1′	37
Exon 5	AE1Ex5L/AE1Ex5R	94°C, 1′	63°C, 1′	72°C, 1’	37
Exon 6	AE1Ex6L/AE1Ex6R	94°C, 1′	63°C, 1′	72°C, 1′	37
Exon 7	AE1Ex7L/AE1Ex7R	94°C, 1′	60°C, 1′	72°C, 1′	37
Exon 8	AE1Ex8L/AE1Ex8R	94°C, 1′	60°C, 1′	72°C, 1′	37
Exon 9	AE1Ex9L/AE1Ex9R	94°C, 1′	60°C, 1′	72°C, 1′	37
Exon 10	AE1Ex10L/AE1Ex10R	94°C, 1′	58°C, 1′	72°C, 1′	37
Exon 11	AE1Ex11L/AE1Ex11R	94°C, 1′	62°C, 1′	72°C, 1′	37
Exon 12	AE1Ex12L/AE1Ex12R	94°C, 1′	58°C, 1′	72°C, 1′	37
Exon 13	AE1Ex13L/AE1Ex13R	94°C, 1′	58°C, 1′	72°C, 1′	40
Exon 14	AE1Ex14L/AE1Ex14R	94°C, 1′	60°C, 1′	72°C, 1′	37
Exon 15	AE1Ex15L1/AE1Ex15R1	94°C, 1′	70°C, 1′	72°C, 1′	37
Exon 16	AE1Ex16L/AE1Ex16R	94°C, 1′	68°C, 1′	72°C, 1′	37
Exon 17	AE1Ex17L/AE1Ex17R	94°C, 1′	67°C, 1′	72°C, 1′	37
Exon 18	AE1Ex18L/AE1Ex18R	94°C, 1′	65°C, 1′	72°C, 1′	37
Exon 19	AE1Ex19L/AE1Ex19R	94°C, 1′	60°C, 1′	72°C, 1′	37
Exon 20	AE1Ex20L1/AE1Ex20R1	94°C, 1′	65°C, 1′	72°C, 1′	37

[a] 5 minutes for first cycle

[b] 5 minutes for last cycle

2.4.2 Preparation of polyacrylamide gel

Before preparation of polyacrylamide gel, two glass plates of sequencing set (21 cm x 50 cm x 0.04 cm) (Sequi-Gen™ sequencing gel, Bio-Rad) were assembled. One glass plate was initially coated with dimethyldichlorosilane siliconizing solution to let the gel attached to the other glass plate.

Non-denaturing polyacrylamide gel (5.5%) for RI PCR-SSCP was prepared by mixing 10 ml of stock 40% acrylamide: bis-acrylamide (19:1), 16 ml of 5x TBE, 46 ml of distilled water, 450 µl of 10% ammonium persulphate (see Appendix), and 30 µl of TEMED. The polyacrylamide solution was immediately mixed and poured in a continuous stream at an angle of approximately 45° to the horizontal assembled sequencing set. After the glass plate sandwich had been filled, immediately slided the flat edge of the sharkstooth-comb into the gel. The gel was allowed to polymerize for about 3 hours. After the gel polymerized, the comb was removed and residual polyacrylamide was washed off with deionized water. The gel set was attached to the electrophoresis apparatus and filled with 1x TBE buffer. Then the sharkstooth-comb was gently pressed downward to form sample wells so that the teeth barely penetrated but did not puncture the gel. The top of the gel was rinsed again to remove excess urea. Before loading sample, the gel was pre-electrophoresed at a constant 1,000 volts for 1 hour to equilibrate the gel to the desired temperature (45°C to 55°C).

2.4.3 Sample preparation and loading

Three microliters each of the labeled PCR product were taken into two tubes and a total volume of 25 µl each was made up with SSCP loading buffers for ssDNA or double stranded DNA (dsDNA) preparations (see Appendix). For ssDNA preparation, the diluted sample was denatured by heating at 95°C for 10 minutes and immediately transferred to ice. After 5 minutes on ice, 7 µl of ssDNA sample were loaded into a well of the polyacrylamide gel. A dsDNA control was prepared in the same way except that it is made up in SSCP loading buffers without NaOH and the sample was not preheated before applying to the gel.

2.4.4 Electrophoresis

The gel was electrophoresed in 1x TBE at a constant power (3 W), room temperature for 15-24 hours (depend on fragments' length). The dsDNA was also run for comparison on the same gel.

2.4.5 Gel drying and autoradiography

The gel was transferred onto a sheet of Whatman® paper by gentle placing the paper on top of the gel; this would cause the gel to stick to the paper. Then the gel was turned up and covered with wrapping film. The gel was dried under vacuum gel drier (E-C Apparatus) at 80°C for 2.5 hours. The paper with dried gel was cut into the size of cassette and an X-ray film was placed on the dried gel in dark room. Autoradiography was carried out at -70°C for 1-3 days by exposing the gel to X-ray film with intensifying screen. After that the film was developed by a Kodak automated film developer.

2.5 Nonradioisotopic polymerase chain reaction and single strand conformation polymorphism (non-RI PCR-SSCP)

2.5.1 Polymerase chain reaction (PCR)

PCR reaction was performed by mixing 125 ng of DNA template, 2.5 µl of 10x PCR buffer, 1.5 µl of 25 mM $MgCl_2$, 1.5 µl of 2 mM dNTPs, 12.5 pmol each of forward (L) and reverse (R) primers, and 0.25 units of *Taq* DNA polymerase in a total volume of 25 µl. The reaction mixture was mixed well, spun to collect splashing, and overlaid with 2 drops of mineral oil to prevent vaporization. PCR was performed in the DNA Thermal Cycler 480. The PCR thermal cycling profiles for amplifications of all regions followed that described in 2.4.1.

2.5.2 Detection of PCR product by agarose gel electrophoresis

Five microliters of the PCR amplified product were thoroughly mixed with 1 µl of 6x gel-loading buffer (see Appendix), loaded, and run on 2% agarose gel electrophoresis in 1x TAE buffer at constant 100 volts in an electrophoresis set (Mupid 2, ADVANCE). One hundred-fifty nanograms of ϕX174 DNA digested with *Hae* III was also applied in one well as standard-size markers. After electrophoresis, the gel was stained in 0.5 µg/ml ethidium bromide solution for 10 minutes and destained in a large volume of distilled water for 20 minutes. The stained PCR product was visualized on an UV transilluminator and photographed with a Polaroid camera (Fotodyne) through a red filter.

2.5.3 Preparation of polyacrylamide gel

Ten percent nondenaturing polyacrylamide gels (acrylamide to bis-acrylamide; 49:1), containing 0.5% or 5% (v/v) glycerol, were prepared as described in Table 14.

Table 14 Mixture for preparing 10% nondenaturing polyacrylamide gels.

Reagent	Volume	
	0.5% glycerol gel	**5% glycerol gel**
Stock 40% acrylamide: bis-acrylamide	2.5 ml	2.5 ml
5x TBE	2.0 ml	2.0 ml
Glycerol	50 µl	500 µl
Distilled water	4.95 ml	4.5 ml
10% Ammonium persulphate	70 µl	70 µl
TEMED	4 µl	4 µl

The gel mixture was poured between the assembled glass plates (90x80x1 mm in size) which had been set before preparing the gel. A comb was immediately inserted at the topside in order to make sample wells without allowing air bubbles to become trapped under the teeth. Polyacrylamide was allowed to polymerize for 60 minutes at room temperature. After polymerization, the glass plates (containing gel) were assembled upon the electrophoresis set and the comb was removed.

2.5.4 Sample preparation and loading

Two microliters of PCR product were mixed with 8 µl of SSCP loading buffer (see Appendix) and heated at 95°C for 10 minutes. The sample mixture was immediately chilled on ice and applied into a well of 10% nondenaturing polyacrylamide gel (49:1 acrylamide to bis-acrylamide) containing 0.5% or 5% (v/v) glycerol. A dsDNA control was prepared in the same way except that it was made up in SSCP loading buffer without NaOH and heating.

2.5.5 Electrophoresis

Electrophoresis was performed at either room temperature or 4°C, with constant 20 mA, in 1x TBE buffer. The running times of each exon in 4 different conditions are shown in Table 15.

2.5.6 Silver staining of DNA

After electrophoresis, the polyacrylamide gel was fixed in 40 ml of 40% methanol for 10 minutes, soaked in 160 mM HNO_3 for 6 minutes, then rinsed and washed twice for 5 minutes each with deionized water. It was then stained in silver staining solution (see Appendix) for 20 minutes. After staining, silver staining solution was discarded into a beaker and added with a few drops of HCl to convert $AgNO_3$ to AgCl before discarding into drainage. After staining, the gel was rinsed and washed for 5 minutes with deionized water. Fifty milliliters of chilled developer solution (see Appendix) were added. The gel was shaken well until DNA bands became visible (approximately 5-10 minutes). Once the DNA bands were clearly observed, 50 ml of stop solution (see Appendix) was immediately added into the developer to stop the developing reaction.

Table 15 Running time of SSCP in 4 different conditions for 18 fragments of *AE1*.

Regions	Product size (bp)	SSCP conditions			
		Room temperature		4° C	
		0.5%glycerol gel	5%glycerol gel	0.5%glycerol gel	5%glycerol gel
Promoter	491	7 hours	8 hours	7 hours	8 hours
Exon4	226	2 hours 30 minutes	4 hours 30 minutes	2 hours 45 minutes	4 hours 30 minutes
Exon5	299	3 hours 30 minutes	4 hours	3 hours 30 minutes	5 hours
Exon6	262	3 hours	4 hours	3 hours	4 hours
Exon7	243	3 hours	4 hours 15 minutes	3 hours	4 hours 15 minutes
Exon8	244	3 hours	4 hours	3 hours	4 hours
Exon9	299	3 hours 30 minutes	6 hours	3 hours 30 minutes	6 hours
Exon10	332	4 hours	6 hours	4 hours	6 hours
Exon11	318	4 hours	5 hours	4 hours	6 hours
Exon12	293	3 hours	4 hours 30 minutes	3 hours 30 minutes	5 hours 15 minutes
Exon13	339	3 hours 30 minutes	6 hours	4 hours	6 hours
Exon14	320	4 hours	6 hours	4 hours	6 hours
Exon15	201	2 hours 15 minutes	3 hours 30 minutes	2 hours 15 minutes	3 hours 30 minutes
Exon16	276	3 hours 30 minutes	4 hours 30 minutes	3 hours 30 minutes	6 hours
Exon17	347	5 hours 30 minutes	6 hours 30 minutes	5 hours 30 minutes	6 hours
Exon18	332	3 hours 30 minutes	6 hours 45 minutes	4 hours	6 hours 45 minutes
Exon19	334	4 hours	5 hours 20 minutes	4 hours	5 hours 30 minutes
Exon20	198	2 hours	3 hours 30 minutes	2 hours 15 minutes	3 hours 30 minutes

After incubation with shaking for 5 minutes, the gel was washed with deionized water for 5 minutes. The washing step was repeated at least 2 times to ensure that the gel was washed thoroughly. The gel was placed between two transparency sheets. The SSCP pattern was recorded by scanning into a computer scanner. The gel could also be dried on the piece of filter paper for permanent storage.

2.6 Purification of PCR product for DNA sequencing

The PCR product that showed mobility shift in the SSCP analysis was purified from low melting point (LMP) agarose gel after electrophoresis, by using the QIAquick Gel Extraction Kit (Qiagen), following the manufacturer's instruction. The DNA fragment separated on the agarose gel was excised with a clean sharp blade and placed into a microtube. The gel was weighted and its volume was estimated. Then, three volumes of QG buffer were added to the gel. The incubation was made at 50°C for 10 minutes. After the complete dissolution of the gel, 1 gel volume of isopropanol was added. The solution containing DNA was applied to the QIAquick spin column and centrifuged at 13,000 g (Speedfuge HSC10K, Savant Instrument) for 1 minute. The flow-through was discarded before adding of 0.5 ml of QG buffer and a repeated centrifugation. The column was washed by soaking with 0.75 ml of PE buffer for 2-5 minutes and centrifuged again. After discarding the flow-through, centrifugation was repeated once. DNA was eluted from the QIAquick column by soaking with 30 µl of 10 mM Tris-HCl, pH 8 for 1 minute, before centrifugation. Concentration of the purified DNA was estimated from the band intensity seen on the electrophoresed gel, compared to that of ϕX 174 DNA/*Hae* III standard markers.

2.7 DNA sequencing

The purified PCR product was sequenced by an automated sequencer ABI-PRISM™310 (Applied Biosystems) using ABI-PRISM BigDye™ Terminator Cycle Sequencing Ready Reaction Kit (Applied Biosystems). Normally, the sequencings were performed for both strands of DNA and in parallel with normal DNA fragment.

2.7.1 Preparing cycle sequencing reactions

In the later experiment, the amplified DNA fragment showing mobility shift in SSCP was sequenced by automated sequencing machine (ABI-PRISM™ 310). The sequencing reaction was performed by using ABI-PRISM BigDye™ Terminator Cycle Sequencing Ready Reaction Kit (Applied Biosystems) following the manufacturer's instruction. The reaction mixture was made by mixing 4 µl terminator ready reaction mix, 3.2 pmol primer, 30-90 ng purified PCR product which was used as DNA template, and distilled water to adjust the volume to 20 µl. The cycle sequencing was carried out in the DNA Thermal Cycler 480, by running 25 cycles consisting of 96°C for 30 seconds, 50°C for 15 seconds, and 60°C for 4 minutes.

2.7.2 Precipitation of sequencing products

The sequencing products were purified from the excessive dye terminators by precipitation. The sequencing reaction was added with 2 µl of 3 M sodium acetate (NaOAc), pH 4.6, and 50 µl absolute ethanol to precipitate the sequencing products. After centrifugation at 12,000 rpm for 30 minutes and removing ethanol, the pellet was rinsed with 250 µl of 70% ethanol and dried for 10-15 minutes, in the darkplace.

2.7.3 Sample preparation and loading

The dried pellet was resuspended in 25 µl template suppression reagent (TSR), heated at 95°C for 2 minutes to denature the sequencing product, chilled on ice, and loading to the automated DNA sequencer ABI-PRISM™310 (Applied Biosystems).

2.7.4 Analysis of DNA sequence

Fluorescent signals were detected and recorded by ABI Collection software. Nucleotide sequence determination was performed by using Sequencer Navigator software, and analysed by using MacVector version 4.5.1 program.

2.8 Restriction endonuclease digestion analysis

Following the sequencing and mutation detection, the PCR product was digested with *Hpa*II restriction endonuclease in order to confirm nucleotide change in codon 701 of exon 17. Ten microliters of the PCR product was mixed with 2 µl 10x Buffer A, 2 Units *Hpa*II, and sterile distilled water to make up the total volume of 20 µl. The digestion mixture was incubated at 37°C overnight.

The PCR product was checked for complete digestion by 3% (w/v) agarose gel electrophoresis, which the details had been described on section 2.5.2.

2.9 Linkage analysis

2.9.1 γ-^{32}P ATP -end labeling of primer

Protocol for labeling 5'-end of primer for amplification of microsatellite DNA marker with radioactive [γ-^{32}P]ATP was a 10 µl primer radiolabeling reaction containing

2.5 pmol of the primer, 2.5 pmol of γ-^{32}P ATP (5,000Ci/mmol, Amersham), 2.5 unit of T4 polynucleotide kinase in 1x T4 polynucleotide kinase buffer (New England Biolabs). The reaction mixture was incubated at 37°C for 60 minutes and then the enzyme was inactivated at 90°C for 10 minutes. The labeled primers can be used immediately or stored for up to 5 days at -20°C.

2.9.2 Amplification of microsatellite DNA

PCR reaction was carried out in a 25 µl volume containing 125 ng of genomic DNA template, 1x PCR buffer II, 1.5 mM $MgCl_2$, 0.25 units of *Taq* DNA polymerase, 0.2 mM dNTPs, 12.5 pmol each of unlabeled L- and R-primers, 0.5 µl of ^{32}P labeled primer. The reaction mixture was mixed well, spun to collect splashing, and overlaid with 2 drops of mineral oil to prevent vaporization. PCR was processed through 37 cycles in a DNA Thermal Cycler 480. Each cycle comprised denaturation at 94°C for 1 minute (5 minutes for the first cycle), annealing at 58°C for 1 minute, and extension at 72°C for 1 minute (5 minutes for the final cycle).

2.9.3 Denaturing polyacrylamide gel preparation

Sequencing polyacrylamide gel, 6% concentration of gel (acrylamide to bis-acrylamide; 19:1), containing 7 M urea (see appendix), was prepared as previously described in section 2.4.2.

2.9.4 Sample preparation and loading

Four microliters of the labeled PCR product and 6 µl of sample running buffer (see Appendix) were mixed. The sample was denatured at 95°C for 10 minutes and

immediately transferred to ice. Ten microliters of each sample were loaded into a well of the polyacrylamide gel.

2.9.5 Electrophoresis, gel drying, and autoradiography

The electrophoresis was carried out at constant 1,700 volts for 4 hours. After that, the gel was dried and subjected to autoradiography as previously mentioned in section 2.4.5.

CHAPTER V

RESULTS

1. Amplifications of the 18 regions of the *AE1* gene

To test the primers and establish PCR conditions suitable for amplifications of the 18 regions of the *AE1* gene, PCRs were performed on genomic DNA from normal individual. The 18 regions included kidney *AE1* promoter in intron 3 and exons 4-20. The sequence of PCR primers used for amplifications were summarized in Table 11. After amplifications, PCR products were examined by agarose gel electrophoresis. Figure 15 shows the results of a set of amplifications of all the 18 regions. The PCR products, run in consecutive order on the agarose gel electrophoresis, all showed single bands.

2. Screening for *AE1* mutations in EdRTA patients by RI PCR-SSCP analysis

Mutations of the *AE1* gene were initially screened in 10 EdRTA patients from 4 families by RI-SSCP analysis. All 18 regions of *AE1* were amplified by PCR and simultaneously labeled by addition of α-^{32}P dCTP in the reaction mixture. The labeled PCR products were denatured and run on non-denaturing 5.5% polyacrylamide (19:1 acrylamide to bis-acrylamide) gel electrophoresis at room temperature. The gel was dried on a gel dryer and subjected to autoradiography. Autoradiograms of the RI PCR-SSCP analysis for screening of mutations in all 18 regions of *AE1* are shown in Figures 16a-16r.

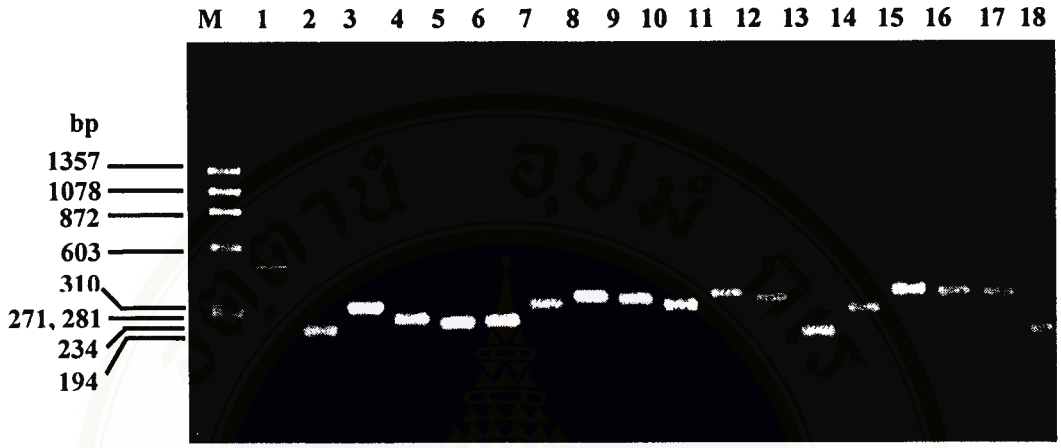

Figure 15 PCR products of the amplified 18 regions of *AE1*, examined by agarose gel electrophoresis and stained with ethidium bromide.

Electrophoresis was performed on 2% agarose-gel slab in 1x TAE buffer at 100 volts for 30 minutes. Lane M is *Hae*III-digested ϕX174 RF DNA markers. Lane 1 is the PCR product of kidney *AE1* promoter region in intron 3 with the size of 491 base pairs (bp). Lanes 2-18 are PCR products of exons 4-20 with the size of 226, 299, 262, 243, 244, 299, 332, 318, 293, 339, 320, 201, 276, 347, 332, 334, and 198 bp, respectively.

Mobility shifts of single stranded DNA (ssDNA), indicating mutations or polymorphisms of the *AE1* gene, were observed in DNA samples of 9 patients (P1, P2, P3, P4, P5, P6, P7, P8, and P9). Five patients (P1, P3, P4, P5, and P6) had the same pattern of the mobility shift involving both exons 4 and 17 (Figures 16b and 16o). Four patients (P2, P7, P8, and P9) had the different pattern (pattern 2) of mobility shift in exon 17 (Figure 16o). One patient (P8) showed a mobility shift of only exon 12 (Figure 16j) but another (P9) demonstrated mobility shifts of three exons comprising exons 4, 5, and 9 (Figures 16b, 16c, and 16g). The shiftment of exon 4 in the last patient was different from that of exon 4 in the previous 5 patients. The results of mobility shifts in RI PCR-SSCP analysis are summarized in Table 16.

3. Screening for *AE1* mutations in members of an EdRTA family by non-RI PCR-SSCP analysis

Non-RI PCR-SSCP method, which is more simple and rapid but less hazardous, was used to screen for mutations in the 18 regions of *AE1* in DNA samples of 7 affected and 1 unaffected members of a selected EdRTA family (Figure 12D), and of 11 normal controls. To enhance screening efficiency of this method, the gel composition and electrophoresis condition were modified. Different concentrations of glycerol (0.5% and 5%) as additive in 10% polyacrylamide gel were used and electrophoresis was performed at either room temperature or 4°C. The SSCP pattern was detected by silver nitrate staining.

a

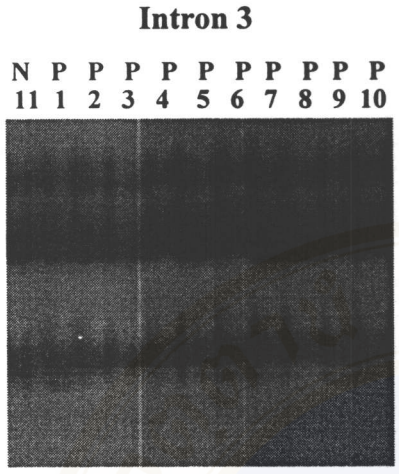

b

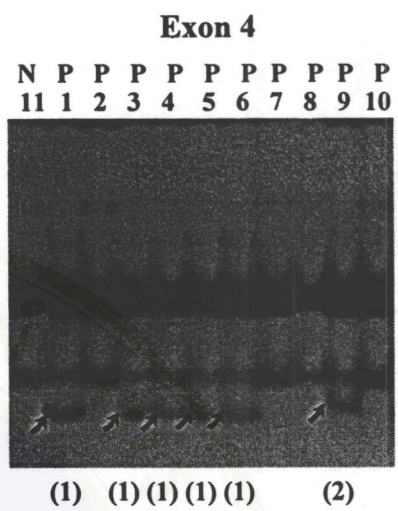

c

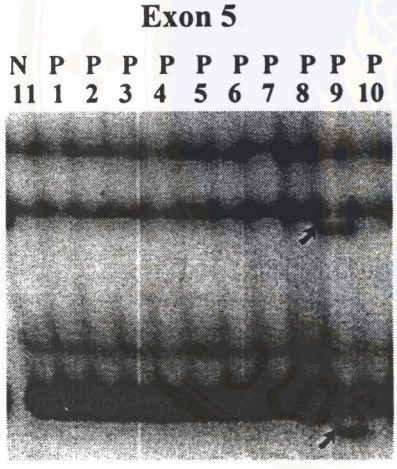

d

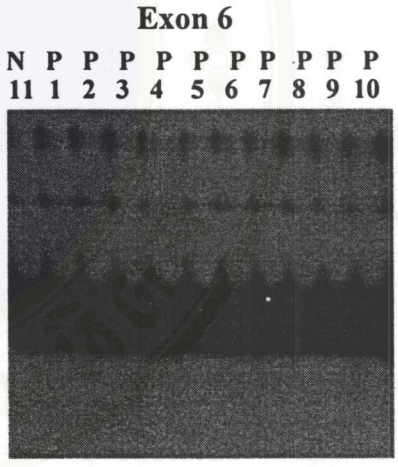

e

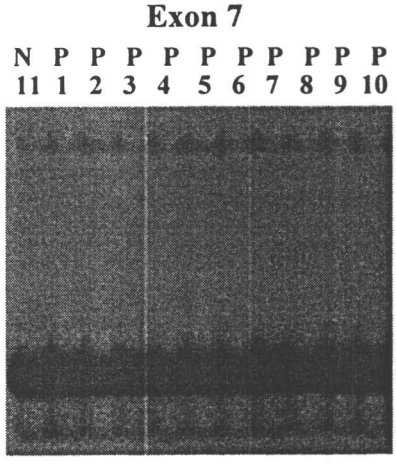

f

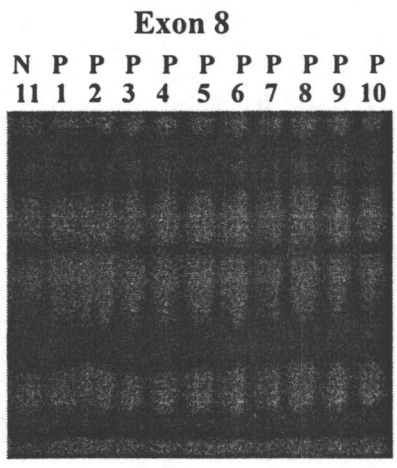

g Exon 9

h Exon 10

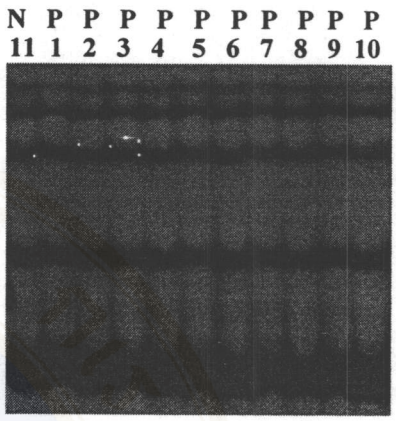

i Exon 11

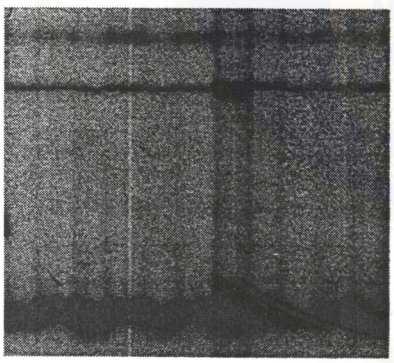

j Exon 12

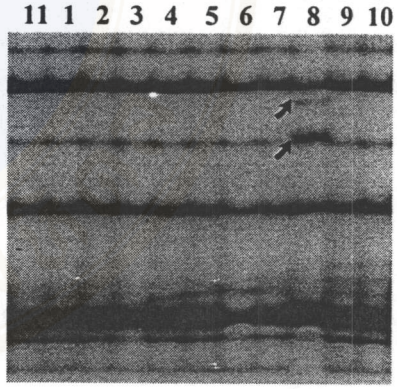

k Exon 13

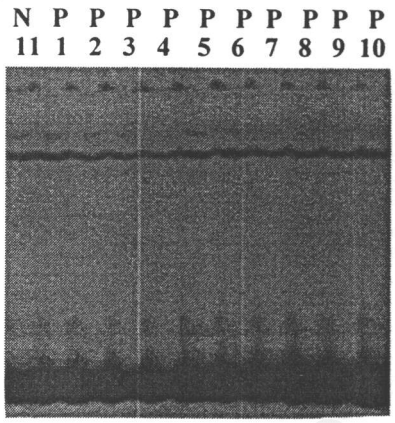

l Exon 14

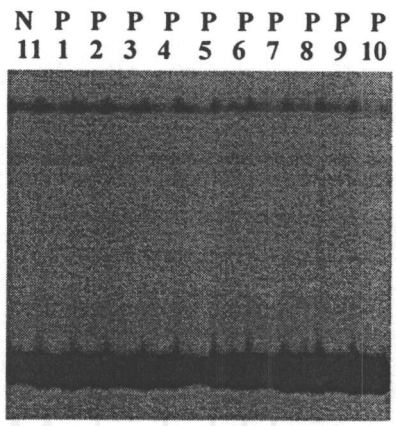

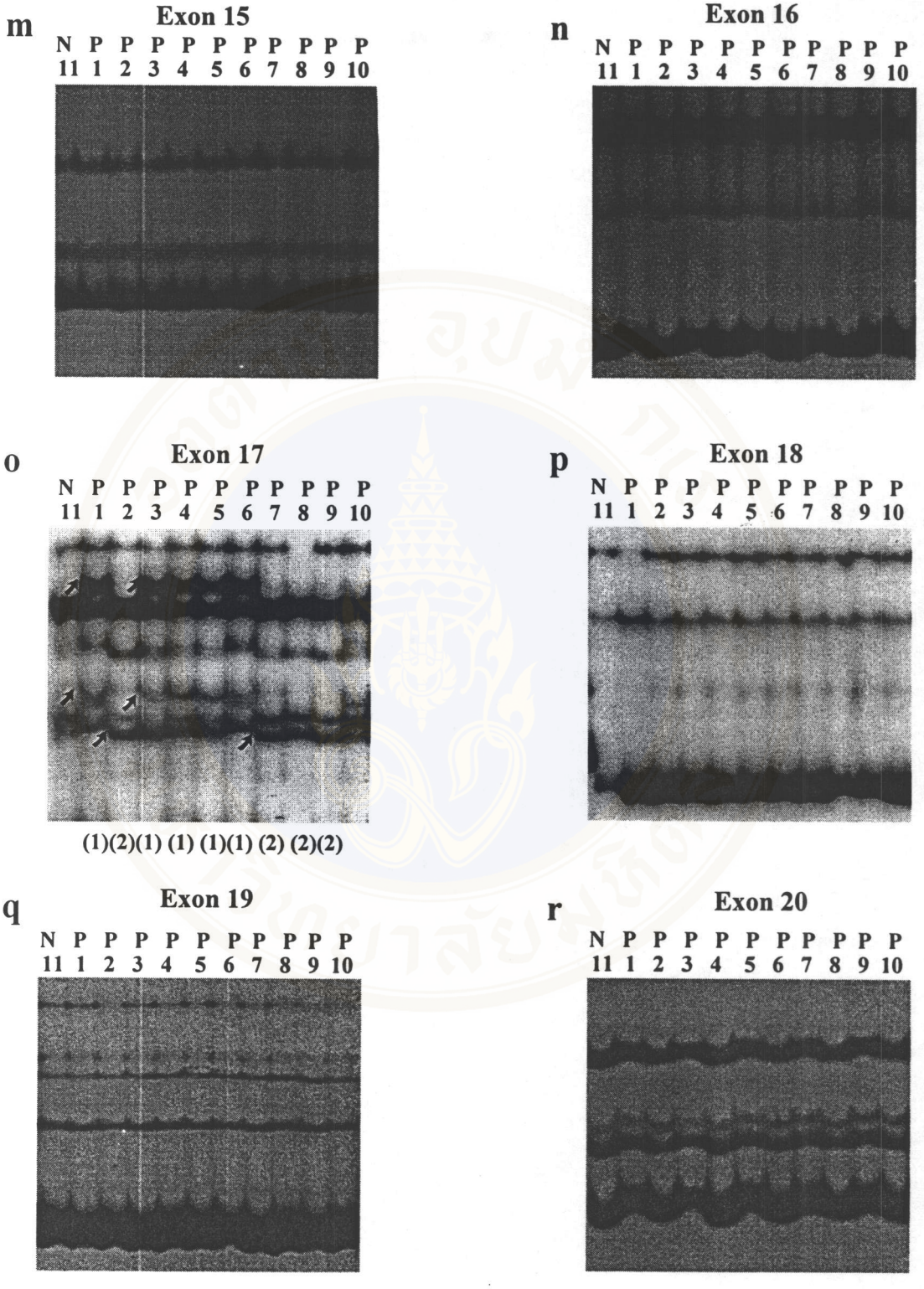

Figure 16 Screening of *AE1* mutations by RI PCR-SSCP analysis.

Eighteen regions of *AE1* (a-r) were amplified from DNA samples of a normal control (N) and 10 EdRTA patients (P1-P10) by radioisotopic PCR and analysed by electrophoresis on non-denaturing 5.5% polyacrylamide gel at room temperature, followed by autoradiography. Arrow (↗) indicates single stranded DNA with mobility shift.

Table 16 Summary of the results of screening for *AE1* mutations in EdRTA patients by RI PCR-SSCP analysis.

EdRTA patient	Region with mobility shift
P1	Exon 4 (1)*
	Exon 17 (1)
P2	Exon 17 (2)
P3	Exon 4 (1)
	Exon 17 (1)
P4	Exon 4 (1)
	Exon 17 (1)
P5	Exon 4 (1)
	Exon 17 (1)
P6	Exon 4 (1)
	Exon 17 (1)
P7	Exon 17 (2)
P8	Exon 12
	Exon 17 (2)
P9	Exon 4 (2)
	Exon 5
	Exon 9
	Exon 17 (2)

Note: *Number in parenthesis indicates pattern of mobility shift of ssDNA.

By performing electrophoresis on 10% polyacrylamide gel with 0.5% glycerol additive at room temperature, it was found that the DNA samples from 8 individuals (3 normal controls, 1 unaffected and 4 affected members) had mobility shifts of ssDNA in the non-RI PCR-SSCP analysis. Of the 3 normal control samples with mobility shifts, two (N2 and N6) occurred similarly in only exon 4 (Figure 17b) and one (N9) in both exons 4 and 5 (Figures 17b and 17c). The DNA sample of unaffected (N12) and two affected (P9 and P12) members showed mobility shifts in three exons including exons 4, 5, and 9 (Figures 17b, 17c, 17g). The DNA samples of two affected members (P11 and P14) had mobility shift in only exon 9 (Figure 17g). The mobility shifts observed in exon 4 consisted of two different patterns (Figure 17b): pattern 1 (faster) was found in DNA samples of two normal controls (N2 and N6), and pattern 2 (slower) in one normal control (N9), one unaffected member (N12), and two affected members (P9 and P12). The pattern 2 seemed to link to the observed mobility shift in exon 5 (Figures 17b and 17c).

The electrophoreses in three other different conditions: *(i)* the gel with 0.5% glycerol additive at 4°C, *(ii)* the gel with 5% glycerol additive at room temperature, and *(iii)* the gel with 5% glycerol additive at 4°C, were carried out for screening mutations in all the 18 regions of *AE1*. The results of these non-RI PCR-SSCP analyses using all four different conditions, which showed mobility shifts of ssDNA in 4 regions of *AE1* (exons 4, 5, 9, and 17), are demonstrated in Figures 4a-4d and summarized in Tables 17 and 18.

a

Intron 3

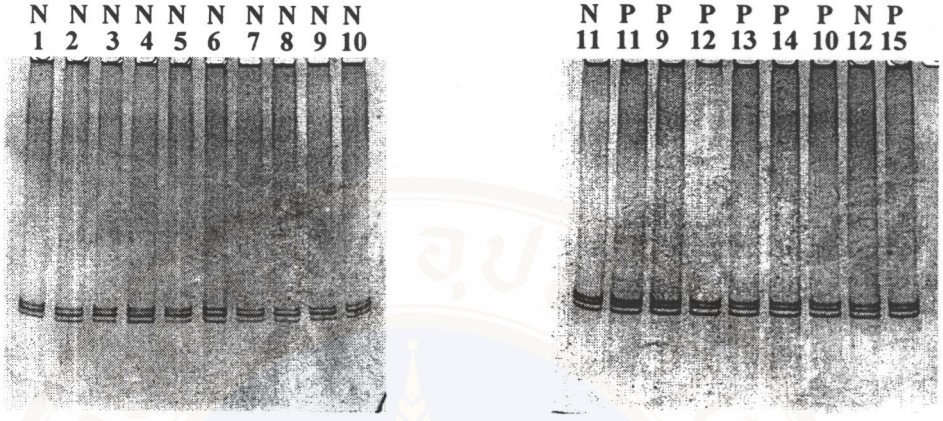

b

Exon 4

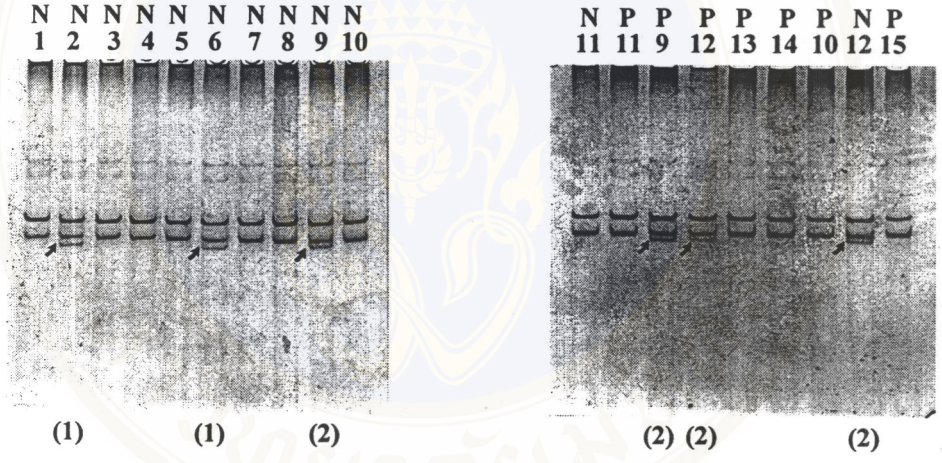

c

Exon 5

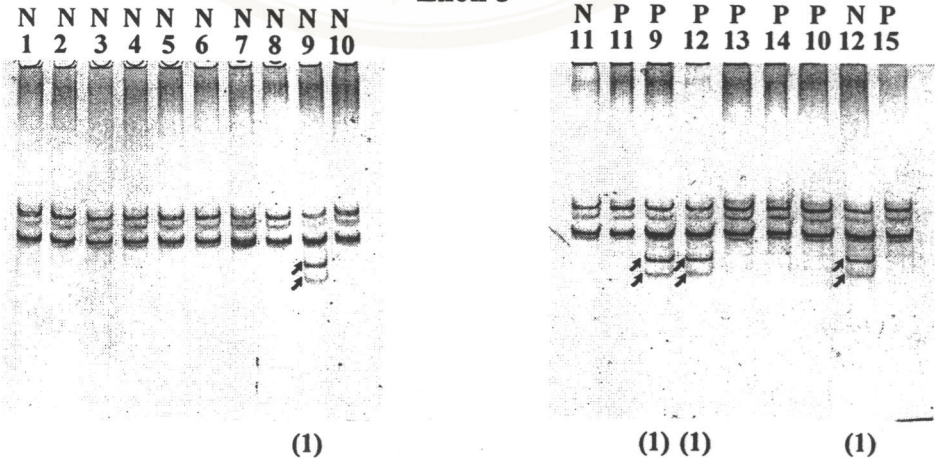

Exon 6

d

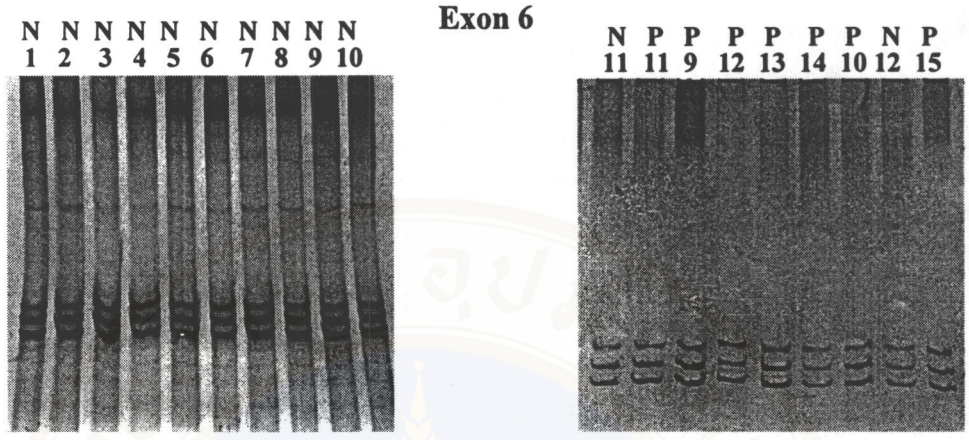

Exon 7

e

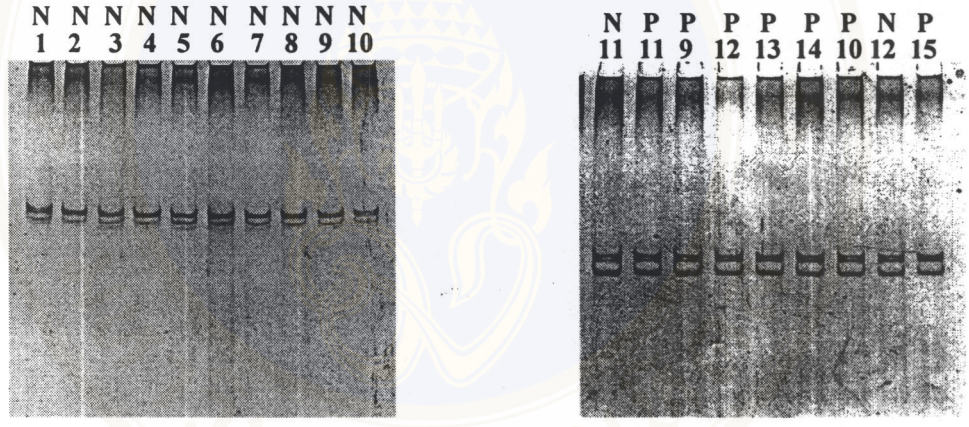

Exon 8

f

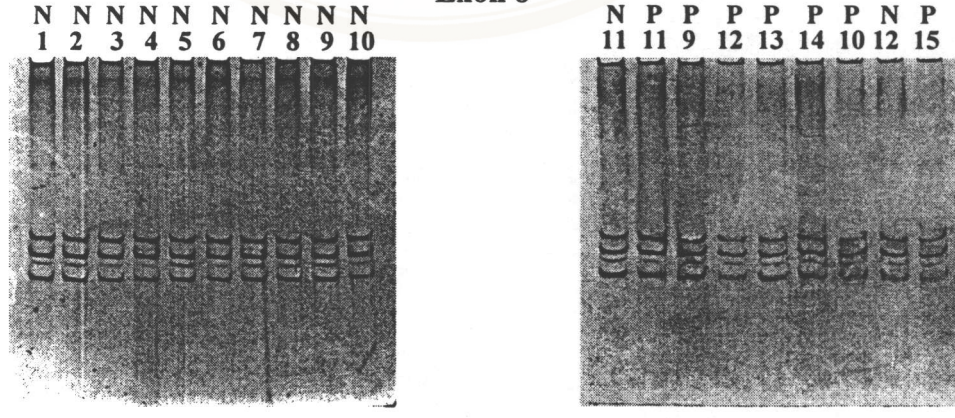

g

Exon 9

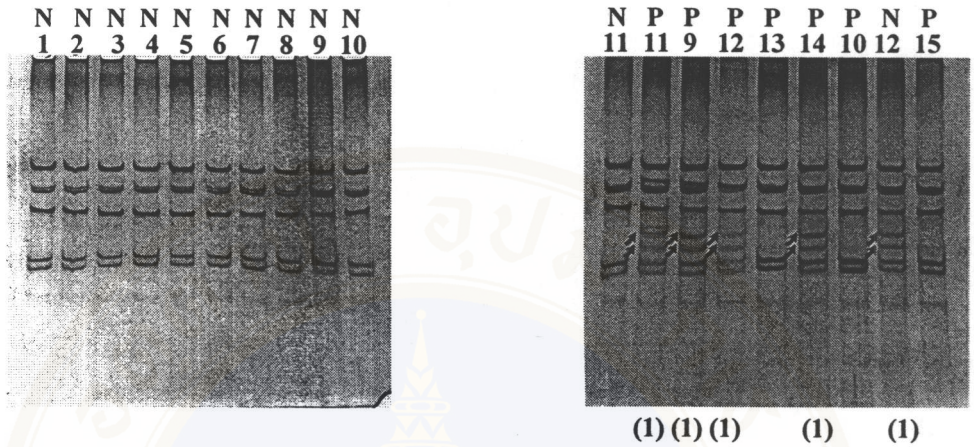

h

Exon 10

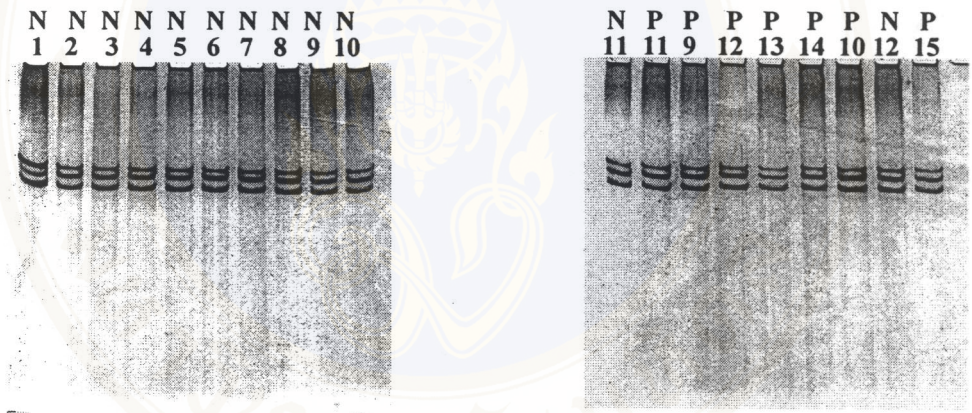

i

Exon 11

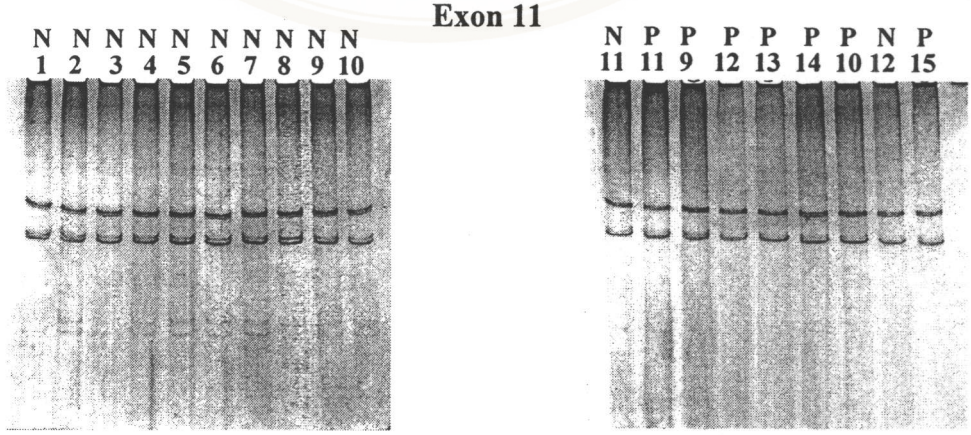

Exon 12

j

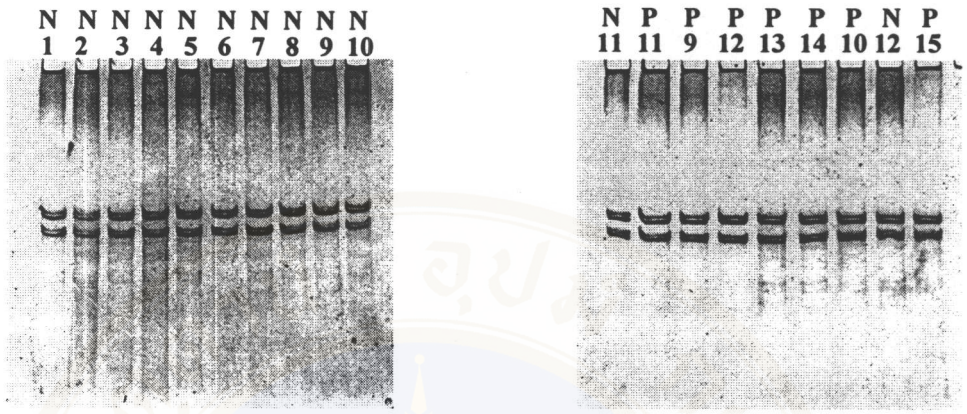

Exon 13

k

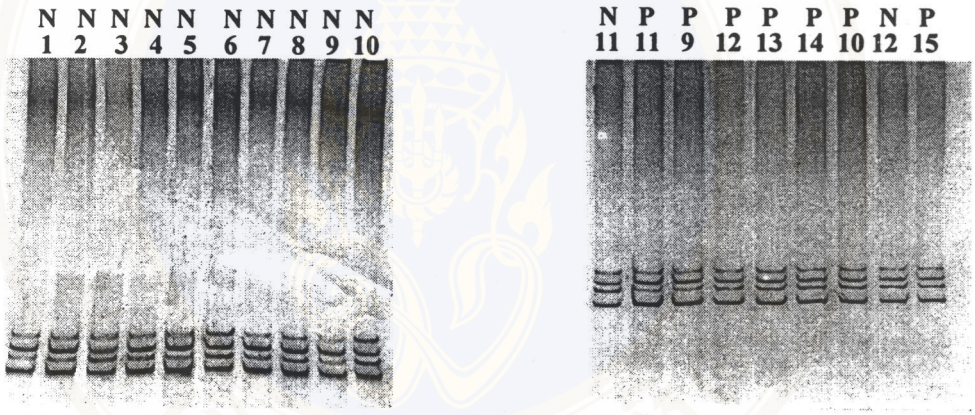

Exon 14

l

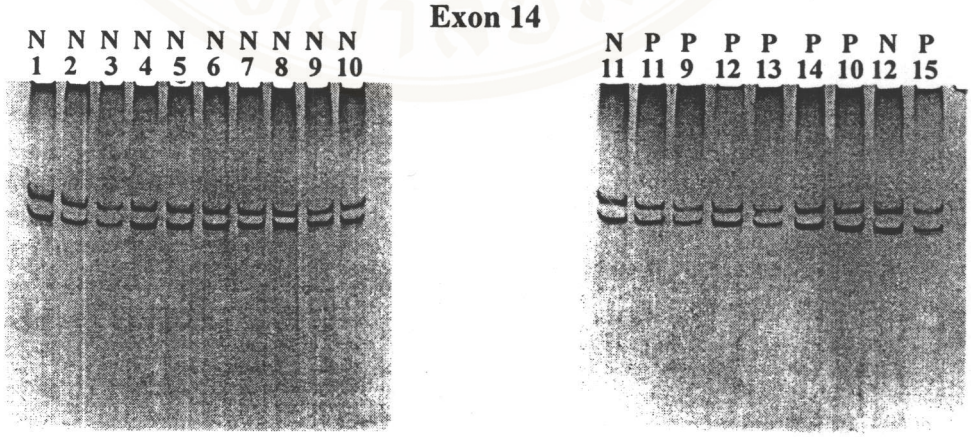

Exon 15

m

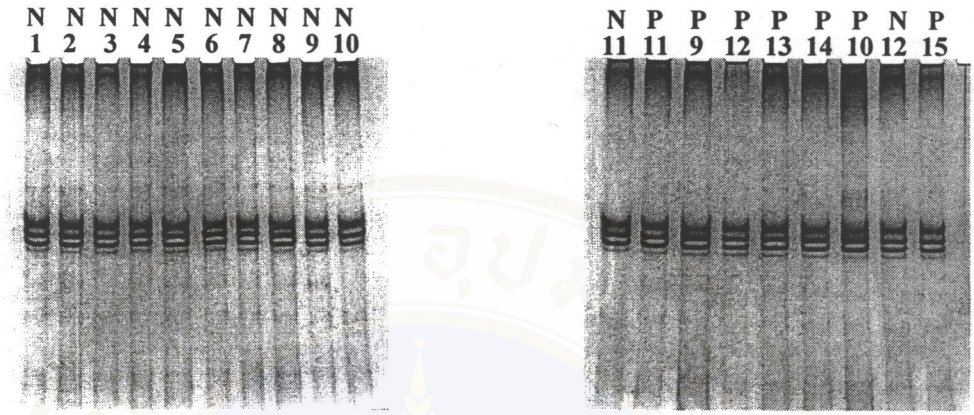

Exon 16

n

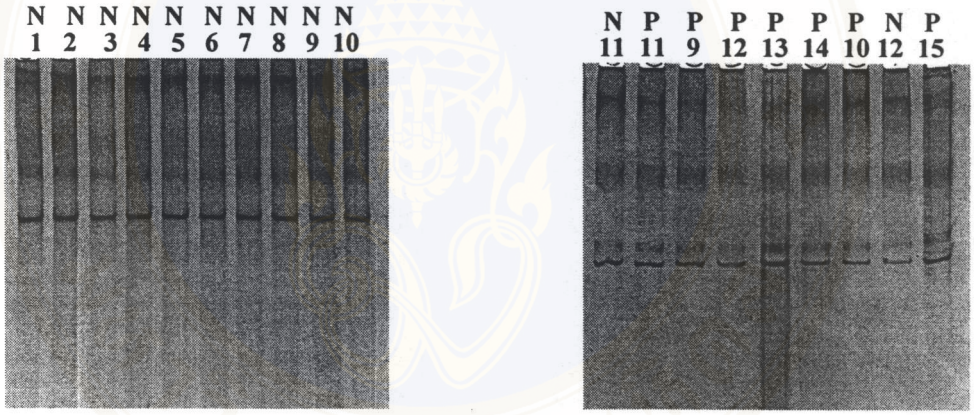

Exon 17

o

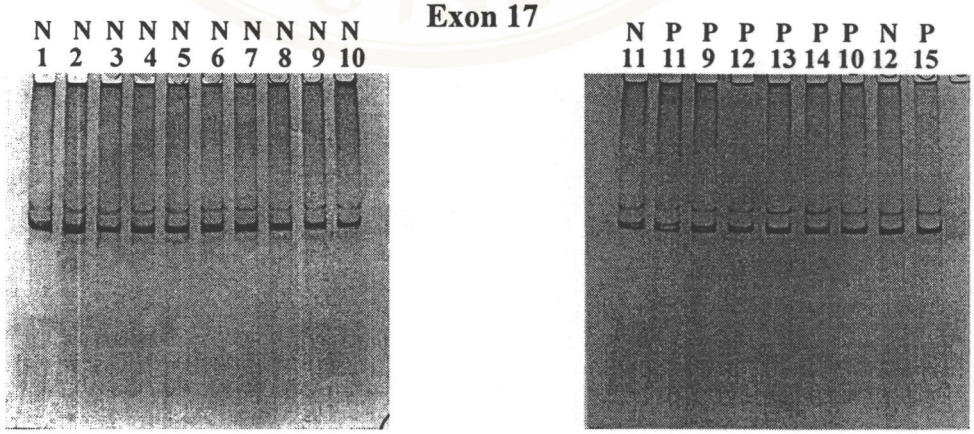

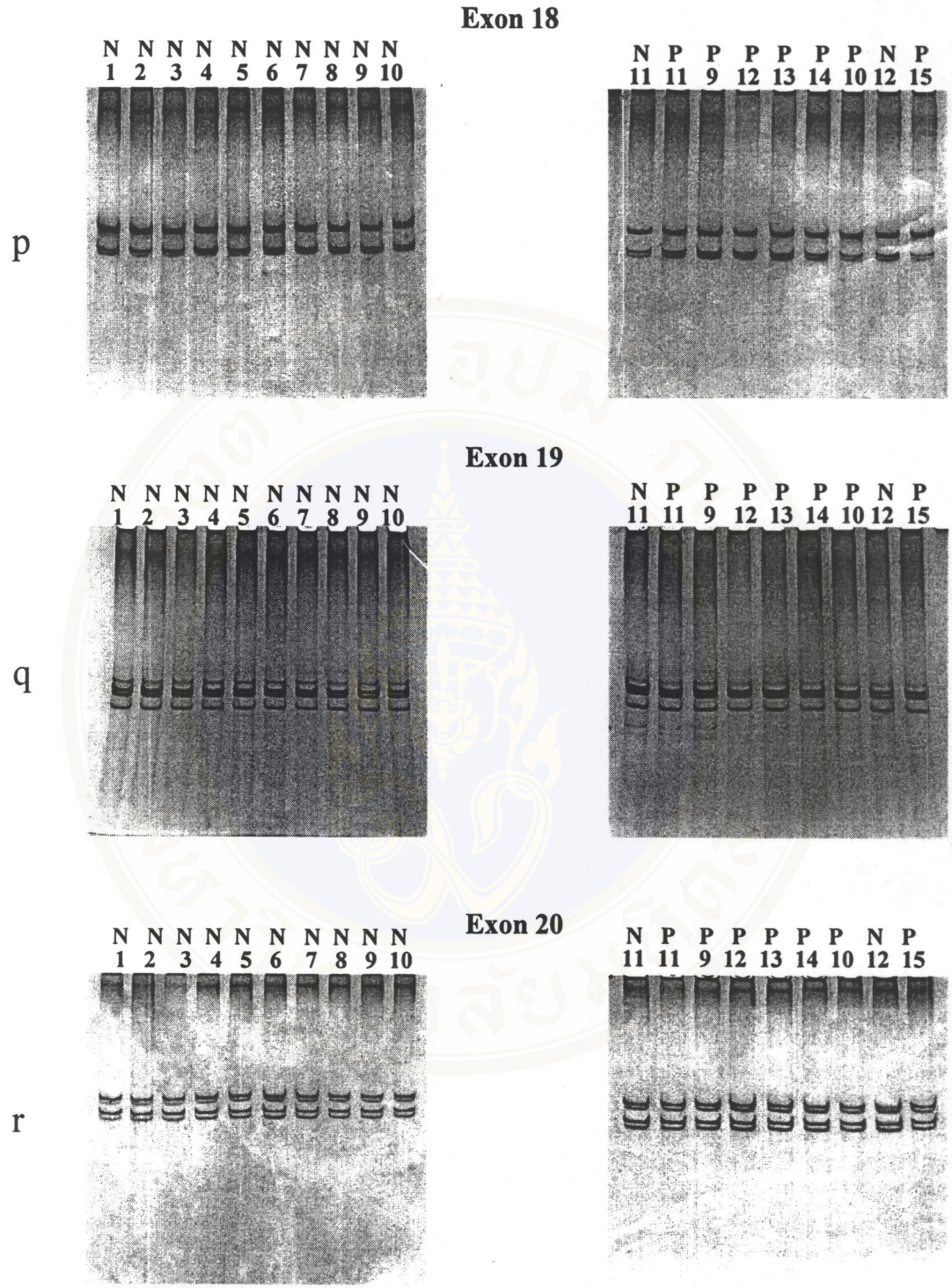

Figure 17 Screening of *AE1* mutations by non-RI PCR-SSCP analysis.

Eighteen regions of *AE1* (a-r) were analysed in DNA samples of 11 normal controls (N1-N11), 7 affected (P9-P15) and an unaffected (N12) members of a selected EdRTA family, by electrophoresis on non-denaturing 10% polyacrylamide gel containing 0.5% glycerol at room temperature, and silver nitrate staining.

Table 17 Summary of mobility shifts in four exons of *AE1* in four different conditions, screened by non-RI PCR-SSCP.

Subject		Exon 4				Exon 5				Exon 9				Exon 17			
		0.5%*		5%		0.5%		5%		0.5%		5%		0.5%		5%	
		RT	4°C	RT	4°C	RT	4°C	RT	4°C	RT	4°C	RT	4°C	RT	4°C	RT	4°C
Normal	N1	- **	-	-	-	-	-	-	-	-	-	-	-	-	+(3)	+(3)	-
	N2	+(1) ***	-	+(1)	-	-	-	-	-	-	-	-	-	-	-	-	-
	N3	-	-	-	-	-	-	-	-	-	-	-	-	-	-	-	-
	N4	-	-	-	-	-	+(2)	+(2)	+(2)	-	-	-	-	-	+(3)	+(3)	-
	N5	-	-	-	-	-	-	-	-	-	-	-	-	-	-	-	-
	N6	+(1)	-	+(1)	-	-	-	-	-	-	-	-	-	-	+(3)	+(3)	-
	N7	-	-	-	-			-	-	-	-	-	-	-	-	-	-
	N8	-	-	-	-	-	+(2)	+(2)	+(2)	-	-	-	-	-	-	-	-
	N9	+(2)	+(2)	+(2)	+(2)	+(1)	+(1)	+(1+2)	+(1+2)	-	-	-	-	-	-	-	-
	N10	-	-	-	-	-	-	-	-	-	-	-	-	-	-	-	-
	N11	-	-	-	-	-	-	-	-	-	-	-	-	-	+(3)	+(3)	-
	N12	+(2)	+(2)	+(2)	+(2)	+(1)	+(1)	+(1)	+(1)	+(1)	+(1)	+(1)	+(1)	-	-	-	-
Patient	P11	-	-	-	-	-	-	-	-	+(1)	+(1)	+(1)	+(1)	-	+(3)	+(3)	-
	P9	+(2)	+(2)	+(2)	+(2)	+(1)	+(1)	+(1)	+(1)	+(1)	+(1)	+(1)	+(1)	-	-	-	-
	P12	+(2)	+(2)	+(2)	+(2)	+(1)	+(1)	+(1)	+(1)	+(1)	+(1)	+(1)	+(1)	-	-	-	-
	P13	-	-	-	-	-	-	-	-	-	-	-	-	-	-	-	-
	P14	-	-	-	-	-	-	-	-	+(1)	+(1)	+(1)	+(1)	-	+(3)	+(3)	-
	P10	-	-	-	-	-	-	-	-	-	-	-	-	-	+(3)	+(3)	-
	P15	-	-	-	-	-	-	+(2)	+(2)	-	-	-	-	-	-	-	-

Notes: * Percentage of glycerol in 10% polyacrylamide gel

** - = Absence of mobility shift, + = Presence of mobility shift

*** Number in parenthesis represents pattern of mobility shift of ssDNA.

Table 18 Summary of the results of screening for *AE1* mutations and polymorphisms in normal controls and members of a selected EdRTA family by non-RI PCR-SSCP.

Subject	Region with mobility shift
N1	Exon 17
N2	Exon 4
N4	Exon 5
	Exon 17
N6	Exon 4
	Exon 17
N8	Exon 5
N9	Exon 4
	Exon 5
N11	Exon 17
N12	Exon 4
	Exon 5
	Exon 9
P11	Exon 9
	Exon 17
P9	Exon 4
	Exon 5
	Exon 9
P12	Exon 4
	Exon 5
	Exon 9
P14	Exon 9
	Exon 17
P10	Exon 17
P15	Exon 5

Seven of 11 DNA samples from normal controls (N1, N2, N4, N6, N8, N9, and N11), one from the unaffected member (N12), and 6 of 7 from the affected members (P11, P9, P12, P14, P10, and P15) had mobility shifts of ssDNA in these 4 exons (Figures 18a-18d, and Tables 17 and 18). DNA samples from 3 normal controls (N2, N6, and N9), the unaffected member (N12), and 2 affected members (P9 and P12) showed the mobility shifts in exon 4 (Figure 18a). DNA samples from 3 normal controls (N4, N8, and N9), the unaffected member (N12), and 3 affected members (P9, P12, and P15) demonstrated the mobility shift in exon 5 (Figure 18b). DNA samples from the unaffected member (N12) and 4 affected members (P11, P9, P12, and P14) contained the mobility shift in exon 9 (Figure 18c). And, DNA samples from 4 normal control (N1, N4, N6, and N11) and 2 affected members (P14 and P10) revealed the mobility shift in exon 17 (Figure 18d).

Sensitivity of each condition of the non-RI PCR-SSCP method for each exon was different. For exon 4, the polyacrylamide gel with both 0.5% and 5% glycerol and the electrophoresis at room temperature were more sensitive than the gels with the same concentrations of glycerol but the electrophoresis was performed at 4°C because in the two former conditions an additional mobility shift (pattern 1) could be detected in 2 DNA samples (from N2 and N6) but could not in the two latter conditions (Figure 18a and Table 17). For exon 5, the polyacrylamide gels with 0.5% glycerol and the electrophoresis at room temperature was less sensitive than all other conditions as a mobility shift (pattern 2) present in 2 DNA samples (N4 and N8) could not be seen, and the polyacrylamide gels with either 0.5% or 5% glycerol and

(a) Exon 4

I. 0.5% glycerol at RT

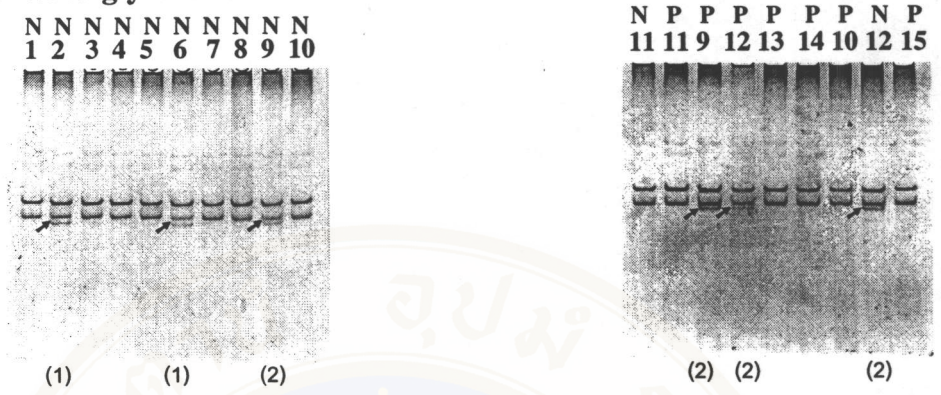

II. 0.5% glycerol at 4°C

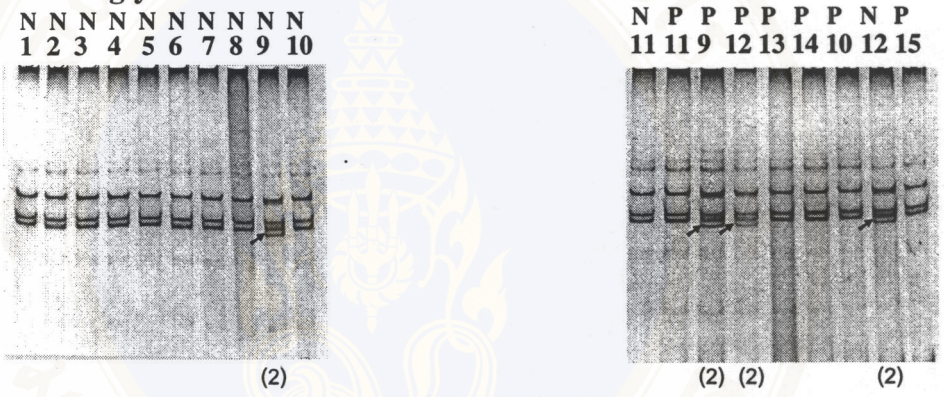

III. 5% glycerol at RT

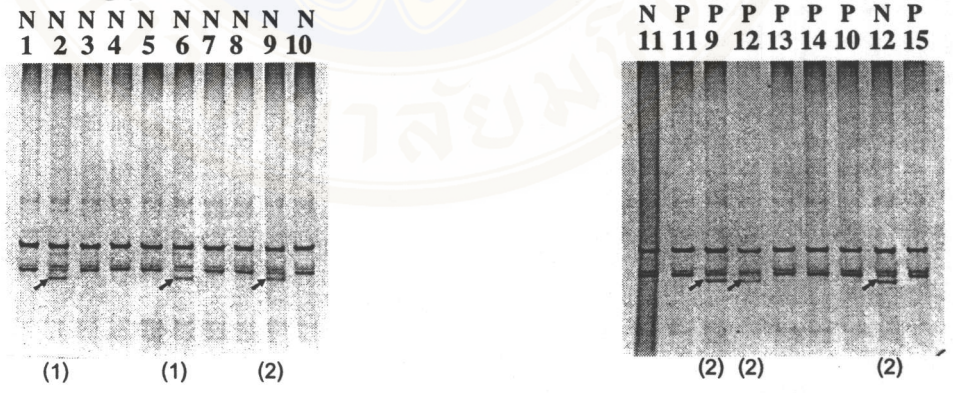

IV. 5% glycerol at 4°C

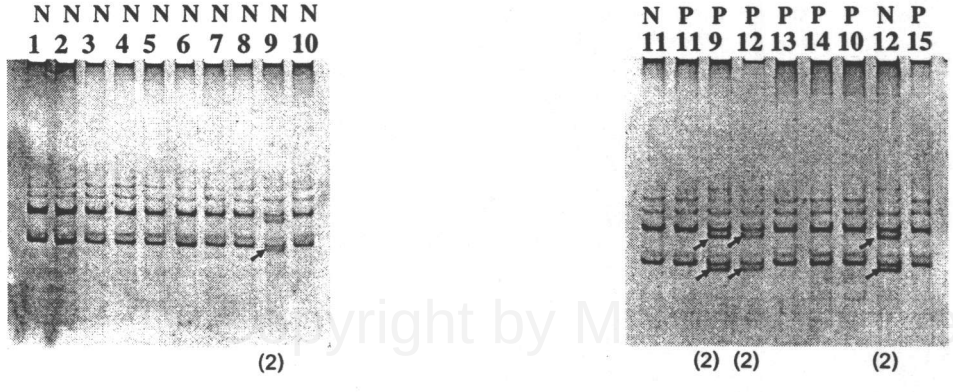

(b) Exon 5

I. 0.5% glycerol at RT

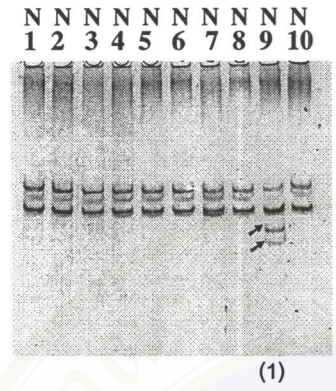

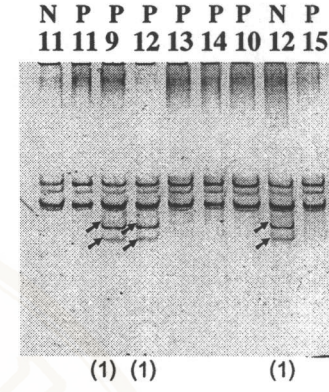

II. 0.5% glycerol at 4°C

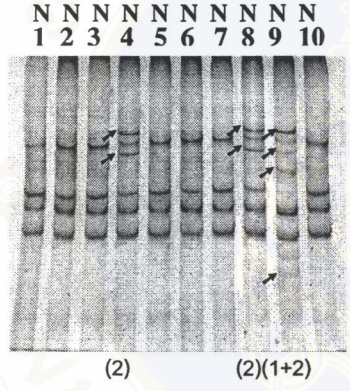

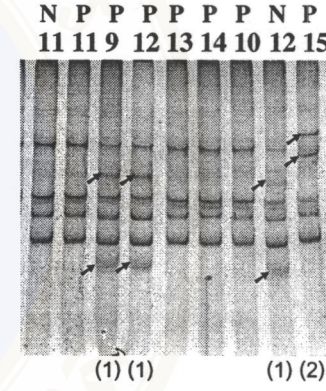

III. 5% glycerol at RT

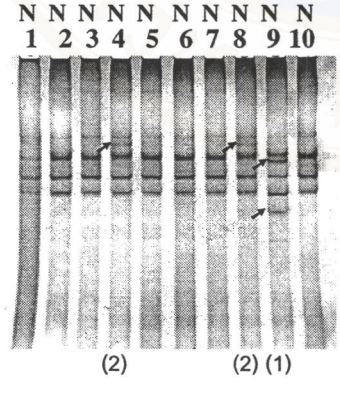

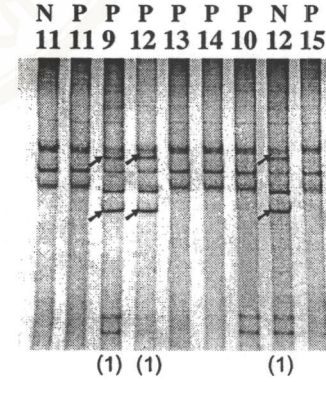

IV. 5% glycerol at 4°C

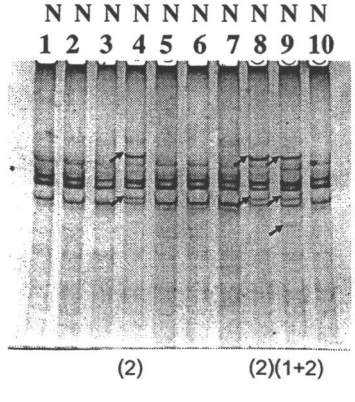

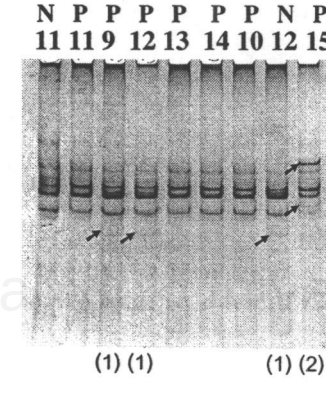

(c) Exon 9

I. 0.5% glycerol at RT

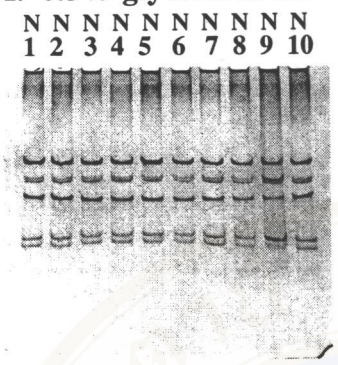

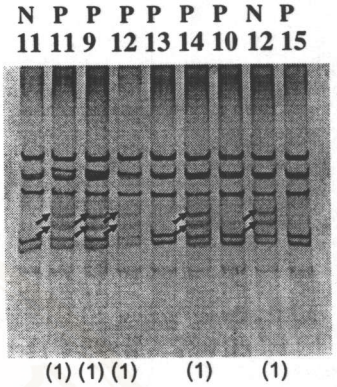

II. 0.5% glycerol at 4°C

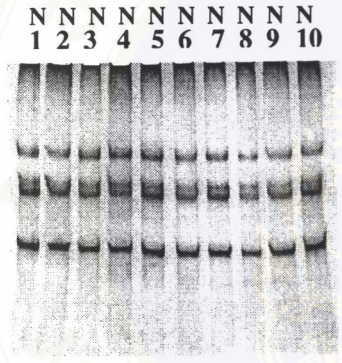

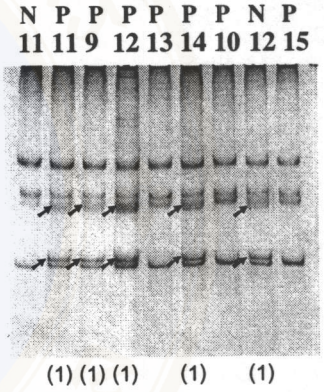

III. 5% glycerol at RT

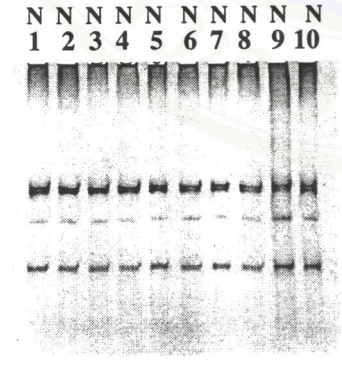

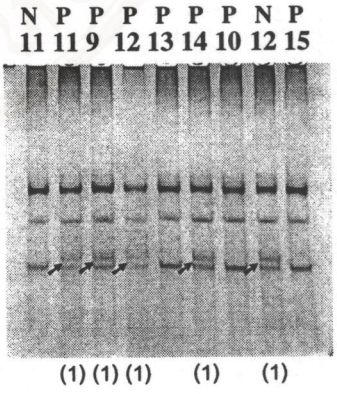

IV. 5% glycerol at RT

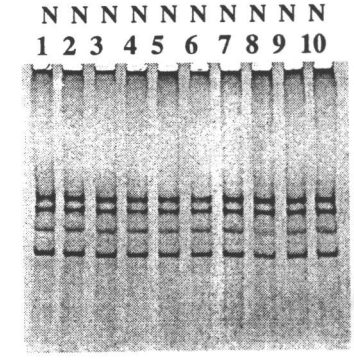

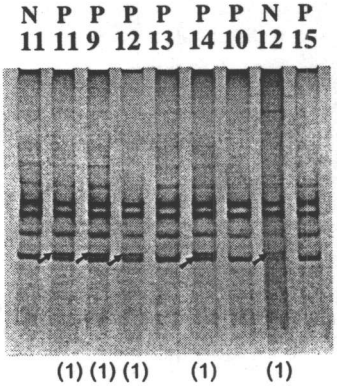

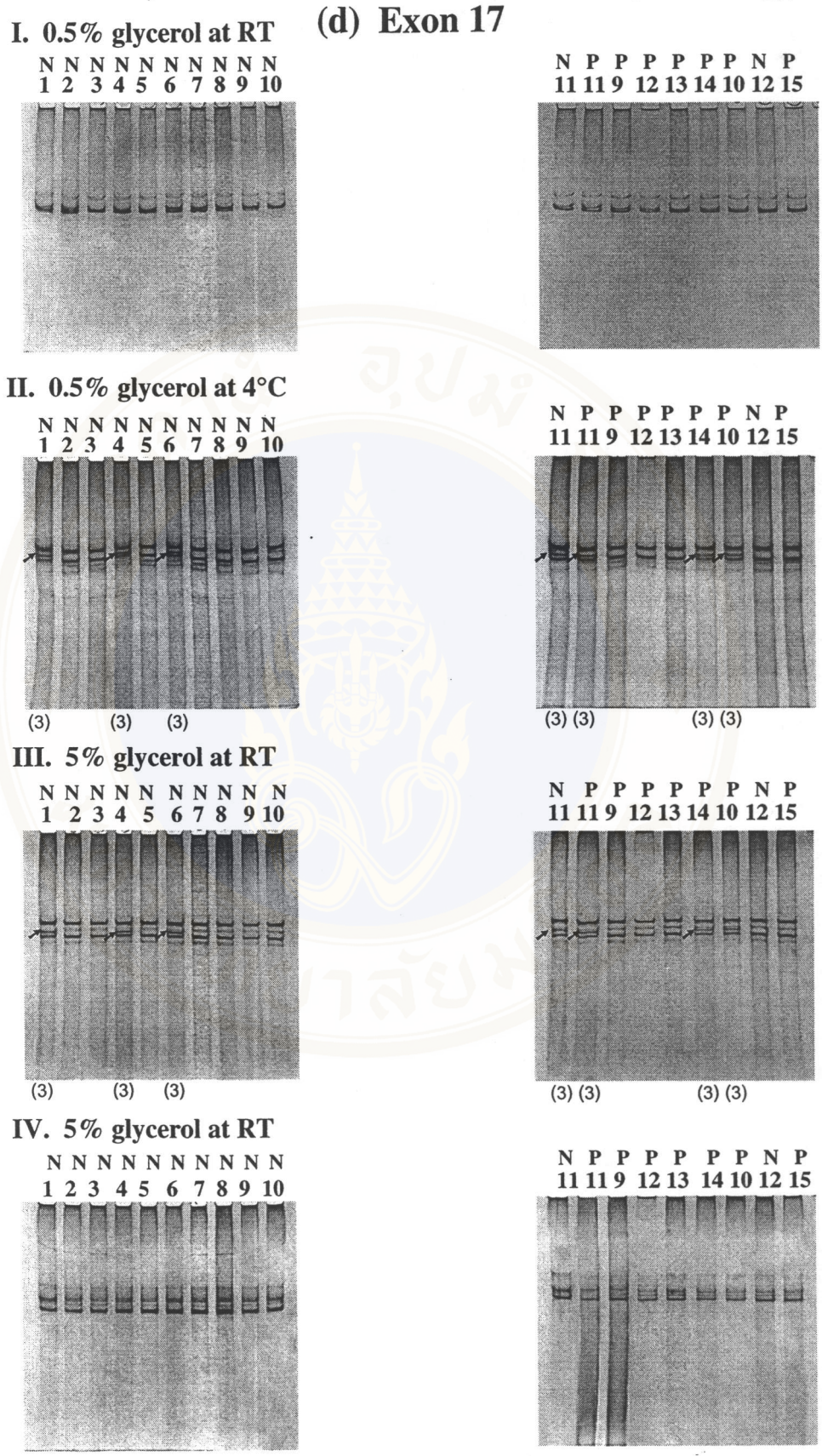

Figure 18 Four regions of *AE1* with mobility shifts of ssDNA (exons 4, 5, 9, and 17) in four different conditions of non-RI PCR-SSCP analysis.

The polyacrylamide gels contained 0.5% glycerol in panels I and II and 5% glycerol in panels III and IV. The electrophoreses were performed at room temperature (RT) for panels I and III, and at 4°C for panels II and IV. Arrow (↗) indicates mobility shift. Numbers in parentheses under the gels are mobility shift patterns.

The electrophoresis at 4°C were relatively most sensitive since more mobility shift were observed in 2 DNA samples (N9 and P15) (Figure 18b and Table 17). For exon 9, the sensitivities of all gel and electrophoretic conditions were the same (Figure 18c and Table 17). For exon 17, either the polyacrylamide gel with 0.5% glycerol and the electrophoresis at 4°C or the gel with 5% glycerol and the electrophoresis at room temperature was equally sensitive but the other two conditions did not show any mobility shift of ssDNA.

4. Characterization of nucleotide alterations in the exons with mobility shifts by direct sequencing analysis

The exons with mobility shifts as observed in the analyses by both RI PCR-SSCP and non-RI PCR-SSCP, indicating the presences of *AE1* mutations or polymorphisms, were further characterized by direct sequencing analysis (section 2.7 of the Methods). Altogether 5 exons with the mobility shifts including exons 4, 5, 9, 12, and 17 from 8 individuals namely P3, P8, P9, P15, N6, N8, N9, and N11 were subjected to the direct sequencing analysis (Table 19). Exons 4 and 5 showed two patterns of mobility shifts in the SSCP analysis and both of each were sequenced. The PCR products with normal mobility patterns from exons 4, 5, 9, and 12 of N11, and from exon 17 of P9 were also sequenced for comparison. The sequencing data of the exons with the mobility shifts were analysed by aligning to the sequence of the corresponding exons with the normal SSCP patterns and to the published human *AE1* genomic sequences available from the public database-*Entrez* (accession numbers:

X77738 and X77739 for 3' and 5' regions of *AE1* submitted from one group, and L35930 submitted from another group).

The sequencing analyses of the PCR products of exon 4 with the mobility shift pattern 1 in N6 and pattern 2 in P9 (Figures 15b, 17b, and 18a, and Table 19) showed that the mobility shift pattern 1 in N6 had an A to G transition at codon 56 (AAG-> GAG) causing substitution of lysine (K) by glutamic acid (E) in one allele of the *AE1* gene (Figure 19a), and the mobility shift pattern 2 in P9 occurred from an A to C transversion at codon 38 (GAC->GCC) resulting in substitution of aspartic acid (D) by alanine (A) in one allele (Figure 19b). Both K56E (Memphis I) and D38A missense polymorphisms have previously been reported (73, 88).

The PCR products of exon 5 also showed two patterns of mobility shifts in the SSCP analysis (Figure 18b and Table 19). The products with mobility shift pattern 1 from P9, pattern 2 from N8 and P15, and pattern 1+2 from N9 were selected for sequencing analysis and their sequences were compared to that of exon 5 from N11 (Figure 20). The results demonstrated that nucleotide changes were present in two regions, at IVS5+27 and codon 72. In the normal control sample (N11), the sequences at IVS5+27 and codon 72 were C and GAG, respectively. In the mobility shift pattern 1 (P9), they were C/T and GAG, and in the mobility shift pattern 2 (N8 and P15), they were C/C and GAG/GAT. And, in the mobility shift pattern 1+2 (N9), they were C/T and GAG/GAT. Comparison of the two published nucleotide sequences (L35930 and X77738) illustrated that the sequence at IVS5+27 could be either T/T or C/C but the codon 72 was only GAG (Table 5). The change of codon 72 from GAG to GAT leads to substitution of glutamic acid (E) by aspartic acid (D).

Table 17 Summary of mobility shifts in four exons of *AE1* in four different conditions, screened by non-RI PCR-SSCP.

Subject		Exon 4				Exon 5				Exon 9				Exon 17			
		0.5%*		5%		0.5%		5%		0.5%		5%		0.5%		5%	
		RT	4°C	RT	4°C	RT	4°C	RT	4°C	RT	4°C	RT	4°C	RT	4°C	RT	4°C
Normal	N1	- **	-	-	-	-	-	-	-	-	-	-	-	-	+(3)	+(3)	-
	N2	+(1) ***	-	+(1)	-	-	-	-	-	-	-	-	-	-	-	-	-
	N3	-	-	-	-	-	-	-	-	-	-	-	-	-	-	-	-
	N4	-	-	-	-	-	+(2)	+(2)	+(2)	-	-	-	-	-	+(3)	+(3)	-
	N5	-	-	-	-	-	-	-	-	-	-	-	-	-	-	-	-
	N6	+(1)	-	+(1)	-	-	-	-	-	-	-	-	-	-	+(3)	+(3)	-
	N7	-	-	-	-			-	-	-	-	-	-	-	-	-	-
	N8	-	-	-	-	-	+(2)	+(2)	+(2)	-	-	-	-	-	-	-	-
	N9	+(2)	+(2)	+(2)	+(2)	+(1)	+(1)	+(1+2)	+(1+2)	-	-	-	-	-	-	-	-
	N10	-	-	-	-	-	-	-	-	-	-	-	-	-	-	-	-
	N11	-	-	-	-	-	-	-	-	-	-	-	-	-	+(3)	+(3)	-
	N12	+(2)	+(2)	+(2)	+(2)	+(1)	+(1)	+(1)	+(1)	+(1)	+(1)	+(1)	+(1)	-	-	-	-
Patient	P11	-	-	-	-	-	-	-	-	+(1)	+(1)	+(1)	+(1)	-	+(3)	+(3)	-
	P9	+(2)	+(2)	+(2)	+(2)	+(1)	+(1)	+(1)	+(1)	+(1)	+(1)	+(1)	+(1)	-	-	-	-
	P12	+(2)	+(2)	+(2)	+(2)	+(1)	+(1)	+(1)	+(1)	+(1)	+(1)	+(1)	+(1)	-	-	-	-
	P13	-	-	-	-	-	-	-	-	-	-	-	-	-	-	-	-
	P14	-	-	-	-	-	-	-	-	+(1)	+(1)	+(1)	+(1)	-	+(3)	+(3)	-
	P10	-	-	-	-	-	-	-	-	-	-	-	-	-	+(3)	+(3)	-
	P15	-	-	-	-	-	-	+(2)	+(2)	-	-	-	-	-	-	-	-

Notes: * Percentage of glycerol in 10% polyacrylamide gel

** - = Absence of mobility shift, + = Presence of mobility shift

*** Number in parenthesis represents pattern of mobility shift of ssDNA.

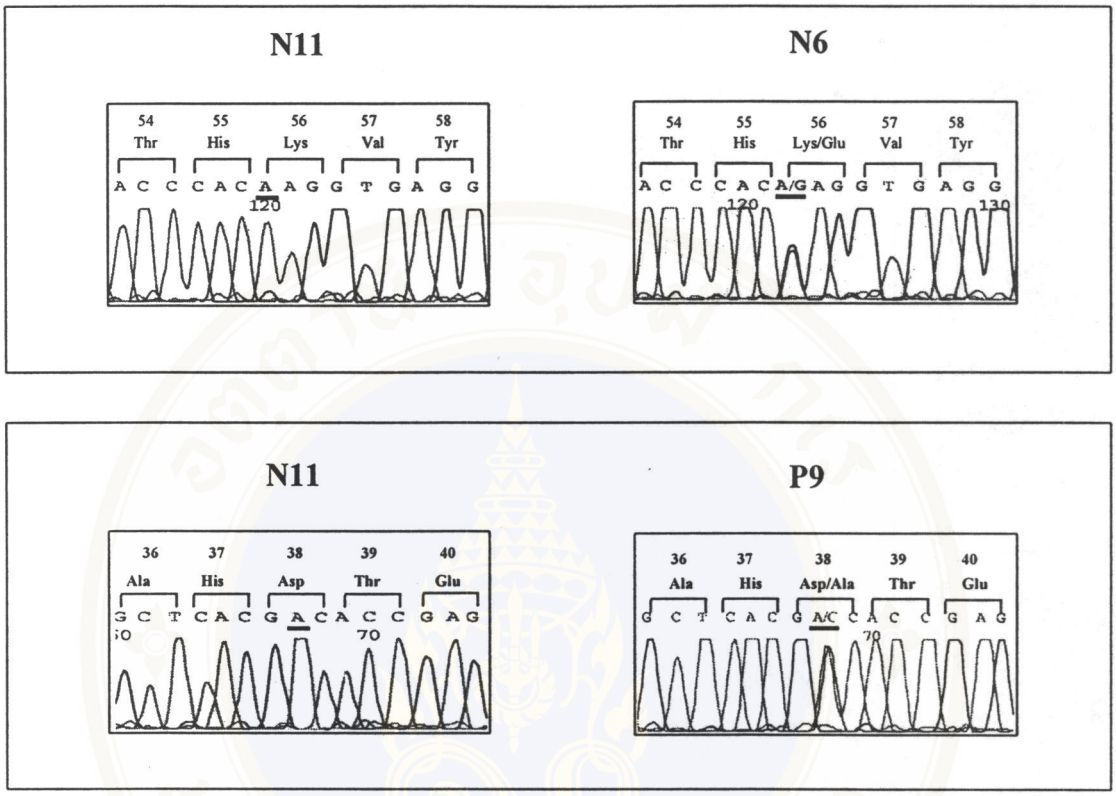

Figure 19 Electropherograms of automated DNA sequencing analyses of exon 4 with the SSCP mobility shift pattern 1 of the normal subject-N6 (a) and pattern 2 of the patient-P9 (b), comparing to the same sequence regions of the normal control-N11.

In a, an A to G transition at codon 56 (AAG->GAG) in exon 4 in N6 causes substitution of lysine (K) by glutamic acid (E) in one allele of the *AE1* gene. And, in b, an A to C transversion at codon 38 (GAC->GCC) in exon 4 in P9 results in substitution of aspartic acid (D) by alanine (A) in one allele.

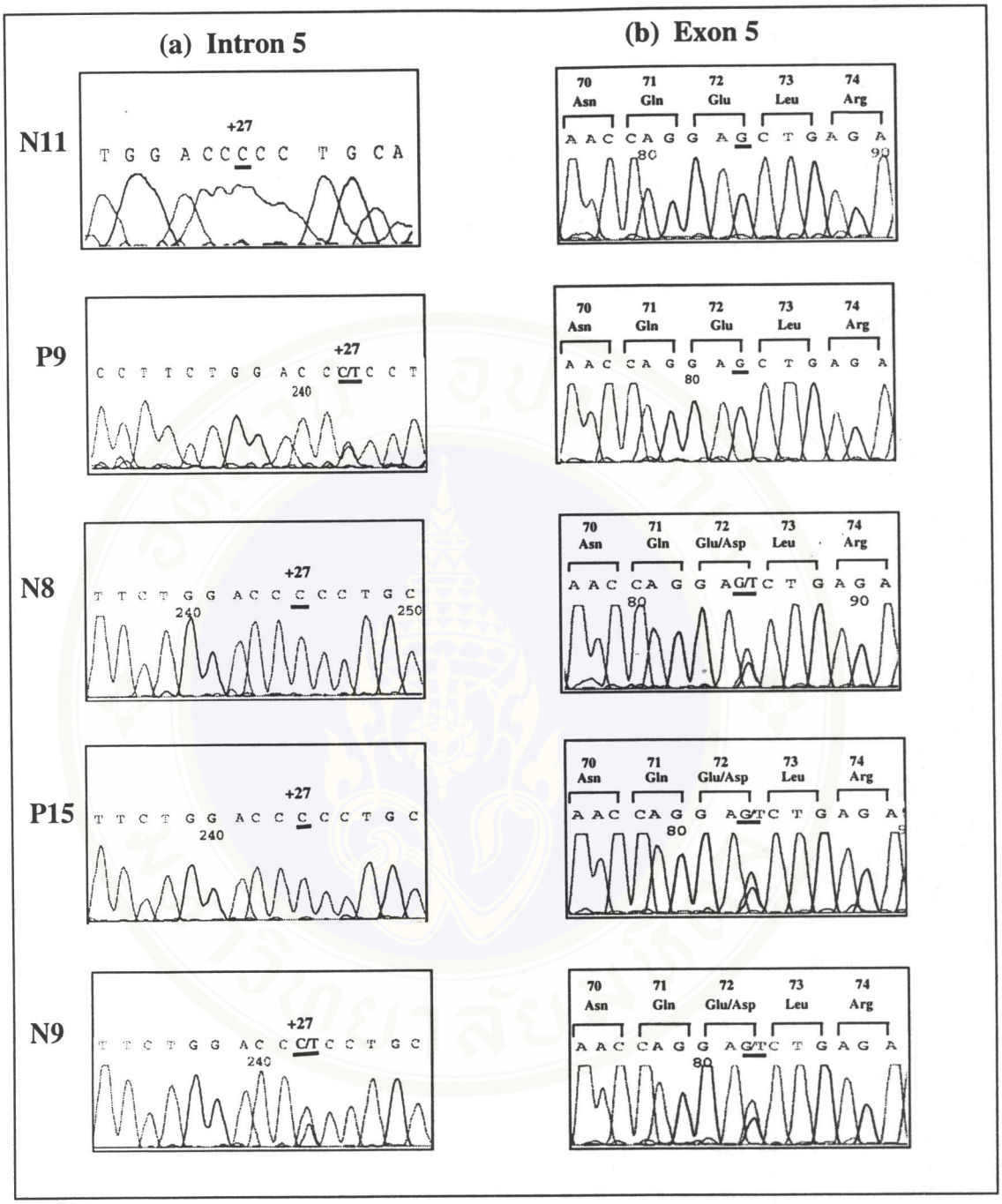

Figure 20 Electropherograms of automated DNA sequencing analyses of exon 5 of the normal control-N11, exon 5 with the SSCP mobility shift pattern 1 of the patient-P9, exon 5 with the mobility shift pattern 2 of the normal control-N8 and the patient-P15, and exon 5 with the mobility shift pattern 1+2 of the normal subject-N9.

The SSCP mobility shift pattern 1 in P9 occurs from intronic nucleotide variation, IVS5+27C/T, the pattern 2 in N8 and P15 from a substitution at codon 72 (GAG->GAT) resulting in the replacement of glutamic acid (E) by aspartic acid (D) in one allele, and the pattern 1+2 in N9 from both IVS5+27C/T and codon 72 (GAG->GAT) in one allele.

Table 20 Summary of DNA sequencing analyses of exon 5 of *AE1* in selected samples with the mobility shifts, compared to two published sequences from *Entrez* databases.

Subject	SSCP Pattern	Sequencing result	
		IVS5+27	Codon 72
N11	-	C/C	GAG/GAG
P9	+(1)	C/T	GAG/GAG
N8	+(2)	C/C	GAG/GAT
P15	+(2)	C/C	GAG/GAT
N9	+(1+2)	C/T	GAG/GAT
L35930*		T/T	GAG/GAG
X77738*		C/C	GAG/GAG

Note: * *Entrez* accession number.

The sequencing analyses of exon 9 from the normal control (N11) and from the patient (P9) who had the SSCP mobility shift in this exon (Figures 15g, 17g, and 18c) showed a nucleotide substitution at codon 266 (TTT->TTC) in one allele (Figure 21). Both TTT and TTC are codons for phenylalanine; therefore, it was a silent mutation.

The SSCP mobility shift in exon 12 of the patient-P8 (Figure 15j) was characterized and found to result from a nucleotide substitution at codon 438 (TCG-> TCA) in one allele (Figure 22). The TCG and TCA are codons for serine; therefore, it was also a silent mutation.

Two patterns of SSCP mobility shift were observed in the RI-PCR SSCP analysis of exon 17 in DNA samples from almost all patients. The mobility shift pattern 1 was found in the samples from 5 patients (P1, P3, P4, P5, and P6) and pattern 2 was observed in the samples from 4 patients (P2, P7, P8, and P9) (Figure 15o). In addition, 4 DNA samples each from the normal controls (N1, N4, N6, and N11) and from the patients (P11, P14, and P10) showed a mobility shift (pattern 3) in the non-RI PCR-SSCP (Figure 18d). One normal control DNA sample (N11) that had the mobility shift in the non-RI PCR-SSCP did not show the mobility shift in the RI-PCR SSCP.

The PCR products of exon 17 from N11, P3, and P9 were selected, representing each group of the SSCP mobility shift, for sequencing analysis. The results (Figure 23) showed that the PCR products of N11 had an intronic substitution at IVS17+19 where G was changed to A in one allele, of P3 contained a heterozygous G to A substitution at codon 701, changing GGC codon for glycine (G) to GAC

codon for aspartic acid (D) or resulting in G701D missense mutation, and of P9 did not have nucleotide change at these two and other positions.

In this study, almost all the PCR products with the SSCP mobility shifts were sequenced in both directions, except for the exon 4 of N6 and the exon 17 of P3. The G701D missense mutation observed in P3 was confirmed by restriction endonuclease digestion (see result in next section). All the mutations in the coding regions and nucleotide changes in the non-coding regions of the *AE1* gene identified in this study are summarized in Tables 21 and 22, respectively.

The PCR products with the SSCP mobility shifts in the normal control subjects and the patients which were determined by the sequencing analysis were assumed to carry the same mutations or nucleotide changes as those identified (Table 23).

5. Restriction endonuclease digestion analysis

The G701D missense mutation in exon 17 of the *AE1* gene occurred at the sequence of CCGG, which is a recognition, and digestion of the *Hpa*II restriction endonuclease. The mutation changed the sequence to CCGA, which destroys this *Hpa*II site. Since the RI PCR-SSCP mobility shift of exon 17 (pattern 1) was detected in 5 patients (P1, P3, P4, P5, and P6) (Figure 15o) but one of them (P3) was identified by DNA sequencing analysis, the *Hpa*II digestion analysis was therefore used to confirm this mutation in other patients. After the *Hpa*II digestions, 5 patients (P1, P3, P4, P5, and P6) showed both undigested and digested PCR products of exon 17

(Figure 24), indicating that they carried the G701D missense mutation in heterozygous state, and consistent to the result of RI PCR-SSCP. The other 5 patients (P2, P7, P8, P9, and P10) had only digested PCR products; therefore they did not carry this mutation.

Figure 21 Electropherograms of automated DNA sequencing analyses of exon 9 of the normal control-N11, and of the patient-P9 with the SSCP mobility shift.

The sequencing results showed a nucleotide substitution at codon 266 (TTT->TTC) in one allele without changing the encoded amino acid (phenylalanine) at this position of the AE1 protein; therefore, it was a silent mutation.

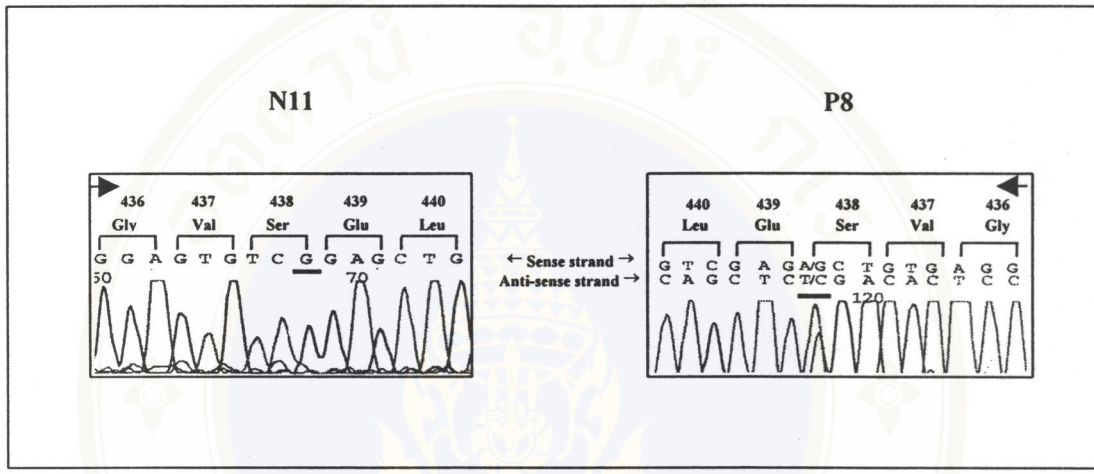

Figure 22 Electropherograms of automated DNA sequencing analyses of exon 12 of the normal control-N11, and of the patient-P8 with the SSCP mobility shift.

The sequencing results showed a nucleotide substitution at codon 438 (TCG->TCA) in one allele without changing the encoded amino acid (serine) at this position of the AE1 protein; therefore, it was a silent mutation. The sequencing analysis of exon 12 in the patient was carried out on anti-sense strand.

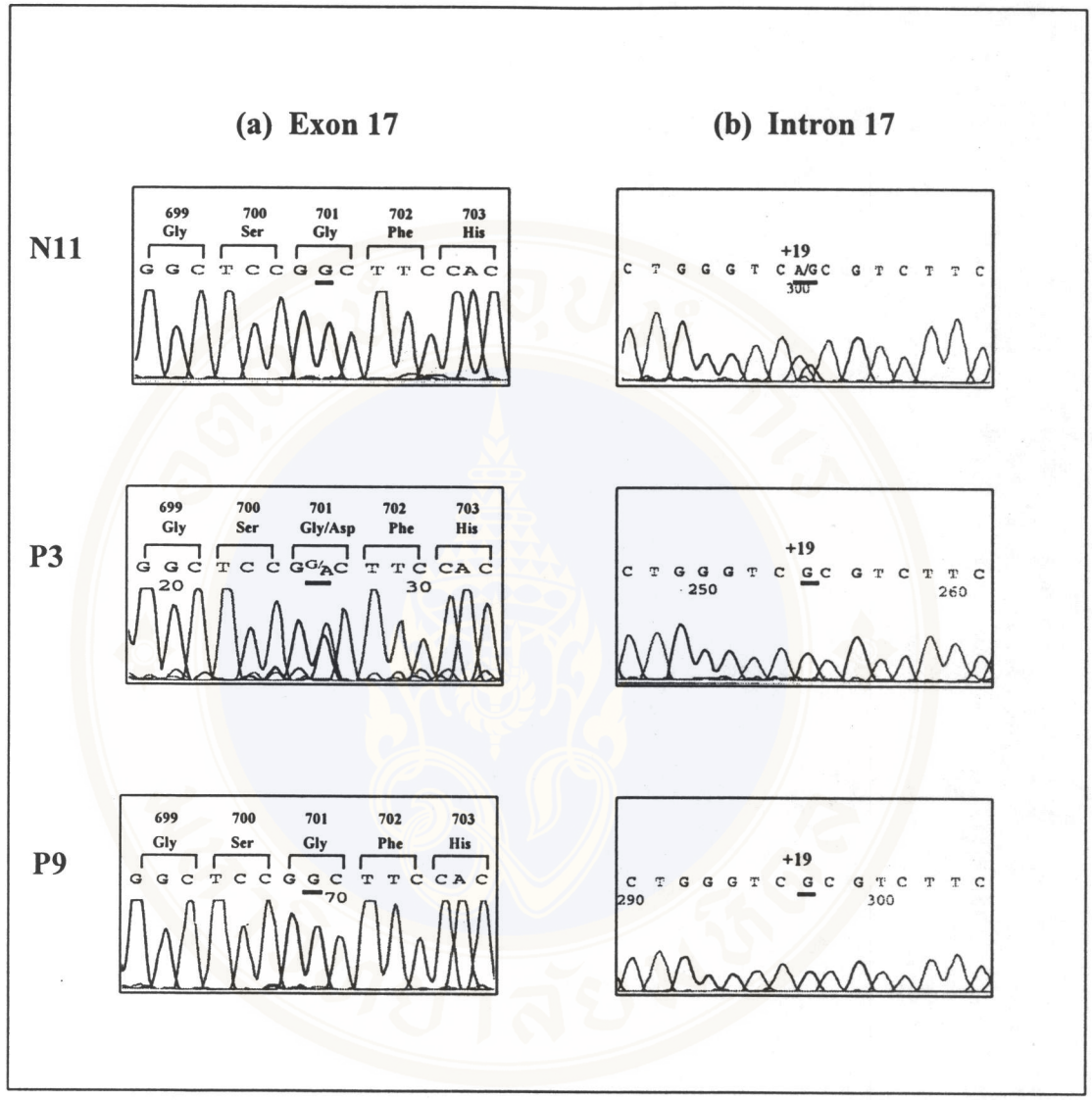

Figure 23 Electropherograms of automated DNA sequencing analyses of exon 17 of the normal control-N11 (also with the SSCP mobility shift pattern 3), of the patient-P3 with the SSCP mobility shift pattern 1, and of the patient-P9 with the SSCP mobility shift pattern 2.

The sequencing results showed a heterozygous nucleotide change at IVS17+19G>A in N11, and a heterozygous G to A substitution at codon 701 in P3, which changes the GGC codon for glycine (G) to GAC codon for aspartic acid (D) and results in G701D missense mutation. The result of sequencing analysis of exon 17 of P9 did not show any nucleotide change in both positions.

Table 21 Summary of mutations occurred in coding regions of the *AE1* gene.

Subject	Codon	Exon no.	Nucleotide change	Amino acid change	Type of mutation
N6	56	4	AAG > GAG	K56E	missense
N8	72	5	GAG > GAT	E72D	missense
N9	72	5	GAG > GAT	E72D	missense
P3	701	17	GGC > GAC	G701D	missense
P8	438	12	TCG > TCA	S438S	silent
P9	38	4	GAC > GCC	D38A	missense
	266	9	TTT > TTC	F266F	silent
P15	72	5	GAG > GAT	E72D	missense

Table 22 Summary of nucleotide changes identified in non-coding regions of the *AE1* gene.

Subject	Intron no.	Nucleotide change
N9	5	IVS5+27C>T
N11	17	IVS17+19G>A
P9	5	IVS5+27C>T

Table 23 Summary of mutations and nucleotide changes identified in this study.

Subject	Exon/ Intron no.	Amino acid change
N6 (N2, P1, P3, P4, P5, P6)*	4	K56E
N8 (N4)	5	E72D
P9 (N9, N12, P12)	5	E72D
N9	5	E72D
	5	IVS5+27C>T
N11 (N1, P10, P11, P14)	17	IVS17+19G>A
P3 (P1, P4, P5, P6)	17	G701D
P8	12	S438S
P9 (N9, N12, P12)	4	D38A
	9	F266F
P15	5	E72D

* Subject codes in parentheses represent the ones who had the PCR products with mobility shifts which were not directly sequenced, presumably carrying the same mutations as in the PCR products of those who were identified by the sequencing analysis.

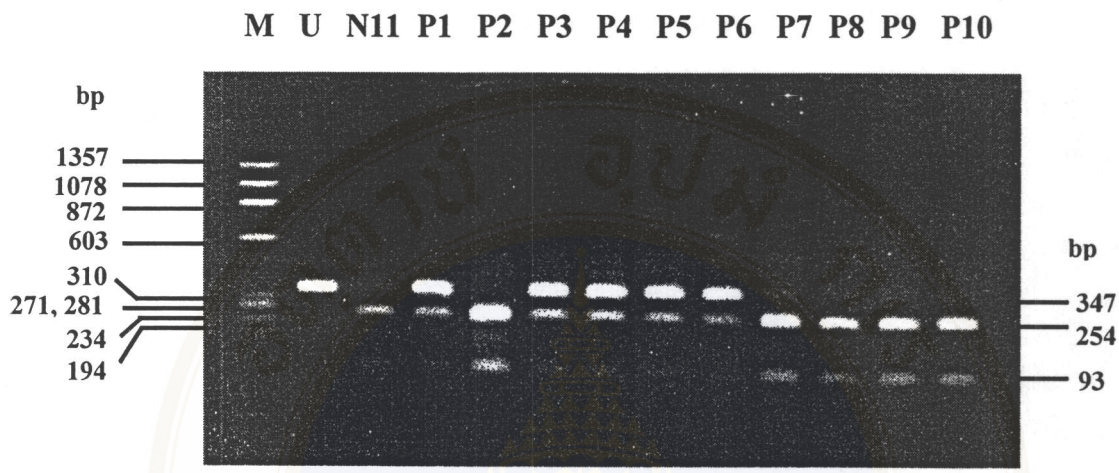

Figure 24 Agarose-gel electrophoresis of PCR products of exon 17 digested with *Hpa*II restriction endonuclease for detection of G701D missense mutation.

Lane M is *Hae*III-digested PhiX174 RF DNA marker. Lane U is undigested PCR product of a normal control (N11) sample, showing a DNA fragment with the size of 347 bp. Lane N11 is digested PCR product of the normal control sample, presenting the DNA fragments with the sizes of 254 and 93 bp. Lanes P1-P10 are digested PCR products of 10 patients. Five patients (P1, P3, P4, P5, and P6) had both undigested PCR products (347) bp and digested (254 and 93 bp), indicating the presence of heterozygous G701D missense mutation. The other 5 patients showed only the digested PCR products (254 and 93 bp), indicating the absence of this mutation.

6. DNA linkage analysis

DNA linkage analysis was also carried out to investigate whether or not the *AE1* gene would be involved as the causative defective-gene of EdRTA in the patients, which would provide a broader information concerning the involvement of the *AE1* gene in this disease. The DNA linkage analysis using a microsatellite, D17S787, marker mapped at about 3 cM from the *AE1* gene, was performed in the family which was also selected for the mutation screening by non-RI PCR-SSCP method (Figure 25). In this family, 5 sibs (P11, P9, P12, P14, and P10) and 1 cousin (P15) were affected while 1 sib (N12) was not affected. In addition, an affected male (P13) married to an affected member (P12) of the family was also included. Unfortunately, all parents of the major branch of the family were expired and members of only a single generation of the family were available for the study.

The result (Figure 25) showed that this marker was very polymorphic; altogether 6 alleles (A-F) were detected. Four alleles (B, C, D, and F) were segregated in the family. Alleles A and E were found in P13 who was the husband of P12. Two genotypes, CF and BD, were observed in the 6 affected sibs and cousin. However, one unaffected sib also had the BD genotype.

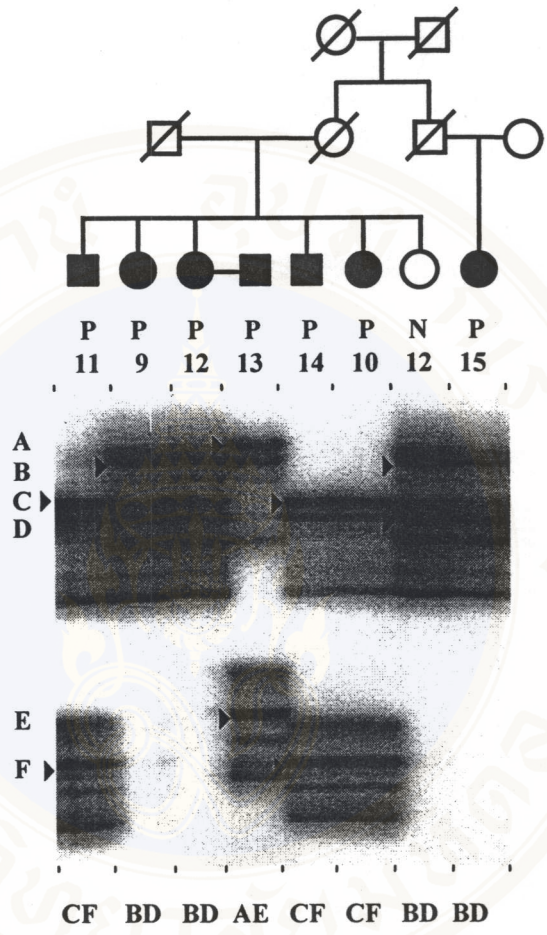

Figure 25 DNA linkage analysis of a selected family with EdRTA by using a microsatellite, D17S787, marker located in the *AE1* region.

The family pedigree is shown above the autoradiogram. The family member codes are under the symbols. Square is male and circle is female. Filled symbols (● , and ■) represent affected members and blank symbol represents unaffected member. Alleles (A-F) are shown on the left of the autoradiogram and the arrow head (‣) points to the location of each allele in the autoradiogram. The genotypes identified by the analysis using this marker are indicated under the lanes of samples of the autoradiogram.

CHAPTER VI

DISCUSSION

Endemic distal renal tubular acidosis (EdRTA) is a group of medical conditions which are major public health problems in the northeast of Thailand (1, 3). The etiology of EdRTA is still unknown. The disease is found within an area in which the population is fairly homogeneous and their nutritional and socioeconomic status are poor, suggesting the role of environmental factors in its pathogenesis (1, 3). No autoimmunity background has been found, since the results of autoantibody screenings were negative (1). Potassium deficiency (2, 3) and vanadium toxicity (6, 12, 42, 43) were suggested to play role as the pathogenic factors. The spectrum of EdRTA was observed and proposed to be due to tubulointerstitial damage associated with potassium deficiency (2). No evidence that the vanadium toxicity really exists. Therefore, the hypothesis based on environmental factors has not yet definitely been proved. As familial dRTA has been well documented (18, 19, 133) and high incidence of familial association was found in the study of EdRTA in the northeastern population of Thailand (1), genetic factors may also be involved in the pathogenesis of this disease. In the study by Nilwarangkur *et al.*, an autosomal dominant mode of inheritance were found in five families and possible in another five families (1).

Although the defects of several enzymes or proteins responsible for the acid secretion and/or acid-base regulation in renal tubular epithelial cells, including

H^+-ATPase, H^+/K^+-ATPase, carbonic anhydrase II (CA II), and anion exchanger 1 (AE 1), can potentially result in dRTA, AE1 is the most likely candidate of EdRTA. The mutations in the gene encoding B1 subunit of the H^+-ATPase were found in autosomal recessive dRTA patients with sensorineural deafness (22) and that of *CA II* gene was observed in autosomal recessive syndrome of osteopetrosis with RTA and cerebral calcification (16). The clinical characteristics of these two groups of defects are not compatible to that was described for EdRTA (1). The defect of *H^+/K^+-ATPase* in humans has not yet been observed.

Recently, mutations of the *AE1* gene were found to be associated with familial dRTA in both autosomal dominant (28-31) and autosomal recessive (32, 33) forms. The autosomal dominant dRTA associated with *AE1* mutations was usually found in adults while the autosomal recessive dRTA associated with *AE1* mutations was frequently observed in children. Different types of *AE1* mutations were discovered in these two categories of dRTA, which had particular clinical manifestations and distinct modes of inheritance. Mutations of *AE1* at the same codon, codon 589, were independently observed in autosomal dominant dRTA by three research groups (28-31). The heterozygous missense mutations (R589H, R589C, or R589S) were found in several unrelated families with autosomal dominant dRTA, which R589H was most common. Other mutations of *AE1* associated with autosomal dominant dRTA were IVS12+1G>A (band 3 Pribram), S613F, and 13-bp duplication in exon 20 of *AE1* (28-30).

The work presented in this thesis was initiated from the question that whether or not *AE1* mutation is involved in EdRTA in the northeastern people of

Thailand. The *AE1* gene was therefore considered in the study as a candidate gene for EdRTA and was extensively investigated by mutation screening and sequencing analysis.

The PCR-SSCP technique was used to screen mutations of *AE1* in this study. This technique offers advantages over several currently used methods, particularly in terms of its simplicity and rapidity. Although, its sensitivity is not 100%, the high efficiency, which appears to be achievable with PCR-SSCP, has made it a powerful method for screening mutations (134). The RI PCR-SSCP was primarily used because it was first developed and widely used as a standard method for PCR-SSCP. However, it still has two important problems. It is laborious because it requires the use of radioisotope and large-formatted sequencing gel. The other is time consuming. Because the gel temperature is the most important parameter affecting the conformation of ssDNA, the electrophoresis must be run at low voltage (usually overnight) to avoid heat-induced conformational changes. Therefore, there are now several reports describing non-radioisotopic protocols for PCR-SSCP analysis. The main options that have been explored are silver staining, ethidium bromide staining, chemiluminescence, or fluorescence (97, 107, 135-137). In addition, the large formatted gel in conventional radioisotopic protocol is modified by using mini gel, semiautomated electrophoresis or automated sequencer for SSCP analysis (97, 107, 136, 137).

In this study, non-RI PCR-SSCP analysis using a mini gel system and silver-staining method was performed. This technique has many advantages in comparison with the radioisotopic and others non-RI PCR-SSCP methods reported

earlier (95, 96, 138, 139), since it eliminates problems concerning safety, handling, cost, and time. The advantages are as follows: *(i)* this technique does not use radioisotope, *(ii)* the handling of a mini gel is much easier than that of a large gel, *(iii)* a mini gel apparatus is cheaper than a semiautomated electrophoresis or automated sequencer, and *(iv)* this technique is dramatically increased speed than conventional radioactive method.

Although, non-RI PCR-SSCP is a rapid, inexpensive and relatively safe method, its sensitivity may be lower than that of the conventional radioactive technique. The longer electrophoresis of the radioactive labeled DNA fragment on a thinner and longer gel normally gives a better resolution. From the results of study in this thesis, the sensitivities of RI and non-RI PCR-SSCP methods could not be compared because different sets of DNA samples were analysed by the two methods. However, all DNA samples showing mobility shifts in the RI PCR-SSCP method were also found to have mobility shifts in the non-RI PCR-SSCP technique.

The sensitivity of PCR-SSCP analysis is generally mentioned to be about 80% if PCR fragments are shorter than 300 bp (94, 140). There are several factors that critically influence the sensitivity of PCR-SSCP analysis, including the size and sequence of DNA fragment, electrophoresis temperature, gel additives, percentage of polyacrylamide, acrylamide cross-linking, and ionic strength of the buffer (100-102, 104, 107, 108).

In this study, the sizes of PCR products of 18 regions of *AE1* gene were usually less than 350 bp, except for that from the amplification of the kidney promoter (intron 3) which was 491 bp in size (Table11). A study by Orita *et al* (96) has shown

that the sensitivity of detection of mobility shift may be dropped to 70-80% for the fragment up to 400 bp. However, there are many reports showing that combination of many different conditions increase the sensitivity of SSCP analysis (93, 141, 142). Therefore, 4 different combinations of gel components and electrophoresis conditions of the non-RI PCR-SSCP method were used to optimize its sensitivity. The electrophoresis was performed at both room temperature and 4°C because the conformation of intrastrand bonds, and thereby the conformation of ssDNA, is temperature dependent. In addition to temperature, the presence of glycerol in the gel affects the conformation of ssDNA significantly. Hence, glycerol in varied concentrations, 0.5% or 5%, was used in this experiment.

From the results of mutations screening in 18 regions of *AE1* by the silver-stained PCR-SSCP in the 4 different conditions, the mobility shifts were observed in 4 regions which were exons 4, 5, 9, and 17. These mobility shifts were detected in the DNA samples from both EdRTA patients and normal subjects. In addition, the sensitivity for detection of mobility shift in each condition was different for each exon (section 3 of the Results). The most suitable conditions for detections of the mobility shifts in these 4 exons were summarized in Table 24. These findings that the overall sensitivity was increased by increasing the number of conditions for SSCP analysis agree with those reported by others (93, 141, 142). However, employing the number of conditions for each region is time consuming and has to weigh against the improved sensitivity.

Table 24 Summary of the most suitable conditions for detections of mobility shifts in 4 exons of *AE1*.

Region	Optimal condition
Exon 4	Polyacrylamide gel with 0.5% glycerol, and electrophoresis at room temperature for 2 hours and 30 minutes Polyacrylamide gel with 5% glycerol, and electrophoresis at room temperature for 4 hours and 30 minutes
Exon 5	Polyacrylamide gel with 5% glycerol, and electrophoresis at room temperature or 4°C for 3 hours and 30 minutes
Exon 9	Polyacrylamide gel with 0.5% glycerol, and electrophoresis at room temperature or 4°C for 3 hours and 30 minutes Polyacrylamide gel with 5% glycerol, and electrophoresis at room temperature or 4°C for 6 hours
Exon 17	Polyacrylamide gel with 0.5% glycerol, and electrophoresis at 4°C or Polyacrylamide gel with 5% glycerol, and electrophoresis at room temperature for 5 hours and 30 minutes

From the results of screening of mutations in 18 regions of the *AE1* gene by both RI PCR-SSCP and non-RI PCR-SSCP analyses, mobility shifts were observed in 8 normal control subjects (N1, N2, N4, N6, N8, N9, N11, and N12) and 14 EdRTA patients (P1, P2, P3, P4, P5, P6, P7, P8, P9, P11, P12, P14, P10, and P15), in 5 regions, exons 4, 5, 9, 12, and 17, of the *AE1* gene. More than one pattern of mobility shifts was found in all exons, except for exons 9 and 12. Several individuals shared the same pattern of mobility shift in the same exon (Table 19).

Sequencing analyses were performed in all 5 exons with the mobility shifts in 8 individuals (N6, N8, N9, N11, P3, P8, P9, and P15) who were selected as representatives of each group. Altogether 15 PCR products (one exon each from N6, N8, N9, P3, P8, and P15, four exons from P9, and five exons from N11) were subjected to the sequencing analysis (Table 19). The results of sequencing analysis showed that one pattern of mobility shift each of exons 5 and 17 occurred from nucleotide changes in the non-coding regions, IVS5+27C>T and IVS17+19G>A, respectively (Tables 22 and 23). The IVS5+27C>T was found in only N9 and the IVS17+19G>A in N11 and presumably also in N1, P10, P11, and P14. As the former was found in a normal control subject (N9) and the latter seemed to be present in both normal control subjects (N11 and N1) and patients (P10, P11, and P14), and as the two nucleotide changes occurred in the non-coding regions, they were unlikely to be significant alterations.

Two silent mutations, F266F and S438S, were observed in two patients, P9 and P8, respectively (Table 21). The former might also be present in N9, N12, and P12 while the latter was in only P8 (Table 23). Since these two mutations did not change amino acids, it is obvious that they have no effect to the AE1 protein.

Four missense mutations including K56E, D38A, E72D, and G701D were identified by the sequencing analysis in N6 (K56E), P9 (D38A), N8, N9, and P15 (E72D), and P3 (G701D) (Table 21). These missense mutations were also likely to be present in other individuals who had the same pattern of the mobility shift of the same PCR product i.e. K56E in N2, P1, P3, P4, P5, and P6; D38A in N9, N12, and P12; E72D in N4; and G701D in P1, P4, P5, and P6 (Table 23). The presence of G701D

missense mutation in P1, P4, P5, and P6 could also be confirmed by the inability to digest the PCR products of exon 17 from these patients by *Hpa*II restriction endonuclease (Figure 23). The K56E and G701D missense mutations seemed to have linkage disequilibrium (Figure 16b and 16o); this finding has also previously been recorded (32, 33).

The K56E (band 3 Memphis I) and D38A (band 3 Darmstadt) missense mutations which were found in normal control subjects and patients in this study have previously been reported to be polymorphisms (73, 88). Both mutations were unlikely to be associated with EdRTA. E72D is a new *AE1* missense mutation and proposed to be called 'band 3 Siriraj I'. It was observed in a patient (P15), two normal control subjects (N8 and N9), and probably an additional normal control subject (N4) who had the same mobility shift in exon 5. It is most likely to be a non-disease mutation for the reason that it was present in normal control subjects as well as a patient. Another reason is that E72D is a conservative amino-acid substitution; glutamic acid (E) and aspartic acid (D) are both negatively charged amino acids. The substitution of glutamic acid by aspartic acid should not change the normal function of the AE1 protein.

The G701D (band 3 Bangkok I) missense mutation was found in five patients (P3, P1, P4, P5, and P6) without detecting the normal control subjects. It is a reported disease mutation which causes autosomal recessive dRTA in children (32, 33). Heterozygous G701D mutation does not result in dRTA as evident by that the parents of the children with dRTA caused by homozygous G701D or compound heterozygous G701D/exon 11Δ27 did not have dRTA. In addition, the results of

G701D mutation analysis by the group in the Division of Medical Molecular Biology showed that it could be found in heterozygous state in both normal and affected members of some families with EdRTA from the northeast of Thailand and it did not seem to have association with the disease (unpublished data). Since the G701D mutation as found in five patients with EdRTA in this study was also in heterozygous condition, it is unlikely to cause the disease in these patients.

Some genetic diseases have been found to result from two hits of mutations in the different alleles of the same locus; the first hit is an inherited germline mutation and the second hit is a non-inherited somatic mutation occurring in the cell of the affected organ (143). This group of diseases is phenotypically dominant but cellularly and molecularly recessive. They are often malignant disorders and their characteristics relate to clonal expansion of the abnormal cells harboring both germline and somatic mutations. Autosomal dominant polycystic kidney disease (ADPKD) which is caused by mutations of the *PKD1* or *PKD2* genes is also suggested to result from such two-hit mutations (144-147). Although it is not a malignant disease in nature, the cyst formation may involve clonal expansion of the defective renal epithelial cell (144). The two-hit model of pathogenesis may be applicable to explain adult-type dRTA and EdRTA which are late-onset autosomal dominant disorder, if they have the characteristics of malignancy or clonal expansion. However, this is not found to be the case for both adult-type dRTA and EdRTA. In addition, if the G701D mutation was involved in the pathogenesis of EdRTA as the first hit, it should be always or frequently observed in the patients. However, the results in the present study did not suggest so.

Since no specific *AE1* mutation potentially considered to be a disease mutation causing EdRTA was observed in the patients studied and it was still possible that such mutation might escape the screening procedure used, the DNA linkage analysis using microsatellite (D17S787) marker mapped closed to the *AE1* gene was also carried out in a selected family with several members who were affected by EdRTA. This analysis would provide the information concerning the involvement of the *AE1* gene in EdRTA in the family studied, albeit mutations were unable to be detected. If the *AE1* gene is involved in EdRTA, it is expected that in autosomal dominant mode of inheritance, a specific allele of the marker, or in autosomal recessive mode of inheritance, a specific genotype (two combined alleles of the marker) will be present in all the affected members and not present in the unaffected member. The result (Figure 24) did not demonstrate as what was expected; a specific allele or genotype was not found in the affected members but four alleles (B, C, D, and F) or two genotypes (BD and CF) could be seen in the affected members. From this result, if the *AE1* gene was involved in EdRTA either in the autosomal dominant or autosomal recessive model, all four alleles would be the disease-associated alleles. This seems to be very unlikely, unless these disease-associated alleles were extremely common. Furthermore, the same genotype (BD) that was present in the affected members was also noticed in the only available unaffected member.

The failure to find a specific allele or genotype of this marker in the affected members from this family does not absolutely exclude that *AE1* mutation is not involved the pathogenesis of EdRTA since the disease-associated alleles might be very common and the unaffected individual who had the same genotype as the

affected individuals might have not developed the disease. In addition, the genetic distance between *AE1* and D17S787 marker is not known with precision. This marker probably lies about 3 cM of *AE1*. Therefore, the possibility of recombination in the region between *AE1* and D17S787 marker is about 3%. Additional results of DNA linkage analysis as studied by the group in the Division of Medical Molecular Biology showed that no specific allele or genotype of this marker was found to be linked to the disease in other 7 families with EdRTA (unpublished data).

In conclusion, the results of mutation analysis and DNA linkage study presented in this thesis did not support the hypothesis that mutation of the *AE1* gene is involved as the etiology of EdRTA in the northeastern population of Thailand. The pathogenesis of EdRTA is still not known. The hypotheses based on both the environmental and genetic factors should be tested and verified. Considering the genetic factors, there are several other genes that encode the proteins and enzymes that regulate acid secretion at the renal distal tubules. These genes are interesting to be further investigated. With the advanced techniques in molecular genetics and molecular biology, the pathogenesis of EdRTA in this population will potentially be elucidated in the near future.

CHAPTER VII

CONCLUSION

The study in this thesis was based on the hypothesis that mutations of the *AE1* gene may be involved in the pathogenesis of EdRTA in the patients from the northestern population of Thailand. This hypothesis would be validated if specific mutation or mutations of *AE1* were constantly found to be present in the EdRTA patients, without detection in normal individuals. In the autosomal dominant mode of inheritance, one abnormal *AE1* allele would be observed, while in the autosomal recessive mode of inheritance, two abnormal *AE1* alleles would be detected.

Two different methods including mutation screening and characterization, and DNA linkage analysis were employed to test the hypothesis. In the mutation screening, RI PCR-SSCP and non-RI PCR SSCP with modified conditions were carried out, in which mobility shifts were detected in 5 regions of AE1. Sequencing analyses of these regions demonstrated two nucleotide changes in the non-coding regions (IVS5+27C>T and IVS17+19G>A), two silent mutations (F266F and S438S), and four missense mutations (K56E, D38A, E72D, and G701D). Of these nucleotide changes and mutations, G701D (band 3 Bangkok I) was reported to be a diseases causing mutation. This mutation results in autosomal recessive dRTA in children when it is present in homozygous or compound heterozygous conditions. In heterozygous state, it does not cause dRTA. G701D was found in five patients in heterozygous state in this study, which was unlikely to cause the disease.

To broadly investigate the involvement of AE1 as a cause of EdRTA, DNA linkage analysis using microsatellite (D17S787) marker was also studied in an affected family. The result of this study did not show that a specific allele or genotype of the marker was linked to the disease.

From the evidences of both mutation analysis and linkage study, it was concluded that AE1 mutation might not be involved in the pathogenesis of EdRTA in the group of patients from the northeastern population of Thailand studied in this thesis.

REFERENCES

1. Nilwarangkur S, Nimmannit S, Chaovakul V, Susaengrat W, Ong-aj-Yooth S, Vasuvattakul S, *et al*. Endemic primary distal renal tubular acidosis in Thailand. Q J Med 1990;74(275):289-301.

2. Vasuvattakul S, Nimmannit S, Chaovakul V, Susaengrat W, Shayakul C, Malasit P, *et al*. The spectrum of endemic renal tubular acidosis in the northeast of Thailand. Nephron 1996;74(3):541-7.

3. Nimmannit S, Malasit P, Susaengrat W, Ong-Aj-Yooth S, Vasuvattakul S, Pidetcha P, *et al*. Prevalence of endemic distal renal tubular acidosis and renal stone in the northeast of Thailand. Nephron 1996;72 (4):604-10.

4. Nilwarangkur S, Malasit P, Nimmannit S, Susaengrat W, Ong-Aj-Yooth S, Vasuvattakul S, *et al*. Urinary constituents in an endemic area of stones and renal tubular acidosis in northeastern Thailand. Southeast Asian J Trop Med Public Health 1990;21(3):437-41.

5. Tungsanga K, Sriboonlue P, Borwornpadungkitti S, Tosukhowong P, Sitprija V. Urinary acidification in renal stone patients from northeastern Thailand. J Urol 1992;147(2):325-8.

6. Inaba Y, Chiba M, Igarashi T, Komats Y, Murai Y, Endou H, *et al*. Endemic primary distal renal tubular acidosis and sudden unexplained death

syndrome in Thailand. In: Endou H, Nilwarangkur S, editors. Lai Tai, sudden unexplained death syndrome. Bangkok; 1995. Contact No.: 91-II-259, 92-III-044, 04041041. Sponsored by Toyota Foundation and the Ministry of Education, Science and Culture of Japan.

7. Halperin M, Carlisle E, Donnelly S, Kamel K, Vasuvattakul S. Renal tubular acidosis. In: Narins R, editor. Clinical disorders of fluid and electrolyte metabolism. New York: McGraw Hill; 1994. p. 875-910.

8. DuBose TD, Alpern RJ. Renal tubular acidosis. In: Scriver CR, Beaudet AL, Sly WS, Valle D, editors. The metabolic and molecular bases of inherited disease. 7th ed. New York: McGraw-Hill; 1995. p. 3655-89.

9. Smulders YM, Frissen PHJ, Slaats EH, Silberbusch J. Renal tubular acidosis: pathophysiology and diagnosis. Arch Intern Med 1996;156(26):1629-36.

10. Gregory MJ, Schwartz GJ. Diagnosis and treatment of renal tubular disorders. Semin Nephrol 1998;18(3):317-29.

11. Nimmannit S, Malasit P, Chaovakul V, Susaengrat W, Vasuvattakul S, Nilwarangkur S. Pathogenesis of sudden unexplained nocturnal death (lai tai) and endemic distal renal tubular acidosis [see comments]. Lancet 1991;338(8772):930-2.

12. Sitprija V, Tungsanga K, Tosukhowong P, Leelhaphunt N, Kruerklai D, Sriboonlue P, *et al.* Metabolic problems in northeastern Thailand: possible role of vanadium. Miner Electrolyte Metab 1993;19(1):51-6.

13. Sriboonlue P, Tungsanga K, Tosukhowong P, Sitprija V. Seasonal changes in serum and erythrocyte potassium among renal stone formers from northeastern Thailand. Southeast Asian J Trop Med Public Health 1993;24(2):287-92.

14. Arruda JA, Cowell G. Distal renal tubular acidosis: molecular and clinical aspects. Hosp Pract (Off Ed) 1994;29(1):75-8, 82-8.

15. Tanner MJ. Physiology: The acid test for band 3 [news]. Biochim Biophys Acta 1996;1282(2):263-73.

16. Bastani B, Gluck SL. New insights into the pathogenesis of distal renal tubular acidosis. Miner Electrolyte Metab 1996;22(5-6):410-22.

17. Richards P, Wrong OM. Dominant inheritance in a family with familial renal tubular acidosis. Lancet 1972;2(7785):998-9.

18. Seedat YK. Familial renal tubular acidosis. Ann Intern Med 1968;69(6):1329.

19. Chaabani H, Hadj-Khlil A, Ben-Dhia N, Braham H. The primary hereditary form of distal renal tubular acidosis: clinical and genetic studies in 60-member kindred. Clin Genet 1994;45(4):194-9.

20. Cohen T, Brand-Auraban A, Karshai C, Jacob A, Gay I, Tsitsianov J, *et al.* Familial infantile renal tubular acidosis and congenital nerve deafness: an autosomal recessive syndrome. Clin Genet 1973;4 (3):275-8.

21. McKusick VA. Renal tubular acidosis, distal, autosomal recessive. In Online Mendelian Inheritance in Man (OMIM)[Online]: Online; 1998, updated 17 Decmber 1999. Available from:

http://www.ncbi.nlm.nih.gov/htbin-post/Omim/dispmim?602722 [Accessed 2000 Mar 6].

22. Karet FE, Finberg KE, Nelson RD, Nayir A, Mocan H, Sanjad SA, *et al.* Mutations in the gene encoding B1 subunit of H^+-ATPase cause renal tubular acidosis with sensorineural deafness [In Process Citation]. Nat Genet 1999;21(1):84-90.

23. Tanner MJ. The structure and function of band 3 (AE1): recent developments (review). Mol Membr Biol 1997;14(4):155-65.

24. Tse WT, Lux SE. Red blood cell membrane disorders. Br J Haematol 1999;104 (1):2-13.

25. Schofield AE, Martin PG, Spillett D, Tanner MJ. The structure of the human red blood cell anion exchanger (*EPB3, AE1, band 3*) gene. Blood 1994;84(6):2000-12.

26. Baehner RL, Gilchrist GS, Anderson EJ. Hereditary elliptocytosis and primary renal tubular acidosis in a single family. Am J Dis Child 1968;115 (4):414-9.

27. Thong MK, Tan AA, Lin HP. Distal renal tubular acidosis and hereditary elliptocytosis in a single family. Singapore Med J 1997;38(9):388-90.

28. Rysava R, Tesar V, Jirsa M, Jr., Brabec V, Jarolim P. Incomplete distal renal tubular acidosis coinherited with a mutation in the *band 3* (*AE1*) gene. Nephrol Dial Transplant 1997;12(9):1869-73.

29. Bruce LJ, Cope DL, Jones GK, Schofield AE, Burley M, Povey S, *et al.* Familial distal renal tubular acidosis is associated with mutations in

the red cell anion exchanger (*Band 3, AE1*) gene. J Clin Invest 1997;100(7):1693-707.

30. Karet FE, Gainza FJ, Gyory AZ, Unwin RJ, Wrong O, Tanner MJ, *et al.* Mutations in the *chloride-bicarbonate exchanger* gene *AE1* cause autosomal dominant but not autosomal recessive distal renal tubular acidosis. Proc Natl Acad Sci U S A 1998;95(11):6337-42.

31. Jarolim P, Shayakul C, Prabakaran D, Jiang L, Stuart-Tilley A, Rubin HL, *et al.* Autosomal dominant distal renal tubular acidosis is associated in three families with heterozygosity for the R589H mutation in the AE1 (band 3) Cl^-/HCO_3^- exchanger. J Biol Chem 1998;273(11):6380-8.

32. Tanphaichitr VS, Sumboonnanonda A, Ideguchi H, Shayakul C, Brugnara C, Takao M, *et al.* Novel AE1 mutations in recessive distal renal tubular acidosis. Loss-of- function is rescued by glycophorin A. J Clin Invest 1998;102(12):2173-9.

33. Vasuvattakul S, Yenchitsomanus PT, Vachuanichsanong P, Thuwajit P, Kaitwatcharachai C, Laosombat V, *et al.* Autosomal recessive distal renal tubular acidosis associated with Southeast Asian ovalocytosis. Kidney Int 1999;56(5):1674-1682.

34. Thibodeau GA, Patton KT. Anatomy & physiology. St. Louis: Mosby; 1995.

35. Eiam-Ong S, Kurtzman NA. Renal tubular acidosis. In: Massry SG, Glassock R, editors. Text of nephrology. 3rd ed. Baltimore: Williams&Wilkins; 1995. p. 457-68.

36. Tanner GA. Regulation of acid-base physiology. In: Rhoades R, Pflanzer R, editors. Human Physiology. 3rd ed. Florida: Saunder College Publishing; 1996. p. 761-823.

37. Morris R, C., Ives HE. Inherited disorders of the renal tubule. In: Brenner BM, editor. The kidney. 5th ed. Philadelphia: W.B. Saunders Company; 1996. p. 1764-?

38. Kamel KS, Briceno LF, Sanchez MI, Brenes L, Yorgin P, Kooh SW, *et al.* A new classification for renal defects in net acid excretion. Am J Kidney Dis 1997;29(1):136-46.

39. Toto RD, Alpern RJ. Metabolic acid-base disorders. In: Kokko JP, Tennen RL, editors. Fluids and electrolytes. 3rd ed. Philadelphia: W. B. Saunders company; 1996. p. 201-65.

40. DuBose TD, Cogan MG, Rector FC. Acid-base disorders. In: Brenner BM, editor. The kidney. 5th ed. Philadelphia: W.B. Saunders Company; 1996. p. 929-98.

41. Barakat A, Der Kaloustian V, Mufarrij A, Beirbari A. The kidney in genetic disease. New York; 1986.

42. Sitprija V, Eiam-Ong S, Suvanapha R, Kullavanijaya P, Chinayon S. Gastric hypoacidity in distal renal tubular acidosis [letter]. Nephrologie 1988;9(6):259-61.

43. Sitprija V, Tungsanga K, Eiam-Ong S, Leelhaphunt N, Sriboonlue P. Renal tubular acidosis, vanadium and buffaloes. Nephron 1990;54(1):97-8.

44. Mujais SK. Transport enzymes and renal tubular acidosis. Semin Nephrol 1998;18(1):74-82.

45. Sabatini S. Experimental studies in distal urinary acidification: bringing the bedside to the bench. Semin Nephrol 1999;19(2):188-94.

46. Hersey SJ, Sachs G. Gastric acid secretion. Physiol Rev 1995;75(1):155-89.

47. Eiam-Ong S, Dafnis E, Spohn M, Kurtzman NA, Sabatini S. H-K-ATPase in distal renal tubular acidosis: urinary tract obstruction, lithium, and amiloride. Am J Physiol 1993;265(6 Pt 2):F875-80.

48. Dafnis E, Spohn M, Lonis B, Kurtzman NA, Sabatini S. Vanadate causes hypokalemic distal renal tubular acidosis [published erratum appears in Am J Physiol 1992 Aug;263(2 Pt 2):section F following table of contents]. Am J Physiol 1992;262(3 Pt 2):F449-53.

49. Showe LC, Ballantine M, Huebner K. Localization of the gene for the erythroid anion exchange protein, band 3 (EMPB3), to human chromosome 17. Genomics 1987;1(1):71-6.

50. Lux SE, John KM, Kopito RR, Lodish HF. Cloning and characterization of band 3, the human erythrocyte anion- exchange protein (AE1). Proc Natl Acad Sci U S A 1989;86(23):9089-93.

51. Tanner MJ. Molecular and cellular biology of the erythrocyte anion exchanger (AE1). Semin Hematol 1993;30(1):34-57.

52. McKusick AV. Solute carrier family 4, anion exchanger, member 1; SLC4A1. In Online Mendelian Inheritance in Man (OMIM)[Online]: Online;1986, updated 12 Jun 1998. Available from:

http://www.ncbi.nlm.nih.gov/htbin-post/Omim/dispmim?178900 [Accessed 2000 Feb 3].

53. Sahr KE, Taylor WM, Daniels BP, Rubin HL, Jarolim P. The structure and organization of the human erythroid anion exchanger (*AE1*) gene. Genomics 1994;24(3):491-501.

54. Tanner MJ, Martin PG, High S. The complete amino acid sequence of the human erythrocyte membrane anion-transport protein deduced from the cDNA sequence. Biochem J 1988;256(3):703-12.

55. Kollert-Jons A, Wagner S, Hubner S, Appelhans H, Drenckhahn D. Anion exchanger 1 in human kidney and oncocytoma differs from erythroid AE1 in its NH_2 terminus. Am J Physiol 1993;265(6 Pt 2):F813-21.

56. Ding Y, Casey JR, Kopito RR. The major kidney AE1 isoform does not bind ankyrin (Ank1) in vitro. An essential role for the 79 NH_2-terminal amino acid residues of band 3. J Biol Chem 1994;269(51):32201-8.

57. Wang DN, Sarabia VE, Reithmeier RA, Kuhlbrandt W. Three-dimensional map of the dimeric membrane domain of the human erythrocyte anion exchanger, Band 3. Embo J 1994;13(14):3230-5.

58. Hamasaki N, Okubo K. Band 3 protein: physiology, function and structure. Cell Mol Biol (Noisy-le-grand) 1996;42(7):1041-51.

59. Kopito RR. Molecular biology of the anion exchanger gene family. Int Rev Cytol 1990;123:177-99.

60. Vince JW, Reithmeier RA. Structure of the band 3 transmembrane domain. Cell Mol Biol (Noisy-le-grand) 1996;42(7):1053-63.

61. Reithmeier RA, Landolt-Marticorena C, Casey JR, Sarabia VE, Wang J. Molecular characterization of the erythrocyte chloride-bicarbonate exchanger. Soc Gen Physiol Ser 1993;48:161-8.

62. Popov M, Tam LY, Li J, Reithmeier RA. Mapping the ends of transmembrane segments in a polytopic membrane protein. Scanning N-glycosylation mutagenesis of extracytosolic loops in the anion exchanger, band 3. J Biol Chem 1997;272(29):18325-32.

63. Fujinaga J, Tang XB, Casey JR. Topology of the membrane domain of human erythrocyte anion exchange protein, AE1. J Biol Chem 1999;274 (10):6626-33.

64. Askin D, Bloomberg GB, Chambers EJ, Tanner MJ. NMR solution structure of a cytoplasmic surface loop of the human red cell anion transporter, band 3. Biochemistry 1998;37(33):11670-8.

65. Bruce LJ, Tanner MJ. Structure-function relationships of band 3 variants. Cell Mol Biol (Noisy-le-grand) 1996;42(7):975-84.

66. Jarolim P, Palek J, Amato D, Hassan K, Sapak P, Nurse GT, *et al.* Deletion in erythrocyte *band 3* gene in malaria-resistant Southeast Asian ovalocytosis. Proc Natl Acad Sci U S A 1991;88(24):11022-6.

67. Peters LL, Shivdasani RA, Liu SC, Hanspal M, John KM, Gonzalez JM, *et al.* Anion exchanger 1 (band 3) is required to prevent erythrocyte membrane surface loss but not to form the membrane skeleton. Blood 1996;88(7):2745-53.

68. Eber SW, Gonzalez JM, Lux ML, Scarpa AL, Tse WT, Dornwell M, *et al.* Ankyrin-1 mutations are a major cause of dominant and recessive hereditary spherocytosis. Nat Genet 1996;13(2):214-8.

69. Jarolim P, Murray JL, Rubin HL, Taylor WM, Prchal JT, Ballas SK, *et al.* Characterization of 13 novel *band* 3 gene defects in hereditary spherocytosis with band 3 deficiency. Blood 1996;88(11):4366-74.

70. Jenkins PB, Abou-Alfa GK, Dhermy D, Bursaux E, Feo C, Scarpa AL, *et al.* A nonsense mutation in the erythrocyte *band 3* gene associated with decreased mRNA accumulation in a kindred with dominant hereditary spherocytosis. Exp Hematol 1996;24(3):445-52.

71. Alloisio N, Maillet P, Carre G, Texier P, Vallier A, Baklouti F, *et al.* Hereditary spherocytosis with band 3 deficiency. Association with a nonsense mutation of the *band 3* gene (allele Lyon), and aggravation by a low-expression allele occurring in trans (allele Genas). Clin Exp Immunol 1996;105(2):313-20.

72. Dhermy D, Galand C, Bournier O, Boulanger L, Cynober T, Schismanoff PO, *et al.* Heterogenous band 3 deficiency in hereditary spherocytosis related to different *band 3* gene defects [published erratum appears in Br J Haematol 1997 Nov;99(2):474]. Br J Haematol 1997;98(1):32-40.

73. Miraglia del Giudice E, Vallier A, Maillet P, Perrotta S, Cutillo S, Iolascon A, *et al.* Novel band 3 variants (bands 3 Foggia, Napoli I and Napoli II) associated with hereditary spherocytosis and band 3 deficiency: status

of the D38A polymorphism within the EPB3 locus. Br J Haematol 1997;96(1):70-6.

74. Jarolim P, Murray JL, Rubin HL, Smart E, Moulds JM. Blood group antigens Rb(a), Tr(a), and Wd(a) are located in the third ectoplasmic loop of erythroid band 3. Transfusion 1997;37(6):607-15.

75. Lima PR, Gontijo JA, Lopes de Faria JB, Costa FF, Saad ST. Band 3 Campinas: a novel splicing mutation in the band 3 gene (*AE1*) associated with hereditary spherocytosis, hyperactivity of Na^+/Li^+ countertransport and an abnormal renal bicarbonate handling. Blood 1997;90(7):2810-8.

76. Jarolim P, Rubin HL, Brabec V, Chrobak L, Zolotarev AS, Alper SL, *et al.* Mutations of conserved arginines in the membrane domain of erythroid band 3 lead to a decrease in membrane-associated band 3 and to the phenotype of hereditary spherocytosis. Blood 1995;85 (3):634-40.

77. Maillet P, Vallier A, Reinhart WH, Wyss EJ, Ott P, Texier P, *et al.* Band 3 Chur: a variant associated with band 3-deficient hereditary spherocytosis and substitution in a highly conserved position of transmembrane segment 11. Am J Physiol 1995;269(6 Pt 2):F900-10.

78. Kanzaki A, Hayette S, Morle L, Inoue F, Matsuyama R, Inoue T, *et al.* Total absence of protein 4.2 and partial deficiency of band 3 in hereditary spherocytosis. Br J Haematol 1997;99(3):522-30.

79. Bianchi P, Zanella A, Alloisio N, Barosi G, Bredi E, Pelissero G, *et al.* A variant of the *EPB3* gene of the anti-Lepore type in hereditary spherocytosis. Br J Haematol 1997;98(2):283-8.

80. Jarolim P, Palek J, Rubin HL, Prchal JT, Korsgren C, Cohen CM. Band 3 Tuscaloosa: Pro327->Arg327 substitution in the cytoplasmic domain of erythrocyte band 3 protein associated with spherocytic hemolytic anemia and partial deficiency of protein 4.2. Blood 1992;80(2):523-9.

81. Rybicki AC, Qiu JJ, Musto S, Rosen NL, Nagel RL, Schwartz RS. Human erythrocyte protein 4.2 deficiency associated with hemolytic anemia and a homozygous 40 glutamic acid->lysine substitution in the cytoplasmic domain of band 3 (band 3 Montefiore). Blood 1993;81 (8):2155-65.

82. Alloisio N, Texier P, Vallier A, Ribeiro ML, Morle L, Bozon M, *et al.* Modulation of clinical expression and band 3 deficiency in hereditary spherocytosis. Blood 1997;90(1):414-20.

83. Inoue T, Kanzaki A, Kaku M, Yawata A, Takezono M, Okamoto N, *et al.* Homozygous missense mutation (band 3 Fukuoka: G130R): a mild form of hereditary spherocytosis with near-normal band 3 content and minimal changes of membrane ultrastructure despite moderate protein 4.2 deficiency. Br J Haematol 1998;102(4):932-9.

84. Jarolim P, Rubin HL, Liu SC, Cho MR, Brabec V, Derick LH, *et al.* Duplication of 10 nucleotides in the erythroid band 3 (*AE1*) gene in a

kindred with hereditary spherocytosis and band 3 protein deficiency (band 3PRAGUE). J Clin Invest 1994;93(1):121-30.

85. Perrotta S, Polito F, Cone ML, Nobili B, Cutillo S, Nigro V, *et al.* Hereditary spherocytosis due to a novel frameshift mutation in AE1 cytoplasmic COOH terminal tail: band 3 Vesuvio. Blood 1999;93(6):2131-2.

86. Delaunay J. Red cell membrane polypeptides under normal conditions and in genetic disorders. Adv Exp Med Biol 1995;383(1):67-93.

87. Yannoukakos D, Vasseur C, Driancourt C, Blouquit Y, Delaunay J, Wajcman H, *et al.* Human erythrocyte band 3 polymorphism (band 3 Memphis): characterization of the structural modification (Lys 56-> Glu) by protein chemistry methods. Blood 1991;78(4):1117-20.

88. Jarolim P, Rubin HL, Zhai S, Sahr KE, Liu SC, Mueller TJ, *et al.* Band 3 Memphis: a widespread polymorphism with abnormal electrophoretic mobility of erythrocyte band 3 protein caused by substitution AAG-> GAG (Lys->Glu) in codon 56. Blood 1992;80(6):1592-8.

89. Zelinski T, Punter F, McManus K, Coghlan G. The ELO blood group polymorphism is located in the putative first extracellular loop of human erythrocyte band 3. Vox Sang 1998;75(1):63-5.

90. Zelinski T, McManus K, Punter F, Moulds M, Coghlan G. A Gly565->Ala substitution in human erythroid band 3 accounts for the Wu blood group polymorphism. Transfusion 1998;38(8):745-8.

91. Bruce LJ, Ring SM, Anstee DJ, Reid ME, Wilkinson S, Tanner MJ. Changes in the blood group Wright antigens are associated with a mutation at

amino acid 658 in human erythrocyte band 3: a site of interaction between band 3 and glycophorin A under certain conditions [see comments]. J Biol Chem 1995;270(3):1315-22.

92. Cotton RG. Slowly but surely towards better scanning for mutations [published erratum appears in Trends Genet 1997 May;13(5):208]. Trends Genet 1997;13(2):43-6.

93. Sheffield VC, Beck JS, Kwitek AE, Sandstrom DW, Stone EM. The sensitivity of single-strand conformation polymorphism analysis for the detection of single base substitutions. Genomics 1993;16(2):325-32.

94. Hayashi K, Kukita Y, Inazuka M, Tahira T. Single-strand conformation polymorphism analysis. In: Cotton RG, Edkins E, Forrest S, editors. Mutation Detection. Oxford: Oxford University Press; 1998. p. 7-24.

95. Orita M, Iwahana H, Kanazawa H, Hayashi K, Sekiya T. Detection of polymorphisms of human DNA by gel electrophoresis as single-strand conformation polymorphisms. Proc Natl Acad Sci U S A 1989;86(8):2766-70.

96. Orita M, Suzuki Y, Sekiya T, Hayashi K. Rapid and sensitive detection of point mutations and DNA polymorphisms using the polymerase chain reaction. Genomics 1989;5(4):874-9.

97. Jaeckel S, Epplen JT, Kauth M, Miterski B, Tschentscher F, Epplen C. Polymerase chain reaction-single strand conformation polymorphism or how to detect reliably and efficiently each sequence variation in

many samples and many genes. Electrophoresis 1998;19(18):3055-61.

98. Ellison J, Dean M, Goldman D. Efficacy of fluorescence-based PCR-SSCP for detection of point mutations. Biotechniques 1993;15(4):684-91.

99. Wallace AJ. Combined single strand conformation polymorphism and heteroduplex analysis. In: Taylor GR, editor. Laboratory method for the detection of mutations and polymorphisms in DNA. Boca Raton: CRC Press; 1997. p. 79-94.

100. Spinardi L, Mazars R, Theillet C. Protocols for an improved detection of point mutations by SSCP. Nucleic Acids Res 1991;19(14):4009.

101. Michaud J, Brody LC, Steel G, Fontaine G, Martin LS, Valle D, *et al*. Strand-separating conformational polymorphism analysis: efficacy of detection of point mutations in the human ornithine delta-aminotransferase gene. Genomics 1992;13(2):389-94.

102. Markoff A, Savov A, Vladimirov V, Bogdanova N, Kremensky I, Ganev V. Optimization of single-strand conformation polymorphism analysis in the presence of polyethylene glycol [published erratum appears in Clin Chem 1997 Apr;43(4):692]. Clin Chem 1997;43(1):30-3.

103. Humphries SE, Gudnason V, Whittall R, Day IN. Single-strand conformation polymorphism analysis with high throughput modifications, and its use in mutation detection in familial hypercholesterolemia. International Federation of Clinical Chemistry Scientific Division:

Committee on Molecular Biology Techniques. Clin Chem 1997;43 (3):427-35.

104. Savov A, Angelicheva D, Jordanova A, Eigel A, Kalaydjieva L. High percentage acrylamide gels improve resolution in SSCP analysis. Nucleic Acids Res 1992;20(24):6741-2.

105. Hongyo T, Buzard GS, Calvert RJ, Weghorst CM. 'Cold SSCP': a simple, rapid and non-radioactive method for optimized single-strand conformation polymorphism analyses. Nucleic Acids Res 1993;21(16):3637-42.

106. White MB, Carvalho M, Derse D, O'Brien SJ, Dean M. Detecting single base substitutions as heteroduplex polymorphisms. Genomics 1992;12 (2):301-6.

107. Bannai M, Tokunaga K, Lin L, Kuwata S, Mazda T, Amaki I, *et al.* Discrimination of human HLA-DRB1 alleles by PCR-SSCP (single-strand conformation polymorphism) method. Eur J Immunogenet 1994;21(1):1-9.

108. Kukita Y, Tahira T, Sommer SS, Hayashi K. SSCP analysis of long DNA fragments in low pH gel. Hum Mutat 1997;10(5):400-7.

109. Prosser J. Detecting single-base mutations. Trends Biotechnol 1993;11(6):238-46.

110. Nilsson P, Larsson A, Lundeberg J, Uhlen M, Nygren PA. Mutational scanning of PCR products by subtractive oligonucleotide hybridization analysis. Biotechniques 1999;26(2):308-16.

111. Fischer SG, Lerman LS. DNA fragments differing by single base-pair substitutions are separated in denaturing gradient gels: correspondence with melting theory. Proc Natl Acad Sci U S A 1983;80(6):1579-83.

112. Losekoot M, Fodde R. Denaturing gradient gel electrophoresis. In: Taylor GR, editor. Laboratoy methods for the detection of mutations and polymorphisms in DNA. Boca Raton: CRC Press; 1997. p. 95-107.

113. Lerman LS, Beldjord C. Comprehensive mutation detectionwith denaturing gradient gel electrophoresis. In: Cotton RGH, editor. Mutation Detection. Oxford: Oxford University Press; 1998. p. 35-61.

114. Sarkar G, Yoon HS, Sommer SS. Dideoxy fingerprinting (ddF): a rapid and efficient screen for the presence of mutations. Genomics 1992;13 (2):441-3.

115. Liu Q, Sommer SS. Parameters affecting the sensitivities of dideoxy fingerprinting and SSCP. PCR Methods Appl 1994;4(2):97-108.

116. Blaszyk H, Hartmann A, Schroeder JJ, McGovern RM, Sommer SS, Kovach JS. Rapid and efficient screening for p53 gene mutations by dideoxy fingerprinting. Biotechniques 1995;18(2):256-60 the above report in.

117. Myers RM, Larin Z, Maniatis T. Detection of single base substitutions by ribonuclease cleavage at mismatches in RNA:DNA duplexes. Science 1985;230(4731):1242-6.

118. Goldrick MM, Kimball GR, Liu Q, Martin LA, Sommer SS, Tseng JY. NIRCA: a rapid robust method for screening for unknown point mutations. Biotechniques 1996;21(1):106-12.

119. Murthy KK, Shen SH, Banville D. A sensitive method for detection of mutations--a PCR-based RNase protection assay. DNA Cell Biol 1995;14(1):87-94.

120. Nagase H, Nakamura Y. Cleavage using RNase to detect mutations. In: Cotton RGH, editor. Mutation detection. Oxford: Oxford University Press; 1998. p. 63-80.

121. Prosser J. Chemical cleavage of mismatch in heteroduplexes. In: Taylor GR, editor. Laboratory methods for the detection of mutations and polymorphisms in DNA. Boca Raton: CRC Press; 1997. p. 225-35.

122. Giannelli F, Green PM, Ramus SJ. Cleavage of mismatched bases using chemical reagents. In: Cotton RGH, editor. Mutation detection. Oxford: Oxford University Press; 1998. p. 81-97.

123. Babon JJ, Youil R, Cotton RG. Improved strategy for mutation detection--a modification to the enzyme mismatch cleavage method. Nucleic Acids Res 1995;23(24):5082-4.

124. Youil R. Mutation detection using T4 endonuclease VII. In: Cotton RGH, editor. Mutation detection. Oxford: Oxford University Press; 1998. p. 99-112.

125. Ganguly A, Rock MJ, Prockop DJ. Conformation-sensitive gel electrophoresis for rapid detection of single-base differences in double-stranded PCR

products and DNA fragments: evidence for solvent-induced bends in DNA heteroduplexes [published erratum appears in Proc Natl Acad Sci U S A 1994 May 24;91(11):5217]. Proc Natl Acad Sci U S A 1993;90(21):10325-9.

126. Korkko J, Annunen S, Pihlajamaa T, Prockop DJ, Ala-Kokko L. Conformation sensitive gel electrophoresis for simple and accurate detection of mutations: comparison with denaturing gradient gel electrophoresis and nucleotide sequencing. Proc Natl Acad Sci U S A 1998;95 (4):1681-5.

127. van der Luijt RB, Fodde R, den Dunnen JT. The protein truncation test (PTT). In: Cotton RGH, editor. Mutation detection. Oxford: Oxford University Press; 1998. p. 189-210.

128. Hamzehloei T, West S. Coupled transcription- translation. In: Taylor GR, editor. Laboratory methods for the detection of mutations and polymorphisms. Boca Raton: CRC Press; 1997. p. 109-21.

129. Maxam AM, Gilbert W. A new method for sequencing DNA. Proc Natl Acad Sci U S A 1977;74(2):560-4.

130. Werle E. Direct sequencing of polymerase chain reaction products. In: Taylor GR, editor. Laboratory methods for the detection of mutations and polymorphisms. Boca Raton: CRC Press; 1997. p. 163-74.

131. Hoheisel JD. Oligomer-chip technology. TIBTECH 1997;15:465-9.

132. Wrong O, Davies H. The secretion of acid in renal disease. Q J Med 1959;28:259-313.

133. Randall RE, Jr. Familial renal tubular acidosis revisited. Mod Treat 1967;4 (3):515-21.

134. Whittall R, Gudnason V, Weavind GP, Day LB, Humphries SE, Day IN. Utilities for high throughput use of the single strand conformational polymorphism method: screening of 791 patients with familial hypercholesterolaemia for mutations in exon 3 of the low density lipoprotein receptor gene. J Med Genet 1995;32(7):509-15.

135. Binder T, Berg T, Siegert W, Schmidt CA. PCR-SSCP: nonradioisotopic detection with biotinylated primers and streptavidin-alkaline phosphatase conjugate. Biotechniques 1995;18(5):780-1.

136. Oto M, Miyake S, Yuasa Y. Optimization of nonradioisotopic single strand conformation polymorphism analysis with a conventional minislab gel electrophoresis apparatus. Anal Biochem 1993;213(1):19-22.

137. Boutin P, Chevre JC, Hani EH, Gomis R, Pardini VC, Guillausseau PJ, et al. An automated fluorescent single-strand conformation polymorphism technique for screening mutations in the hepatocyte nuclear factor-1alpha gene (maturity-onset diabetes of the young). Diabetes 1997;46 (12):2108-9.

138. Ainsworth PJ, Surh LC, Coulter-Mackie MB. Diagnostic single strand conformational polymorphism, (SSCP): a simplified non-radioisotopic method as applied to a Tay-Sachs B1 variant. Nucleic Acids Res 1991;19(2):405-6.

139. Mohabeer AJ, Hiti AL, Martin WJ. Non-radioactive single strand conformation polymorphism (SSCP) using the Pharmacia 'PhastSystem'. Nucleic Acids Res 1991;19(11):3154.

140. Glavac D, Dean M. Optimization of the single-strand conformation polymorphism (SSCP) technique for detection of point mutations. Hum Mutat 1993;2(5):404-14.

141. Leren TP, Solberg K, Rodningen OK, Ose L, Tonstad S, Berg K. Evaluation of running conditions for SSCP analysis: application of SSCP for detection of point mutations in the LDL receptor gene. PCR Methods Appl 1993;3(3):159-62.

142. Vidal-Puig A, Moller DE. Comparative sensitivity of alternative single-strand conformation polymorphism (SSCP) methods. Biotechniques 1994;17(3):490-2, 494, 496.

143. Knudson AG, Mutation and cancer: statstiscal study of retinoblastoma. Proc Natl Acad Sci USA 1971;20:820-3.

144. Qian F, Watnick TJ, Onuchic LF, Germino GG. The molecular basis of focal cyst formation in human autosomal dominant polycystic kidney disease type I. Cell 1996;87(6):979-87.

145. Brasier JL, Henske EP. Loss of the polycystic kidney disease (*PKD1*) region of chromosome 16p13 in renal cyst cells supports a loss-of-function model for cyst pathogenesis. J Clin Invest 1997;99(2):194-9.

146. Koptides M, Constantinides R, Kyriakides G, Hadjigavriel M, Patsalis PC, Pierides A, *et al.* Loss of heterozygosity in polycystic kidney disease

with a missense mutation in the repeated region of *PKD1*. Hum Genet 1998;103(6):709-17.

147. Koptides M, Hadjimichael C, Koupepidou P, Pierides A, Constantinou Deltas C. Germinal and somatic mutations in the *PKD2* gene of renal cysts in autosomal dominant polycystic kidney disease. Hum Mol Genet 1999;8(3):509-13.

APPENDIX

1. Chemicals

Chemicals	Molecular weight (g/ml)	Source
Absolute ethanol (C_2H_5OH)	46.07	BDH Laboratory Supplies England.
Absolute methanol (CH_3OH)	32.04	E.Merck, Germany.
Acrylamide (C_3H_5NO)	71.08	Sigma Chemical, USA.
Agarose type I:low EEO $(C_{12}H_{18}O_9)_n$		Sigma Chemical, USA.
Ammonium Chloride (NH_4Cl)	53.49	Sigma Chemical, USA.
Ammonium persulfate $((NH_4)_2S_2O_8$	228.20	Sigma Chemical, USA.
Bromophenol blue ($C_{19}H_9Br_4O_5SNa$)	670.00	Promega, USA.
Chloroform ($CHCl_3$)	119.38	E.Merck, Germany.
Citric acid (C (OH)COOH)(CH2-COOH)	210.14	BDH Laboratory Supplies, England.
3′-Deoxyadenosine 5′-triphosphate or dATP ($C_{10}H_{12}N_5O_{12}P_3Na_4$)	579.2	Promega, USA.
3′-Deoxycytosine 5′-triphosphate or dCTP ($C_9H_{12}N_3O_{13}P_3Na_4$)	555.1	Promega, USA.
3′-Deoxyguanosine 5′-triphosphate or dGTP ($C_{10}H_{12}N_5O_{13}P_3Na_4$)	595.1	Promega, USA.

3′-Deoxythymidine 5′-triphosphate or dTTP ($C_{10}H_{13}N_2O_{14}P_3Na_4$)	570.1	Promega, USA.
Dimethyldichlorosilane ($C_2H_6Cl_3Si$)	129.06	Fluka, Switzerland
Ethylenediamine tetra acetic acid tetrasodium salt or EDTA ($C_{10}H_{12}N_2Na_2O_8$)	380.2	E.Merck, Germany.
Ficoll (Type 400)	400,000	Sigma Chemical, USA.
Formaldehyde solution (Formalin) (CH_2O)	30.2	A.N.H Products Ltd., Thailand.
Glycerol ($C_3H_8O_3$)	92.09	BDH Laboratory Supplies, England.
Hydrochloric acid (HCl)	36.50	E.Merck, Germany.
Isoamyl alcohol ($C_5H_{12}O$)	88.15	E.Merck, Germany.
Isopropanol ($CH_3CHOHCH_3$)	60.10	E.Merck, Germany.
Low melting point (LMP) agarose		Sigma Chemical, USA.
Magnesium chloride ($MgCl_2.6H_2O$)	203.08	E.Merck, Germany.
N,N′-Methylene-bis-acrylamide($C_7H_{10}N_2O_2$)	154.20	Sigma Chemical, USA.
Nitric acid (HNO_3)	63.01	AJAX Chemicals, Australia.
Mineral oil		Sigma Chemical, USA.
Phenol (C_6H_5OH)	94.11	E.Merck, Germany.
Potassium chloride (KCl)	74.56	E.Merck, Germany.
Potassium hydrogen carbonate ($KHCO_3$)	100.12	E.Merck, Germany.
Silver nitrate ($AgNO_3$)	169.87	E.Merck, Germany.

Sodium acetate (CH_3COONa)	82.03	E.Merck, Germany.
Sodium carbonate (Na_2CO_3)	105.99	E.Merck, Germany.
Sodium chloride (NaCl)	58.44	E.Merck, Germany.
Sodium dodecyl sulphate or SDS ($C_{12}H_{25}O_4SNa$)	288.38	Sigma Chemical, USA.
Sodium dihydrogen phosphate monohydrate ($NaH_2PO_4.H_2O$)	137.99	E.Merck, Germany.
Sodium hydrogen phosphate (Na_2HPO_4)	141.96	E.Merck, Germany.
Sodium hydroxide (NaOH)	40.00	E.Merck, Germany.
N, N, N′, N′-Tetramethyl ethylenediamine or TEMED ($C_4H_{11}NO_3$)	166.21	Bio-Rad Laboratories, Hong Kong.
Tris (Hydroxymethyl aminomethane) ($C_4H_{11}NO_3$)	121.1	Sigma Chemical, USA.
Xylene cyanol FF ($C_{25}H_{27}N_2O_6Na$)	538.60	BDH Laboratory Supplies, England.
α-^{32}P dCTP		Amersham Pharmacia Biotech, England.
γ-^{32}P ATP		Amersham Pharmacia Biotech, England.

2. Instruments

2.1 Automatic Pipettes, Gilson, France.

2.2 Biofreezer (-70°C), Forma Scientific, USA.

2.3 Centrifuge, High Speed Micro Refrigerated Centrifuge, Tomy, MTX-150, Seiko Co., Ltd., Japan.

2.4 Centrifuge, Microfuge®E Centrifuge, Beckman J3-MC, USA.

2.5 Centrifuge, Refrigerated Centrifuge, Hermle ZK 380, Germany.

2.6 Centrifuge, Refrigerated Centrifuge, Hermle ZK 383K, Germany.

2.7 Centrifuge, Speedfuge HSC10K, Savant Instruments, Inc., USA.

2.8 Computer Scanner, UMAX Data systems, Inc., Taiwan.

2.9 Convection Oven, SANYO, MOV-212F, SANYO Electric Co.,Ltd., Japan.

2.10 Cooled Incubator, SANYO, MIR-152, SANYO Electric Co.,Ltd., Japan.

2.11 DNA Thermal Cycler 480, Perkin-Elmer Cetus, Norwolk, USA.

2.12 Electronic Analytical and Precision Balance, Sartorius, B3105, Germany.

2.13 Fume Hood, TOXICAP® 1000, CAPTAIR LABX, USA.

2.14 Geiger Counter, Mini-Monitor G-M tube, Series 900, Mini-Instruments Ltd., England.

2.15 Horizontal Electrophoresis Apparatus, BRL Life technologies, England.

2.16 Horizontal Electrophoresis Apparatus, Mupid 2, ADVANCE Co., Ltd., Japan.

2.17 Hot Air Oven, Model 600 Memmert GmbH+ Co., Germany.

2.18 Magnetic Stirrer Hotplate, Stuart Scientific, England.

2.19 Medical freezer (-30°C), Sanyo MDFFO 535, Japan.

2.20 Microwave, Mitsubishi Cube-62, Mitsubishi Co., Ltd., Japan.

2.21 Minigel electrophoresis apparatus (90x80x1 mm), EIDO, Japan.

2.22 Mili-Q plus, Milipore Co., USA.

2.23 pH Meter, Orion 520 A, USA.

2.24 Polaroid Camera, Forodyme, USA.

2.25 Powersupply, E-C Apparatus EC 135, Bio-Rad Laboratories, USA.

2.26 Powersupply, Model 3000xi, Bio-Rad Laboratories, USA.

2.27 Powersupply, Power Pac 300, Bio-Rad Laboratories, USA.

2.28 Powersupply, Power Pac 3000, Bio-Rad Laboratories, USA.

2.29 Refrigerator, Sanyo SR-S58 GY, SANYO Electric Co., Ltd., Thailand.

2.30 Refrigerator, Sanyo SR-NF97 EG, SANYO Electric Co.,Ltd., Thailand.

2.31 Sequencing Gel Electrophoresis Apparatus, Sequi-Gen ™ Sequencing Gel, Bio-Rad Laboratories, Inc., USA.

2.32 Shaking Incubator, Lab-Line Instruments, USA.

2.33 Shaking Waterbath, Julabo SW-20C, Julabo Labortechnik, Germany.

2.34 Slab Gel Dryer, E-C Apparatus EC 355, USA.

2.35 Sterilizer Autoclave, Sanyo MLS-3000, Japan.

2.36 Transilluminator, TVC 312A, Spectronics, USA.

2.37 Ultrasonic Bath, Decon F54006, Decon Laboratories Ltd., England.

2.38 UV-Visible Spectrophotometer, Shimadzu UV-160A, Japan.

2.39 Vacuum Pumps, KNF Neuberger, Inc., USA.

2.40 Vortex-Mixer, Vortex Gene2, Scientific Industries, USA.

3. Enzymes

3.1 Proteinase K, Promega, USA.

3.2 *Taq* DNA polymerase, Perkin Elmer, USA or Promega, USA.

3.3 T4 polynucleotide kinase, New England Biolabs, USA.

4. DNA markers

4.1 *Hae*III digested ϕx 174 DNA, Promega, USA.

5. Commercial kits

5.1 ABI PRISM BigDye™ Terminator Cycle Sequencing Ready Reaction Kit, Perkin Elmer, USA.

5.2 QIAquick Gel Extraction Kit ,Qiagen, USA.

6. Reagents

6.1 Reagents for white blood cell harvesting

6.1.1. 10x Phosphate buffer saline (PBS)

NaCl	40	g
KCl	1	g
Na_2HPO_4	0.1	g
KH_2PO_4	1	g
Distilled water to	500	ml

The prepared 10x PBS solution was steriled by autoclaving for 15 minutes at 121°C, 15 lb/square inches and stored in a refrigerator. It was

diluted to 1x before use (1x PBS consists of 137 mM NaCl, 2.7 KCl, 4.3 mM Na_2HPO_4, 1.4 mM KH_2PO_4, pH~7.3)

6.1.2. 10x RBC lysis buffer

NH_4Cl	0.829	g
$KHCO_3$	0.1	g
EDTA	0.0037	g
Distilled water to	100	ml

The solution was steriled by autoclaving for 15 minutes at 121°C, 15 lb/square inches and stored in a refrigerator. It was diluted to 1x before use.

6.2 Reagents for DNA preparation

6.2.1. 70% Ethanol

Absolute ethanol	70	ml
Sterile distilled water to	100	ml

The solution was mixed and stored at –20 °C.

6.2.2. 10 mM Tris-HCl, pH 8.0

Tris base (Sigma)	12.11	g

Dissolved in distilled water and adjusted pH to 8.0 with HCl.

Distilled water to	100	ml

The solution was sterilized by autoclaving for 15 minutes at 121°C, 15 lb/square inches and stored in a refrigerator.

6.2.3. 0.5 M EDTA pH 8.0

EDTA	18.60	g

Dissolved in distilled water and adjusted pH to 8.0 with NaOH.

Distilled water to	100	ml

The solution was mixed and stored at room temperature.

6.2.4. TE 20-5 (20 mM Tris-HCl and 5 mM EDTA) buffer

1 M Tris –HCl, pH 8.0	20	ml
0.5 mM EDTA	10	ml
Distilled water to	1,000	ml

The solution was sterilized by autoclaving for 15 minutes at 121°C, 15 lb/square inches and stored stored in a refrigerator.

6.2.5. 10% (w/v) SDS solution

Sodium dodecyl sulfate	10	g
Distilled water to	100	ml

The solution was sterilized by autoclaving for 15 minutes at 121°C, 15 lb/square inches and stored stored in a refrigerator.

6.2.6. 2 mg/ml Proteinase K in TE 20-5

Proteinase K	2	mg
Sterile TE 20-5 buffer	1000	µl

The solution was mixed and immediately used.

6.2.7. Phenol (equilibrated with 0.1 m Tris-HCl pH 8.0, containing 0.1% w/v 8-hydroxyquinoline)

Liquefied phenol	1	volume

8-Hydroxyquinoline was added to a final concentration of 0.1%

The solution was melted at 68°C and mixed well with equal volume of 0.1 M Tris-HCl, pH 8.0. After leaving until two phases separated, the upper aqueous phase was removed. Equilibration was repeated until the pH of phenolic phase is >7.8.

β-Mercaptoethanol was added to a final concentration of 0.2%

The phenol solution migth be stored in a light tight bottle at 4 °C for periods of up to 1 month.

6.2.8. 4 M NaCl solution

NaCl	23.38	g
Distilled water to	100	ml

The solution was dispensed into aliquots and sterile by autoclaving.

6.2.9. Chloroform-isoamyl alcohol (24:1)

Chloroform	24	volume
Isoamyl alcohol	1	volume

The reagents were mixed and stored in the sterile bottle stored in a refrigerator.

6.3 Reagents for polymerase chain reaction (PCR)

6.3.1. 10 mM dNTPs solution (containing 10 mM dATP, 10 mM dCTP, 10 mM dGTP, and 10 mM dTTP)

100 mM dATP (Promega)	10	µl
100 mM dTTP (Promega)	10	µl
100 mM dCTP (Promega)	10	µl
100 mM dGTP (Promega)	10	µl
DEPC-treated water	60	µl

The solution was kept at -20°C.

6.4 Reagent for agarose gel electrophoresis

6.4.1. 50x Tris-acetate buffer (TAE buffer)

Tris-base (Sigma)	242	g
Glacial acetic acid	57.1	ml
0.5 M EDTA (pH 8.0)	100	ml
Distilled water to	1000	ml

The solution was mixed and stored at room temperature. 1x solution was made before use (1x TAE consists of 0.04 M Tris-acetate and 0.001 M EDTA).

6.4.2. 2% (w/v) Agarose gel in 1x TAE buffer

Agarose gel	2	g
1x TAE buffer	100	ml

The slurry was heated in a microwave oven until the agarose completely dissolved and then pour the warm agarose solution into the gel set containing a comb. The gel thickness was between 3 mm and 5 mm. The gel slab might be kept in 1x TAE buffer in refrigerator.

6.4.3. 6x Gel loading buffer

Bromophenol blue	0.25	g
Xylene cyanol FF	0.25	g
Ficoll (Type 400; Sigma)	15	g
Distilled water to	100	ml

The solution was mixed and stored in aliquots at room temperature.

6.5 Reagent for SSCP analysis

6.5.1. 40% Acrylamide:bis-acrylamide (49:1) stock solution

Acrylamide	39.2	g
N, N′-methylene bis-acrylamide	0.8	g
Deionized water	~80	ml

The solution was dissolved at 65°C for 10 minutes, filtered through a 0.45 mm filter, and adjusted volume to 100 ml with deionized water, and kept at 4°C.

6.5.2. 40% acrylamide:bis-acrylamide (19:1) stock solution

Acrylamide	38	g
N, N′-methylene bis-acrylamide	2	g
Deionized water	~80	ml

The solution was dissolved at 65 °C for 10 minutes, filtered through 0.45 mm filter and adjusted volume to 100 ml with deionized water and kept at 4°C.

6.5.3. 10% Polyacrylamide with 0.5% or 5% glycerol by mixing:

Reagent	Volume	
	0.5% glycerol gel	**5% glycerol gel**
Stock 40% acrylamide: bis-acrylamide (49:1)	2.5 ml	2.5 ml
5x TBE	2.0 ml	2.0 ml
Glycerol	50 µl	500 µl
Distilled water	4.95 ml	4.5 ml
10% Ammonium persulphate	70 µl	70 µl
TEMED	4 µl	4 µl

After mixing, the gel must be used immediately.

6.5.4. 5.5% Polyacrylamide gel

Stock 40% acrylamide : bis-acrylamide(19:1)	10	ml
5x TBE	16	ml

Distilled water	46	ml
TEMED	30	µl
Ammonium persulfate	450	µl
Total volume	73	ml

The reagents were mixed together in the beaker and must be used immediately.

6.5.5. 10% (w/v) Ammonium persulphate

Ammonium persulfate	1.0	g
Distilled water to	10	ml

The solution was kept in the vial at 4 °C.

6.5.6. 5x Tris-borate buffer (TBE buffer)

Tris-base (Sigma)	54	g
Boric acid	27.5	g
0.5 M EDTA (pH 8.0)	20	ml
Distilled water to	1000	ml

The solution was mixed and stored at room temperature.

6.5.7. Sample running buffer for ssDNA

Formamide	950	µl
5% bromophenol blue	10	µl
5% xylene cyanol	10	µl

1 M EDTA	20	µl
1 M NaOH	10	µl

The buffer was aliquoted and stored at 4 °C.

6.5.8. Sample running buffer for dsDNA

Formamide	950	µl
5% bromophenol blue	10	µl
5% xylene cyanol	10	µl
1 M EDTA	20	µl

The buffer was aliquoted and stored at 4 °C.

6.6 Reagent for silver staining

6.6.1. 40% Methanol

Methanol	400	ml
Deionized water to	1000	ml

The solution was mixed and stored at room temperature.

6.6.2. 160 mM Nitric acid (HNO_3)

70% HNO_3	10.19	ml
Deionized water to	1000	ml

The solution was mixed and stored at room temperature.

6.6.3. Silver staining solution

Silver nitrate ($AgNO_3$)	100	mg
Deionized water	50	ml

The solution was mixed and used immediately.

6.6.4. Developer solution

Sodium carbonate (Na_2CO_3)	2.1	g
Deionized water	70	ml
35% Formaldehyde	35	µl

The solution was mixed and used immediately.

6.6.5. Stop solution

Citric acid	100	g
Deionized water	1000	ml

The solution was mixed and stored at room temperature.

6.7 Reagent for purification of PCR product

6.7.1. 2% (w/v) Low melting point (LMP) agarose gel in 1x TAE buffer

Low melting point agarose gel	2	g
1x TAE buffer	100	ml

The gel was prepared as same as that was described in section 6.2.4 and used without storing.

6.8 Reagent for DNA sequencing

6.8.1. 6% Polyacrylamide gel with 7 M urea

Urea	30	g
Distilled water	14.5	ml

The mixture was heated in a microwave oven until the urea completely dissolved.

Stock 40% acrylamide : bis-acrylamide (19:1)	9	ml
5x TBE	12	ml
TEMED	30	µl
Ammonium persulfate	420	µl

The solution was mixed and used immediately.

6.8.2. 3 M Sodium acetate (NaOAc), pH 4.6

Sodium acetate	16.40	g

Dissolved in distilled water and adjusted pH to 5.0 with glacial acetic acid.

Distilled water to	100	ml

The solution was mixed, autoclaved for 15 minutes at 121°C, 15 lb/square inches and stored at room temperature.

BIOGRAPHY

NAME Miss Thitima Tungsirikul

DATE OF BIRTH 23 June 1974

PLACE OF BIRTH Ubolrajathani, Thailand

INSTITUTIONS ATTENDED

Khon Kaen University, 1992-1996:
Bachelor of Science (Medical Technology)

Mahidol University, 1996-2000:
Master of Science (Microbiology)

RESEARCH GRANT

Graduate Fellowship Program National Science and Technology Development Agency (NSTDA)